

SOLUTION OF ONE DIMENSIONAL TRANSIENT FLOW IN COMPOSITE
AQUIFERS USING STEHFEST ALGORITHM

A THESIS SUBMITTED TO
THE GRADUATE SCHOOL OF NATURAL AND APPLIED SCIENCES
OF
MIDDLE EAST TECHNICAL UNIVERSITY

BY

ÜRÜN BAKAR

IN PARTIAL FULFILLMENT OF THE REQUIREMENTS
FOR
THE DEGREE OF MASTER OF SCIENCE
IN
CIVIL ENGINEERING

SEPTEMBER 2010

Approval of the thesis:

**SOLUTION OF ONE DIMENSIONAL TRANSIENT FLOW IN
COMPOSITE AQUIFERS USING STEHFEST ALGORITHM**

submitted by **ÜRÜN BAKAR** in partial fulfillment of the requirements for the degree of **Master of Science in Civil Engineering Department, Middle East Technical University** by,

Prof. Dr. Canan Özgen _____
Dean, Graduate School of **Natural and Applied Sciences**

Prof. Dr. Güney Özcebe _____
Head of Department, **Civil Engineering**

Prof. Dr. Halil Önder _____
Supervisor, **Civil Engineering Dept., METU**

Examining Committee Members:

Prof. Dr. İbrahim Güner _____
Civil Engineering Dept., Gazi University

Prof. Dr. Halil Önder _____
Civil Engineering Dept., METU

Assoc. Prof. Dr. İsmail Aydın _____
Civil Engineering Dept., METU

Assoc. Prof. Dr. Yakup Darama _____
DSİ

Asst. Prof. Dr. Şahnaz Tiğrek _____
Civil Engineering Dept., METU

Date:

15.09.2010

I hereby declare that all information in this document has been obtained and presented in accordance with academic rules and ethical conduct. I also declare that, as required by these rules and conduct, I have fully cited and referenced all material and results that are not original to this work.

Name, Last Name : ÜRÜN BAKAR

Signature :

ABSTRACT

SOLUTION OF ONE DIMENSIONAL TRANSIENT FLOW IN COMPOSITE AQUIFERS USING STEHFEST ALGORITHM

BAKAR, Ürün

M.Sc., Department of Civil Engineering

Supervisor: Prof. Dr. Halil ÖNDER

September 2010, 148 pages

In this study, piezometric heads in a composite aquifer composed of an alluvial deposit having a width adjacent to a semi-infinite fractured rock are determined. One dimensional transient flow induced by a constant discharge pumping rate from a stream intersecting alluvial part of the aquifer is considered. Parts of the aquifer are homogeneous and isotropic. Equations of flow, initial and boundary conditions are converted to dimensionless forms for graphical presentation and the interpretation of results independent of discharge and head inputs specific to the problem. Equations are solved first in Laplace domain and Laplace domain solutions are inverted numerically to real time domain by utilizing Stehfest algorithm.

For this purpose, a set of subroutines in VBA Excel are developed. This procedure is verified by application of code to flow in semi-infinite homogeneous aquifer under constant discharge for which analytical solution is available in literature. VBA codes are also developed for two special cases of finite aquifer with impervious and with recharge boundary on the right hand side. Results of composite aquifer solutions with extreme transmissivity values are compared with these two cases for verification of methodology and sensitivity of results.

Keywords: Composite Aquifer, Double Porosity Model, Laplace Transform, Stehfest Algorithm, Transient Flow

ÖZ

KOMPOZİT AKİFERLERDE TEK BOYUTLU ZAMANA BAĞLI AKIMIN STEHFEST ALGORİTMASI KULLANILARAK ÇÖZÜMÜ

BAKAR, Ürün

Yüksek Lisans, İnşaat Mühendisliği Bölümü

Tez Danışmanı: Prof. Dr. Halil ÖNDER

Eylül 2010, 148 sayfa

Bu çalışmada yarı sonsuz çatlaklı kayaya bitişik alüyonlu birikintiden oluşan kompozit akiferdeki piyezometrik seviyeler belirlenmiştir. Akiferin alüyonlu kısmının kesiştiği nehirden sabit debisiyle başlayan tek boyutlu zamana bağlı akım dikkate alınmıştır. Akiferin kısımları homojen ve izotropdur. Akım denklemleri, ilk ve sınır koşullar, sonuçların soruna özgü debi ve seviye parametrelerinden bağımsız yorumlanabilmesi ve grafiksel sunumu için boyutsuz hale getirilmiştir. Denklemler öncelikle Laplas (Laplace) düzleminde çözülmüş ve çözümler Stehfest algoritması yardımıyla sayısal olarak gerçek zaman düzlemine çevirilmiştir. Bu amaçla Excel Visual Basic Uygulamalarında bir grup alt programlar geliştirilmiştir. Bu işlemler, bilgisayar kodunun literatürde analitik çözümü mevcut olan, yarı sonsuz homojen akiferin sabit debi durumundaki akımına uygulanmasıyla doğrulanmıştır. Visual Basic kodları, sonlu

akiferin sađ sınır kısmında geđirimsiz tabaka ve nehir sınır kořulları olan iki özel durumu için de geliřtirilmiřtir. İletkenlik katsayısının uç deđerleri için birleřik akifer çözümleri bu iki özel durum ile metodun dođruluđu ve sonuçların hassaslıđı için kıyaslanmıřtır.

Anahtar Kelimeler: Kompozit akifer, Çift Gözeneklilik Modeli, Laplas (Laplace) Dönüřümü, Stehfest Algoritması, Zamana Bađlı Akım

To My Family...

ACKNOWLEDGEMENTS

I would like to express sincere appreciation to my supervisor Prof. Dr. Halil Önder for his wise supervision, endless thoughtfulness, valuable suggestions and encouragement, support, contribution and kindness.

I offer very special thanks to my mother Gülderen Bakar and my father Zekayi Bakar. With their endless patience and faith in me, my belief for success will never vanish. Their support whenever I needed at every stage of difficulties leads me on the path of my life.

Gizem Okyay deserves my special thanks for her support and friendship. With her optimism ,support and encouragement, despite of this challenging life I try to keep going on my way and feel lucky to be friends with her at every time.

I would like to express my deepest gratefulness to Onur Arı for his valuable comments about this thesis and sharing his experiences with me.

It is a great pleasure to express my gratitude and thanks to my brother and my best friend Emek Bakar for confronting difficulties together. His high motivation makes me focus on my targets during this work. Despite of far distances between us, I always feel his endless endearment every time.

TABLE OF CONTENTS

ABSTRACT.....	iv
ÖZ.....	vi
ACKNOWLEDGEMENTS.....	ix
TABLE OF CONTENTS.....	x
LIST OF FIGURES.....	xv
LIST OF TABLES.....	xxi
LIST OF SYMBOLS.....	xxiii
CHAPTERS	
1. INTRODUCTION.....	1
1.1 Introductory Remarks	1
1.2 Literature Review	2
1.3 Objective of the Thesis.....	5
1.4 Description of the Thesis	5
2. MATHEMATICAL FORMULATION FOR FLOW IN COMPOSITE AQUIFER.....	7
2.1 Introductory Remarks	7
2.2 Mathematical Formulation of the Problem	8
2.2.1 Assumptions	9
2.2.2 Governing Differential Equations	10
2.2.3 Initial and Boundary Conditions	12
2.3 Non-Dimensional Forms of Equations	14

2.4	Solutions of Dimensionless Groundwater Flow Equations by Laplace Transform Method	17
2.4.1	Laplace Transforms	17
2.4.2	Laplace Transforms of Non-Dimensional Equations, Initial and Boundary Conditions	18
2.5	Stehfest Algorithm for Numerical Inversion	24
3.	TEST OF STEHFEST ALGORITHM IN GROUNDWATER PROBLEMS.....	27
3.1	Introductory Remarks	27
3.2	One Dimensional Transient Flow in a Semi-Infinite Homogeneous Aquifer under Constant Discharge.....	27
3.3	Sensivity Analysis of N Values on the Numerical Solution.....	32
3.4	Analytical and Numerical Solutions for Piezometric Head	35
3.4.1	Variation of piezometric head with time	35
3.4.2	Variation of piezometric head with time	37
3.5	Concluding Remarks	39
4.	APPLICATION OF STEHFEST ALGORITHM TO COMPOSITE AQUIFERS.....	40
4.1	Application Methodology	40
4.2	Variation of Dimensionless Piezometric Head.....	41
4.2.1	Variation of Dimensionless Piezometric Head in Granular Aquifer.....	44
4.2.2	Variation of Dimensionless Piezometric Head in Fractures	46
4.2.3	Variation of Dimensionless Piezometric Head in Blocks	47
4.2.4	Variation of Dimensionless Piezometric Head for Granular Aquifer-Fractures Interface.....	49
4.2.5	Comparison between Dimensionless Piezometric Head of Fractures and Blocks	51
4.3	Sensivity Analysis of Aquifer Characteristics	53

4.3.1	Effect of λ_1 on the Flow through Composite Aquifer.....	53
4.3.1.1	Effect of λ_1 on the dimensionless head of granular aquifer.....	53
4.3.1.2	Effect of λ_1 on the dimensionless head of fractures.....	56
4.3.1.3	Effect of λ_1 on the dimensionless head of blocks.....	57
4.3.1.4	Effect of λ_1 on the dimensionless head on the interface.....	58
4.3.2	Effect of λ_2 on the Flow through Composite Aquifer.....	59
4.3.2.1	Effect of λ_2 on the dimensionless head of granular aquifer.....	59
4.3.2.2	Effect of λ_2 on the dimensionless head of fractures.....	62
4.3.2.3	Effect of λ_2 on the dimensionless head of blocks.....	63
4.3.3	Effect of η_1 on the Flow through Composite Aquifer.....	65
4.3.3.1	Effect of η_1 on the dimensionless head of granular aquifer ...	65
4.3.3.2	Effect of η_1 on the dimensionless head of fractures.....	68
4.3.3.3	Effect of η_1 on the dimensionless head of blocks.....	69
4.3.4	Effect of η_2 on the Flow through Composite Aquifer.....	71
4.3.4.1	Effect of η_2 on the dimensionless head of granular aquifer ...	71
4.3.4.2	Effect of η_2 on the dimensionless head of fractures.....	73
4.3.4.3	Effect of η_2 on the dimensionless head of blocks.....	75
4.3.5	Effect of δ_2 on the Flow through Composite Aquifer.....	76
4.3.5.1	Effect of δ_2 on dimensionless head of granular aquifer.....	77
4.3.5.2	Effect of δ_2 on the dimensionless head of fractures.....	79
4.3.5.3	Effect of δ_2 on the dimensionless head of blocks.....	80
4.4	Concluding Remarks.....	82
5.	FURTHER EVALUATION AND DISCUSSION OF PROPOSED SOLUTION: APPLICATION TO SPECIAL CASES.....	83

5.1	Introduction	83
5.2	One Dimensional Transient Flow in a Finite Aquifer with Impervious Boundary under Constant Discharge	83
5.3	One Dimensional Transient Flow in a Finite Aquifer with Recharge Boundary under Constant Discharge	89
5.3.1	Steady State Condition	94
5.4	Concluding Remarks	96
6.	SUMMARY AND CONCLUSION.....	97
	REFERENCES.....	101
	APPENDICES	
A.	SUBROUTINE IN VBA EXCEL TO SOLVE STEHFEST ALGORITHM FOR SEMI-INFINITE HOMOGENEOUS AQUIFER UNDER CONSTANT DISCHARGE.....	106
B.	SUBROUTINE OF COMPOSITE AQUIFER IN VBA EXCEL TO SOLVE STEHFEST ALGORITHM FOR DIMENSIONLESS PIEZOMETRIC HEAD OF GRANULAR AQUIFER UNDER CONSTANT DISCHARGE.....	115
C.	SUBROUTINE OF COMPOSITE AQUIFER IN VBA EXCEL TO SOLVE STEHFEST ALGORITHM FOR DIMENSIONLESS PIEZOMETRIC HEAD OF FRACTURES UNDER CONSTANT DISCHARGE.....	121
D.	SUBROUTINE OF COMPOSITE AQUIFER IN VBA EXCEL TO SOLVE STEHFEST ALGORITHM FOR DIMENSIONLESS PIEZOMETRIC HEAD OF BLOCKS UNDER CONSTANT DISCHARGE.....	129
E.	SUBROUTINE OF FINITE AQUIFER WITH IMPERVIOUS BOUNDARY IN VBA EXCEL TO SOLVE STEHFEST ALGORITHM FOR DIMENSIONLESS PIEZOMETRIC HEAD UNDER CONSTANT DISCHARGE.....	137

F. SUBROUTINE OF FINITE AQUIFER WITH RECHARGE BOUNDARY IN VBA
EXCEL TO SOLVE STEHFEST ALGORITHM FOR DIMENSIONLESS PIEZOMETRIC
HEAD UNDER CONSTANT DISCHARGE143

LIST OF FIGURES

FIGURES

Figure 1.1 : Typical composite aquifer adjacent to a stream with alluvial formation embedded in fractured rock.....	2
Figure 2.1: One dimensional transient flow in composite aquifer under constant pumping discharge rate, Q . Subscripts 0, 1 and 2 denote granular, fractures and block matrices, respectively.....	8
Figure 3.1: Piezometric head vs. time at $x=300$ m for values of N up to 6	33
Figure 3.2: Piezometric head vs. time at $x=300$ m for values of $N =8, 10, 12, 24$	34
Figure 3.3: Piezometric head vs. time at $x=300$ m for values of $N=26$ and $N=28$	34
Figure 3.4: Piezometric head of numerical and analytical solutions vs. N at $x=300$ m, $t=500000$ secs (139 hrs).....	35
Figure 3.5: Numerical solution of piezometric head vs. time for different values of distance.	36
Figure 3.6: Analytical solution of piezometric head vs. time for different values of distance.	36
Figure 3.7: Numerical and analytical solutions of piezometric head vs. time at $x=300$ m.....	37
Figure 3.8: Numerical solution of piezometric head vs. distance in meters for different values of time.	38
Figure 3.9: Analytical solution of piezometric head vs. distance in meters for different values of time.	38

Figure 3.10: Numerical and analytical solutions of piezometric head vs. distance in meters at $t=90000$ sec.	39
Figure 4.1: Dimensionless piezometric head of granular aquifer z_0 vs. dimensionless time θ for different values of dimensionless distance y	45
Figure 4.2: Dimensionless piezometric head of granular aquifer z_0 vs. dimensionless distance y for different dimensionless time θ	45
Figure 4.3: Dimensionless piezometric head of fractures z_1 vs. dimensionless time θ for different values of dimensionless distance y	46
Figure 4.4: Dimensionless piezometric head of fractures z_1 vs. dimensionless distance y for different values of dimensionless time θ	47
Figure 4.5: Dimensionless piezometric head of blocks z_2 vs. dimensionless time θ for different values of dimensionless distance y	48
Figure 4.6: Dimensionless piezometric head of blocks z_2 vs. dimensionless distance y for different values of dimensionless time θ	49
Figure 4.7: Dimensionless piezometric head of granular aquifer z_0 and fractures z_1 vs. dimensionless time θ at the intersection, $y=1$	50
Figure 4.8: Dimensionless piezometric head of granular aquifer z_0 and fractures z_1 vs. dimensionless distance y for different values of dimensionless time θ ...	51
Figure 4.9: Dimensionless piezometric head of fractures z_1 and blocks z_2 vs. dimensionless distance y for different values of dimensionless time θ	52
Figure 4.10: Dimensionless piezometric head difference between fractures z_1 and blocks z_2 vs. dimensionless time θ for different values of dimensionless distance y	52
Figure 4.11: Dimensionless piezometric head difference between fractures z_1 and blocks z_2 vs. logarithm of dimensionless time θ for different values of dimensionless distance y	53
Figure 4.12: Dimensionless piezometric head of granular aquifer z_0 vs. dimensionless time θ for different values of λ_1 at $y=0.5$	54
Figure 4.13: Dimensionless piezometric head of granular aquifer z_0 vs. dimensionless distance y for different values of λ_1 at $\theta =0.5$	55

Figure 4.14: Dimensionless piezometric head of granular aquifer z_0 vs. dimensionless distance y for different values of λ_1 at $\theta = 10$	55
Figure 4.15: Dimensionless piezometric head of fractures z_1 vs. dimensionless time θ for different values of λ_1 at $y=5$	56
Figure 4.16: Dimensionless piezometric head of fractures z_1 vs. dimensionless distance y for different values of λ_1 at $\theta = 0.5$	57
Figure 4.17: Dimensionless piezometric head of blocks z_2 vs. dimensionless distance y for different values of λ_1 at $\theta = 0.5$	58
Figure 4.18: Dimensionless piezometric heads of granular aquifer and fractures vs. dimensionless distance at $\theta=0.5$ for different values of λ_1	59
Figure 4.19: Dimensionless piezometric head of granular aquifer z_0 vs. dimensionless time θ for different values of λ_2 at $y=0.5$	60
Figure 4.20: Dimensionless piezometric head of granular aquifer z_0 vs. dimensionless distance y for different values of λ_2 at $\theta = 0.5$	61
Figure 4.21: Dimensionless piezometric head of granular aquifer z_0 vs. dimensionless distance y for different values of λ_2 at $\theta = 10$	61
Figure 4.22: Dimensionless piezometric head of fractures z_1 vs. dimensionless time θ for different values of λ_2 at $y=5$	62
Figure 4.23: Dimensionless piezometric head of fractures z_1 vs. dimensionless distance y for different values of λ_2 at $\theta = 0.5$	63
Figure 4.24: Dimensionless piezometric head of blocks z_2 vs. dimensionless time θ for different values of λ_2 at $y=5$	64
Figure 4.25: Dimensionless piezometric head of blocks z_2 vs. dimensionless distance y for different values of λ_2 at $\theta = 0.5$	65
Figure 4.26: Dimensionless piezometric head of granular aquifer z_0 vs. dimensionless time θ for different values of η_1 at $y=0.5$	66
Figure 4.27: Dimensionless piezometric head of granular aquifer z_0 vs. dimensionless distance y for different values of η_1 at $\theta = 0.5$	67
Figure 4.28: Dimensionless piezometric head of granular aquifer z_0 vs. dimensionless distance y for different values of η_1 at $\theta = 10$	67

Figure 4.29: Dimensionless piezometric head of fractures z_1 vs. dimensionless time θ for different values of η_1 at $y=5$	68
Figure 4.30: Dimensionless piezometric head of fractures z_1 vs. dimensionless distance y for different values of η_1 at $\theta =0.5$	69
Figure 4.31: Dimensionless piezometric head of blocks z_2 vs. dimensionless time θ for different values of η_1 at $y=5$	70
Figure 4.32: Dimensionless piezometric head of blocks z_2 vs. dimensionless distance y for different values of η_1 at $\theta =0.5$	70
Figure 4.33: Dimensionless piezometric head of granular aquifer z_0 vs. dimensionless time θ for different values of η_2 at $y=0.5$	71
Figure 4.34: Dimensionless piezometric head of granular aquifer z_0 vs. dimensionless distance y for different values of η_2 at $\theta =0.5$	72
Figure 4.35: Dimensionless piezometric head of granular aquifer z_0 vs. dimensionless distance y for different values of η_2 at $\theta =10$	73
Figure 4.36: Dimensionless piezometric head of fractures z_1 vs. dimensionless time θ for different values of η_2 at $y=5$	74
Figure 4.37: Dimensionless piezometric head of fractures z_1 vs. dimensionless distance y for different values of η_2 at $\theta =0.5$	74
Figure 4.38: Dimensionless piezometric head of blocks z_2 vs. dimensionless time θ for different values of η_2 at $y=5$	75
Figure 4.39: Dimensionless piezometric head of blocks z_2 vs. dimensionless distance y for different values of η_2 at $\theta =0.5$	76
Figure 4.40: Dimensionless piezometric head of granular aquifer z_0 vs. dimensionless time θ for different values of δ_2 at $y=0.5$	77
Figure 4.41: Dimensionless piezometric head of granular aquifer z_0 vs. dimensionless distance y for different values of δ_2 at $\theta =0.5$	78
Figure 4.42: Dimensionless piezometric head of granular aquifer z_0 vs. dimensionless distance y for different values of δ_2 at $\theta =10$	78
Figure 4.43: Dimensionless piezometric head of fractures z_1 vs. dimensionless time θ for different values of δ_2 at $y=5$	79

Figure 4.44: Dimensionless piezometric head of fractures z_1 vs. dimensionless distance y for different values of δ_2 at $\theta = 0.5$	80
Figure 4.45: Dimensionless piezometric head of blocks z_2 vs. dimensionless time θ for different values of δ_2 at $y=5$	81
Figure 4.46: Dimensionless piezometric head of blocks z_2 vs. dimensionless distance y for different values of δ_2 at $\theta = 0.5$	81
Figure 5.1: One dimensional transient flow in a finite aquifer with impervious boundary under constant discharge.....	84
Figure 5.2: Dimensionless piezometric head for finite aquifer with impervious boundary solution vs. dimensionless piezometric head for composite aquifer solution when $\lambda_1 = 10^{-8}$, $\lambda_2 = 10^{-8}$ for different values of dimensionless distance.....	87
Figure 5.3: Dimensionless piezometric head for finite aquifer with impervious boundary solution vs. dimensionless piezometric head for composite aquifer solution when $\lambda_1 = 10^{-8}$, $\lambda_2 = 10^{-8}$ for different values of dimensionless time.	87
Figure 5.4: Dimensionless piezometric head vs. dimensionless distance at $\theta=0.05$ and $\theta=0.5$	88
Figure 5.5: Dimensionless piezometric head vs. dimensionless time at $y=0.5$.	88
Figure 5.6: One dimensional transient flow in a finite aquifer with recharge boundary under constant discharge.....	89
Figure 5.7: Dimensionless piezometric head for finite aquifer with recharge boundary solution vs. dimensionless piezometric head for composite aquifer solution when $\lambda_1=10^8$, $\lambda_2=10^8$ for different values of dimensionless distance ..	92
Figure 5.8: Dimensionless piezometric head for finite aquifer with recharge boundary solution vs. dimensionless piezometric head for composite aquifer solution when $\lambda_1=10^8$, $\lambda_2=10^8$ for different values of dimensionless time.....	93
Figure 5.9: Dimensionless piezometric head vs. dimensionless distance at $\theta=0.05$	93
Figure 5.10: Dimensionless piezometric head vs dimensionless time at $y=0.5$	94

Figure 5.11: Dimensionless piezometric head vs. dimensionless distance and steady state condition at $\theta=10$ 95

Figure 5.12: Dimensionless piezometric head vs. dimensionless time and steady state condition at $y=0.5$ 96

LIST OF TABLES

TABLES

Table 3.1: Summary of equations used in the analysis of flow in semi-infinite homogeneous aquifer under constant discharge.	31
Table 3.2: Outputs of exact analytical solution vs. numerical solution using Stehfest algorithm for different values of N for $\nu = 0.2, Q_d = 0.05$ $x = 300$ m, $t = 500000$ seconds (139 hours).	32
Table 4.1: Dimensional and dimensionless piezometric head symbols used in the equations of groundwater flow	41
Table 4.2: Flow and aquifer parameters in groundwater equations.....	42
Table 4.3: Ranges of storage coefficient for different types of aquifer (Hall, 1996)	43
Table 4.4: Hydraulic conductivity ranges for different representative materials (USBR of Reclamation, 1997).....	43
Table 4.5: Transmissivity ranges for different properties and use (USBR of Reclamation, 1997).....	44
Table A.1: Analytical solution for semi-infinite homogeneous aquifer under constant discharge for $\nu=0.2, Q_d=0.05$	113
Table A.2: Numerical solution by Stehfest for semi-infinite homogeneous aquifer for $N=8, \nu=0.2, Q_d=0.05$	114
Table B.1: Numerical solution in granular region for $\lambda_1=15, \lambda_2=0.01, \eta_1=0.2, \eta_2=2, \delta_2=0.5, Q_b=0.06$	120
Table C.1: Numerical solution of fractures for $\lambda_1=15, \lambda_2=0.01, \eta_1=0.2, \eta_2=2, \delta_2=0.5, Q_b=0.06$	128

Table D.1: Numerical solution of blocks for $\lambda_1=15, \lambda_2=0.01, \eta_1=0.2, \eta_2=2,$ $\delta_2=0.5, Q_b=0.06$	136
Table E.1: Numerical solution by Stehfest Algorithm in finite aquifer with impervious boundary, $Q_b=0.06$	142
Table F.1: Numerical solution by Stehfest Algorithm in finite aquifer with recharge boundary under constant discharge, $Q_b=0.06$	148

LIST OF SYMBOLS

b	:	Thickness of the confined aquifer, [L]
h	:	Piezometric head from water surface, [L]
h_a	:	Analytical solution for piezometric head, [L]
h_n	:	Numerical real time solution for piezometric head by Stehfest algorithm, [L]
H_0	:	Initial value of piezometric head at $t=0$, [L]
h_0	:	Piezometric head in the granular aquifer, [L]
h_1	:	Piezometric head in the fractures, [L]
h_2	:	Piezometric head in the blocks, [L]
\bar{h}	:	Piezometric head in Laplace parameters, [L]
L	:	Length of granular aquifer along x-direction (flow direction), [L]
K_0	:	Coefficient of hydraulic conductivity of granular aquifer, [LT^{-1}]
K_1	:	Coefficient of hydraulic conductivity of fractures, [LT^{-1}]
K_2	:	Coefficient of hydraulic conductivity of blocks, [LT^{-1}]

L	:	Length of granular aquifer along x-direction (flow direction), [L]
N	:	Number of terms in Stehfest algorithm, [-]
p	:	Laplace transform parameter, [-]
Q	:	Volumetric discharge rate per unit length of stream-aquifer boundary, [L ² T ⁻¹]
Q_b	:	Dimensionless discharge relating discharge, transmissivity of the granular aquifer, granular aquifer length and initial value of piezometric head, [-]
Q_d	:	Dimensionless discharge relating discharge and transmissivity of the granular aquifer, [-]
S	:	Coefficient of storage, [L ² T ⁻¹]
S_0	:	Coefficient of storage of the granular aquifer, [-]
S_1	:	Coefficient of storage of the fractures, [-]
S_2	:	Coefficient of storage of the blocks, [-]
T	:	Coefficient of transmissivity, [L ² T ⁻¹]
T_0	:	Coefficient of transmissivity of the granular aquifer, [L ² T ⁻¹]
T_1	:	Coefficient of transmissivity of the fractures, [L ² T ⁻¹]
T_2	:	Coefficient of transmissivity of the blocks, [L ² T ⁻¹]
t	:	Time, [T]
x	:	Distance from stream-confined aquifer intersection along flow direction, [L]

y	:	Dimensionless distance along flow direction, [-]
z_0	:	Dimensionless piezometric head of the granular aquifer, [-]
z_1	:	Dimensionless piezometric head of the fractures, [-]
z_2	:	Dimensionless piezometric head of the blocks, [-]
\bar{z}_0	:	Dimensionless piezometric head of the granular aquifer in Laplace parameters, [-]
\bar{z}_1	:	Dimensionless piezometric head of the fractures in Laplace parameters, [-]
\bar{z}_2	:	Dimensionless piezometric head of the blocks in Laplace parameters, [-]
ε	:	Shape factor depending on geometry of rock, [L ⁻²]
δ_2	:	Dimensionless constant relating granular aquifer length, shape factor, storage and transmissivity ratios of the blocks to the granular aquifer, [-]
η_1	:	Storage ratio of the fractures to the granular aquifer, [-]
η_2	:	Storage ratio of the blocks to the granular aquifer, [-]
λ_1	:	Transmissivity ratio of the fractures to the granular aquifer, [-]
λ_2	:	Transmissivity ratio of the blocks to the granular aquifer, [-]
θ	:	Dimensionless time, [-]
ν	:	Volume of water transfer per unit time from blocks to fractures per unit horizontal area along the depth of aquifer, [L ¹ T ⁻¹]

CHAPTER 1

INTRODUCTION

1.1 Introductory Remarks

Groundwater, covering all water beneath the ground surface as a renewable source, has gained much importance in recent years due to the need of search for new water resources. Demand on water has increased with the excessive population growth and extensive use of water for agriculture, irrigation, industry and domestic needs as a result of development. The issue of meeting the demand requirements may also be further aggravated as a result of climate changes and global warming.

Since seasonal fluctuations in groundwater flow is small and slow motion of flow in aquifers attains large amounts of water storage, groundwater flow behavior has caught the attention of researchers among interdisciplinary sciences such as hydrology, civil engineering, hydrogeology, mining, petroleum engineering and agricultural engineering.

In the regions of the world with limited water due to very low precipitation and lack of adequate resources, analysis of groundwater flow becomes more important than surface water since the former constitutes only source and potential of water. Examples of such locations may be found in Saudi Arabia where water is scarce (Önder, 1989).

A common type of the aquifers is of composite nature formed by fractured rocks with an alluvial part embedded to it and forming interface in between. Typical figure for such aquifers is given in Figure 1.1.

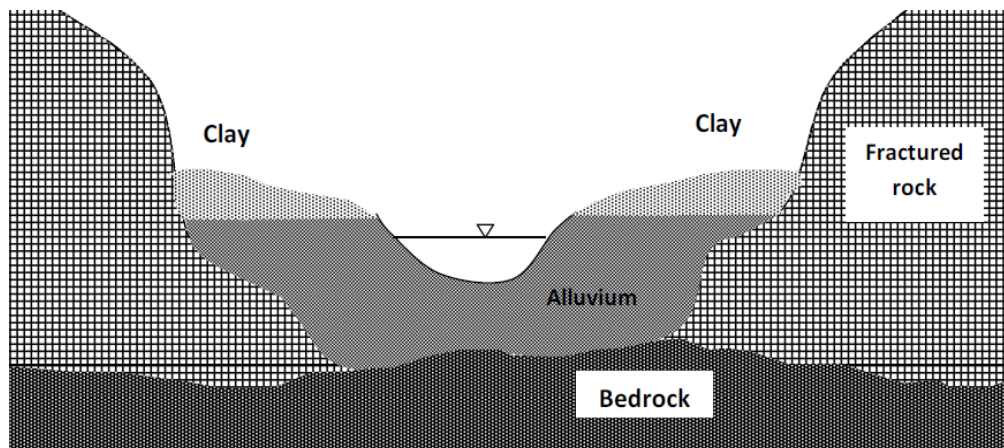


Figure 1.1 : Typical composite aquifer adjacent to a stream with alluvial formation embedded in fractured rock.

Analysis of flow in composite aquifer and method utilized is extremely important for precise determination of head levels, discharge throughout the aquifer, aquifer parameters and system response with limited sources.

1.2 Literature Review

With the developments in technology and in-field applications, the data observation of groundwater flow has become easier. Interpreting the interaction of aquifer with the surrounding requires a detailed study and mathematical model for head and discharge investigations through the aquifer.

Likewise, the characteristics of the aquifer can be determined with prescribed inputs and outputs.

Various efforts have been made by scientists to understand the groundwater flow behavior through the aquifer.

A common type of aquifer, fractured rock, is encountered as a water transmitting and storing unit composed of fractures and rocks. Solutions made for homogeneous aquifers are not valid for such aquifers. Barenblatt et.al (1960) first introduced the double porosity conceptual model in which fractured rock is composed of two overlapping media. This heterogeneous formation assumes low permeability blocks of primary porosity and highly permeable fractures of low fracture. Conducting properties of the aquifer are associated with the fracture permeability while storage properties are related to the primary porosity of blocks. (Barenblatt et al., 1960; Huyakorn & Pinder, 1983)

Warren and Root (1963) have modeled the naturally fractured reservoir as a three dimensional orthogonal fracture system. This model assumes identical rectangular homogeneous and isotropic blocks separated by fractures.

Pseudo-steady state conditions of flow in fractures to blocks have been considered by many researchers (Barenblatt et al., 1960; Warren and Root, 1963; Streltsova, 1988; Önder, 1998; Dündar and Önder, 2006).

Fully transient flow conditions have been taken into account in fractured reservoirs in most studies. (Kazemi, 1969; Najurieta, 1980; Boulton and Streltsova, 1977).

Moench (1984) has analyzed double porosity model with a fracture skin and has proposed that steady state condition is a special case of transient fracture to block flow. This assumption provides a simplified mathematical analysis for the flow in the double porosity medium.

Streltsova (1975) has studied one dimensional flow in a semi-infinite unconfined aquifer and derived sets of type curves. She stated that these solutions are also applicable to the solutions of fractured formations.

A numerical inversion method is proposed by Stehfest (1970) enabling the numerical inversion of Laplace transforms solutions of groundwater problems with transient flow conditions.

Stehfest algorithm in the solution of a variety of groundwater problems has been utilized by Moench and Ogata (1982), Chen (1985), Chen et al. (1993) and Dündar (2005).

Önder (1998) has considered one dimensional flow in a finite fractured system bounded by a stream on one side and by impervious boundary on the other. Transient flow resulting from a sudden rise or fall on the stream stage is analyzed by using Laplace transform and finite Fourier sine transform techniques to the governing equations and analytical solutions are obtained.

Analysis of one dimensional flow in a non-uniform aquifer composed of two different regions separated by a linear vertical discontinuity has been made by Önder (1997). System is excited by a sudden rise or fall on the stream level. Analytical solutions allow the water level fluctuations in the aquifer and time dependent flow rate.

Flow in a composite aquifer formed by fractured rock and alluvial aquifer embedded in has been covered by Önder (1989). Alluvial formation is separated from fractured rock by a linear interface. Equations of flow have been analyzed for three separate regions of homogeneous nature considering double porosity concept. A numerical solution based on finite difference technique is used for the solution of these equations.

1.3 Objective of the Thesis

This thesis aims to find solutions for piezometric head of these formations using Laplace transform method and derive time dependent solutions by numerical inversion method of Stehfest.

The numerical inversion method by Stehfest algorithm is applied to various groundwater problems using subroutines developed in VBA Excel and compared with the available analytical solutions in the literature. The results of subroutine developed for composite aquifer with extreme fracture and blocks transmissivity are compared with the solutions of subroutines for finite aquifer of impervious and recharge boundaries to verify the methodology.

1.4 Description of the Thesis

This thesis is composed of six chapters.

Chapter 2 focuses on the theoretical background of groundwater problem together with the mathematical statement of the problem and assumptions considered in the study. Equations are converted to non-dimensional forms and Laplace transform is applied for the solutions. The methodology of numerical inversion for Laplace equations, Stehfest algorithm is presented.

Chapter 3 verifies the numerical inversion method for Laplace domain solutions. Groundwater problem for semi-infinite homogeneous aquifer under constant discharge which has already an analytical solution available in the literature is solved with the Laplace transform method and Stehfest's numerical inversion. A comparison of results between analytical and numerical methods is presented for the verification of the accuracy of the numerical method.

Chapter 4 involves the application of Stehfest algorithm in the parts of composite aquifer. Subroutines considering the interaction of all parts of

composite aquifer and stream are developed for piezometric heads and run for aquifer parameters that are representative for field data. Variations for dimensionless piezometric head with time and distance are presented by means of charts. Sensivity analyses on the aquifer parameters are made and comments are presented.

Chapter 5 is devoted to a further evaluation of the proposed methodology for composite aquifer. Derivations for finite aquifer with impervious and recharge boundaries on the right hand side are made in the same manner as composite aquifer .Subroutines for these cases are developed. Solutions of composite aquifer subroutine with appropriate adjustment of parameter are compared to finite aquifer solutions and comments are made.

Chapter 6 summarizes the work and conclusions for the thesis are presented in this chapter.

CHAPTER 2

MATHEMATICAL FORMULATION FOR THE FLOW IN COMPOSITE AQUIFER

2.1 Introductory Remarks

Fractured rock, which serves as a water bearing and transmitting unit, is a quite common type of formation encountered beneath the ground surface. It constitutes fracture networks and block matrices, forming a heterogeneous medium due to size and aquifer parameters variations among blocks and uneven distribution of fractures. The heterogeneity of the formation makes modeling of such aquifer very complex. Rather than these complex models in field, theoretical simplified models assuming regular fractured systems are preferable especially for large scale studies.

Barenblatt et al (1960) and Warren and Root (1963) used double porosity concept which assumes two media composed of fractures and blocks. System is characterized by ratios of aquifer parameters like conductivity, transmissivity and storage for each media. Fractures, discontinuities in the solid matrix, serve as high flow transmitting unit whereas porous blocks are considered as high storage units. Exchange of water from fractures to blocks or vice versa take place but no flow occurs between blocks. (Önder, 1998)

It is practically impossible to represent the flow through fractures, pores and openings due to complex geometry of fractured rock. In order to describe flow in this case, representative elementary volume approach is considered such that enough number of fractures and blocks are selected to illustrate flow region and aquifer properties such that including or deducting of elements do not change flow and aquifer properties in that volume. Representative elementary volume (REV) (Bear, 1972) concept enables to apply continuum principle throughout alluvium formation and the fractured rock.

2.2 Mathematical Formulation of the Problem

The idealized cross section of a composite aquifer is shown in Figure 2.1.

Aquifer

is composed of two regions:

- i) a strip of alluvium which has finite length of L in x direction and is made of granular unconsolidated formation.
- ii) a fractured rock adjacent to it and semi-infinite in areal extent.

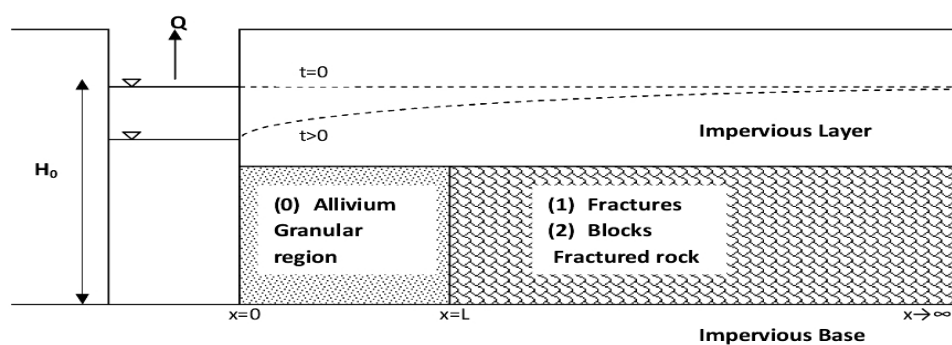


Figure 2.1: One dimensional transient flow in composite aquifer under constant pumping discharge rate, Q . Subscripts 0, 1 and 2 denote granular, fractures and block matrices, respectively.

For the mathematical formulation of the flow in the above aquifer, the following assumptions are considered.

2.2.1 Assumptions

1. Darcy's Law is valid for the flow in granular aquifer, fractures and blocks.
2. Constant aquifer thickness is assumed through the extent of granular aquifer and fractured rock.
3. Essentially horizontal flow occurs in x direction only and vertical component of flow is neglected.
4. All parts of composite aquifer are homogeneous and isotropic.
5. Stream-aquifer and granular aquifer-fractured rock interface form vertical boundary.
6. Composite aquifer is bounded by horizontal impermeable boundaries at the top and at the bottom.
7. Aquifer parameters are independent of time.
8. Stream fully penetrates the aquifer.
9. Flow through the aquifer is laminar.
10. Initial water level in composite aquifer and stream is parallel to the impermeable bottom layer so that initially there is no flow between the stream and the aquifer.
11. No chemical reaction occurs through the aquifer during groundwater flow.
12. Aquifer is non-leaky.
13. Skin effect in the vicinity of stream aquifer is neglected.
14. Water level at the initial instant is the same everywhere in aquifer and stream.

2.2.2 Governing Differential Equations

Conventionally, governing differential equation for the flow through porous medium is obtained by combining Darcy's law with the conservation of mass principle for the parts of composite aquifer. For granular region, basic groundwater equation for one dimensional flow may be obtained by combining Darcy's Law and continuity of fluid principle and expressed as (Bear, 1979):

$$T_0 \frac{\partial^2 h_0}{\partial x^2} = S_0 \frac{\partial h_0}{\partial t}, \quad 0 < x < L, \quad t > 0 \quad (2.1)$$

where

L is the length of granular aquifer along x-direction (flow direction).

T_0 is the coefficient of transmissivity of the granular aquifer.

S_0 is the coefficient of storage of the granular aquifer.

h_0 is the piezometric head in the granular aquifer.

x is the distance from stream-confined aquifer face along flow direction

t is the time.

For fractured rock, double porosity conceptual model, which assumes two overlapping media and a quasi-steady interchange of fluid between fractures and blocks, is applied to describe flow through the aquifer since these two zones have distinct hydraulic properties. Double porosity concept assumes flow between fractures and blocks, but no flow between blocks occurs. (Barenblatt et al., 1960). Two continuity equations for mass of fluid through blocks and fractures are derived each explaining the flow in fractures and blocks in its representative elementary volume and interaction with its surrounding medium.

By representative elementary volume approach, which considers sufficient blocks and fractures in a sample volume of interest such that absence of some

parts do not alter hydraulic properties, equations for fractures can be written as: (Önder,1989)

$$T_1 \frac{\partial^2 h_1}{\partial x^2} = S_1 \frac{\partial h_1}{\partial t} + v, L < x < \infty, t > 0 \quad (2.2)$$

where

v is the volume of water transfer per unit time from blocks to fractures per unit horizontal area along the depth of aquifer.

T_1 is the coefficient of transmissivity of the fractures.

S_1 is the coefficient of storage of the fractures.

h_1 is the piezometric head in the fractures.

and for blocks, equation of flow can be written as:

$$T_2 \frac{\partial^2 h_2}{\partial x^2} = S_2 \frac{\partial h_2}{\partial t} - v, L < x < \infty, t > 0 \quad (2.3)$$

where

T_2 is the coefficient of transmissivity of the blocks.

S_2 is the coefficient of storage of the blocks.

h_2 is the piezometric head in the blocks.

Quasi-steady interaction between fractures and block matrices is described as:

$$v = \varepsilon T_2 (h_1 - h_2), L < x < \infty, t > 0 \quad (2.4)$$

where

ε is a shape factor controlling the flow exchange through interporosity and it depends on fracture network and geometry of blocks which is mainly expressed in terms of cubical block length (Warren & Root, 1963; Zimmerman et al., 1993). Slightly different form of this expression is used earlier by Barenblatt et al. (1960), Streltsova (1976), Huyakorn and Pinder (1983) and Moench (1984).

Equation (2.4) relates the flow between fractures and blocks to the piezometric head difference between two media.

Transmissivity for blocks is much less important than its storage such that the term $T_2 \frac{\partial^2 h_2}{\partial x^2}$ is neglected and using equation (2.4), equations (2.3) and (2.4)

can be modified as:

$$S_2 \frac{\partial h_2}{\partial t} = \varepsilon T_2 (h_1 - h_2), \quad L < x < \infty, \quad t > 0 \quad (2.5)$$

$$T_1 \frac{\partial^2 h_1}{\partial x^2} = S_1 \frac{\partial h_1}{\partial t} + S_2 \frac{\partial h_2}{\partial t}, \quad L < x < \infty, \quad t > 0 \quad (2.6)$$

Equations (2.1), (2.5) and (2.6) are solved for unknown hydraulic heads of granular region, blocks and fractures.

2.2.3 Initial and Boundary Conditions

In this study, transient flow conditions for one dimensional flow for homogeneous and isotropic aquifer are considered; piezometric heads of each zone depend on space and time. Therefore, partial differential equations of flow should be provided with boundary and initial conditions (Önder, 1989):

$$h_0 = H_0, \quad 0 < x < L, \quad t = 0 \quad (2.7)$$

$$h_1 = H_0, \quad L < x < \infty, \quad t = 0 \quad (2.8)$$

$$h_2 = H_0, \quad L < x < \infty, \quad t = 0 \quad (2.9)$$

where

H_0 is the initial value of piezometric head in the entire composite aquifer at $t=0$.

Equations (2.7), (2.8) and (2.9) are initial conditions for the problem.

On the stream-aquifer boundary, specified flux condition may be written as:

$$\lim_{x \rightarrow 0} \frac{\partial h_0}{\partial x} = -\frac{Q}{2T_0}, \quad x=0, t>0 \quad (2.10)$$

where

Q is the volumetric discharge rate per unit length of stream-aquifer boundary.

The conditions on the right hand-side are:

$$h_1 = H_0, \quad x \rightarrow \infty, t>0 \quad (2.11)$$

$$h_2 = H_0, \quad x \rightarrow \infty, t>0 \quad (2.12)$$

The conditions at the surface separating two zones will be the following (Bear, 1979):

1. The piezometric head on each side of the interface remain equal for all times.

$$h_0 = h_1, \quad x=L, t>0 \quad (2.13)$$

2. Flow rate from one zone into another will always be equal.

$$K_0 \frac{\partial h_0}{\partial x} = K_1 \frac{\partial h_1}{\partial x}, \quad x=L, t>0 \quad (2.14)$$

where

K_0 is the coefficient of hydraulic conductivity of the granular aquifer.

K_1 is the coefficient of hydraulic conductivity of the fractures.

In equation (2.14), it has to be underlined that conducting capability of blocks is neglected. In other words, no flow between granular aquifer and blocks of fractured aquifer occurs.

2.3 Non-Dimensional Forms of Equations

To represent the numerical solutions of particular partial differential equations of flow graphically and use the results for comparison, the governing equations of flow, initial and boundary conditions are converted to non-dimensional forms.

In order to non-dimensionalize the equations from (2.1) to (2.14), some dimensionless variables are defined as (Önder,1989):

$$z_0 = \frac{h_0 - H_0}{H_0} \quad (2.15)$$

$$z_1 = \frac{h_1 - H_0}{H_0} \quad (2.16)$$

$$z_2 = \frac{h_2 - H_0}{H_0} \quad (2.17)$$

where

z_0 is the dimensionless piezometric head of the granular aquifer.

z_1 is the dimensionless piezometric head of the fractures.

z_2 is the dimensionless piezometric head of the blocks.

$$y = \frac{x}{L} \quad (2.18)$$

where

y denotes dimensionless distance along flow direction.

$$\theta = \frac{T_0 t}{S_0 L^2} \quad (2.19)$$

where

θ denotes dimensionless time.

In addition, the following dimensionless quantities are defined as:

$$\lambda_1 = \frac{T_1}{T_0} = \frac{bK_0}{bK_1} \quad (2.20)$$

$$\lambda_2 = \frac{T_2}{T_0} = \frac{bK_2}{bK_0} \quad (2.21)$$

$$\eta_1 = \frac{S_1}{S_0} \quad (2.22)$$

$$\eta_2 = \frac{S_2}{S_0} \quad (2.23)$$

$$\delta_2 = \varepsilon L^2 \frac{\lambda_2}{\eta_2} \quad (2.24)$$

where

b is the thickness of confined aquifer.

λ_1 is the transmissivity ratio of the fractures to the granular aquifer.

λ_2 is the transmissivity ratio of the blocks to the granular aquifer.

K_2 is the coefficient of hydraulic conductivity of the blocks.

η_1 is the storage coefficient ratio of the fractures to the granular aquifer.

η_2 is the storage coefficient ratio of the blocks to the granular aquifer.

δ_2 is a dimensionless constant relating granular aquifer length, shape factor, coefficient ratio and transmissivity ratios of the blocks to the granular aquifer.

Inserting equations (2.15) to (2.24) into equations (2.1), (2.5) and (2.6) give non-dimensional form of governing groundwater equations as:

$$\frac{\partial^2 z_0}{\partial y^2} = \frac{\partial z_0}{\partial \theta}, \quad 0 < y < 1, \quad \theta > 0 \quad (2.25)$$

$$\frac{\partial^2 z_1}{\partial y^2} = \frac{\eta_2}{\lambda_1} \frac{\partial z_2}{\partial \theta} + \frac{\eta_1}{\lambda_1} \frac{\partial z_1}{\partial \theta}, \quad y > 1, \quad \theta > 0 \quad (2.26)$$

$$\frac{\partial z_2}{\partial \theta} = \delta_2 (z_1 - z_2), \quad y > 1, \quad \theta > 0 \quad (2.27)$$

Initial conditions in granular aquifer, fractures and blocks in composite aquifer are derived as:

$$z_0 = 0, \quad 0 < y < 1, \quad \theta = 0 \quad (2.28)$$

$$z_1 = 0, \quad 1 < y < \infty, \quad \theta = 0 \quad (2.29)$$

$$z_2 = 0, \quad 1 < y < \infty, \quad \theta = 0 \quad (2.30)$$

At the stream-granular aquifer interface, dimensionless boundary condition is stated in terms of dimensionless discharge, Q_b , as:

$$\lim_{y \rightarrow 0} \frac{\partial z_0}{\partial y} = -Q_b, \quad y = 0, \quad \theta > 0 \quad (2.31)$$

where

$$Q_b = \frac{QL}{2T_0 H_0}$$

Boundary conditions at the interface are expressed in dimensionless form as:

$$z_0 = z_1, \quad y = 1, \quad \theta > 0 \quad (2.32)$$

$$\frac{\partial z_0}{\partial y} = \lambda_1 \frac{\partial z_1}{\partial y}, \quad y = 1, \quad \theta > 0 \quad (2.33)$$

Dimensionless boundary conditions for semi-infinite fractured rock at infinity are expressed as:

$$z_1 = 0, y \rightarrow \infty, \theta > 0 \quad (2.34)$$

$$z_2 = 0, y \rightarrow \infty, \theta > 0 \quad (2.35)$$

2.4 Solutions of Dimensionless Groundwater Flow Equations by Laplace Transform Method

2.4.1 Laplace Transforms

One-dimensional transient groundwater flow in composite aquifer composed of alluvium (granular), fractures and blocks is analyzed in this study by partial differential groundwater equations with corresponding initial and boundary conditions. Transient flow states the unsteady flow conditions therefore flow in the composite aquifer is function of space and time. In order to simplify the complexity of groundwater equations due to time derivative, Laplace transform is a common method in the solution of groundwater flow problems. Laplace transform technique converts the partial differential equations of groundwater flow in composite aquifer into ordinary differential equations by eliminating the time component and these equations become easier to solve.

Laplace transform of a function $u(t)$ defined for $t \geq 0$ is obtained by multiplying the function $u(t)$ by e^{-pt} and integrating this multiplication with respect to time t from $t=0$ to $t=\infty$. This integration yields a function that is only dependent on Laplace parameter p , $\bar{u}(p)$ and it is called as Laplace transform of $u(t)$. Expression for $\bar{u}(p)$ is given as:

$$\bar{u}(p) = \int_0^{\infty} u(t)e^{-pt} dt \quad (2.36)$$

Some basic properties of Laplace transforms which are commonly used in this study are given below; (Edwards & Penney, 2004)

- 1) Linearity of Laplace transforms: If A is a constant, then the Laplace transform of $Au(t)$ is $A\bar{u}(p)$.
- 2) Laplace transform of derivative $\frac{du}{dt}$ is $p\bar{u}(p) - u(0)$.
- 3) Laplace Transform of a constant A is A/p .
- 4) If u is a function of time, t and space, x then the Laplace transform of derivative with respect to space component $\frac{\partial^n u}{\partial x^n}$ is $\frac{\partial^n \bar{u}}{\partial x^n}$.

2.4.2 Laplace Transforms of Non-Dimensional Equations, Initial and Boundary Conditions

Non-dimensional forms of governing groundwater equations are converted to Laplace domain to eliminate complexities due to time derivative. Equations for composite aquifer are transferred to Laplace domain for alluvium (granular aquifer), blocks and fractures denoted by 0, 1, 2 subscripts respectively.

Recalling non-dimensional form of groundwater equation for alluvial region is given in equation (2.25) as:

$$\frac{\partial^2 z_0}{\partial y^2} = \frac{\partial z_0}{\partial \theta}, \quad 0 < y < 1, \quad \theta > 0 \quad (2.25)$$

Applying Laplace transform to granular aquifer groundwater flow equation given in (2.25) yields:

$$\frac{\partial^2 \bar{z}_0}{\partial y^2} = p\bar{z}_0 - z_0(y, 0) \quad (2.37)$$

where

\bar{z}_0 is the dimensionless piezometric head of the granular aquifer in Laplace domain.

Substitution of initial condition given in equation (2.28) into (2.37) results:

$$\frac{\partial^2 \bar{z}_0}{\partial y^2} = p \bar{z}_0 \quad (2.38)$$

General solution for equation (2.38) is:

$$\bar{z}_0 = Ae^{-\sqrt{p}y} + Be^{\sqrt{p}y} \quad (2.39)$$

where A and B are constants of integration. In order to compute A and B in equation (2.38), boundary conditions for granular aquifer are used.

Laplace transforms for boundary conditions given in equations (2.31), (2.32) and (2.33) yield respectively as:

$$\lim_{y \rightarrow 0} \frac{\partial \bar{z}_0}{\partial y} = -\frac{Q_b}{p}, \quad y=0, \quad \theta > 0 \quad (2.40)$$

$$\bar{z}_0 = \bar{z}_1, \quad y=1, \quad \theta > 0 \quad (2.41)$$

$$\frac{\partial \bar{z}_0}{\partial y} = \lambda_1 \frac{\partial \bar{z}_1}{\partial y}, \quad y=1, \quad \theta > 0 \quad (2.42)$$

where

\bar{z}_1 is the dimensionless piezometric head of the fractures in Laplace domain.

Equation (2.39) is differentiated with respect to space variable, y as:

$$\frac{\partial \bar{z}_0}{\partial y} = -A\sqrt{p}e^{-\sqrt{p}y} + B\sqrt{p}e^{\sqrt{p}y} \quad (2.43)$$

As y approaches to zero, equation (2.43) becomes:

$$\lim_{y \rightarrow 0} \frac{\partial \bar{z}_0}{\partial y} = -A\sqrt{p} + B\sqrt{p} \quad (2.44)$$

Equation (2.44) is equated to boundary condition given in equation (2.40) then the relation between coefficients of integration A and B is obtained as:

$$A - B = \frac{Q_b}{p\sqrt{p}} \quad (2.45)$$

Other boundary conditions in Laplace parameters stated with equations (2.40) and (2.41) depend on \bar{z}_1 at the interface of the granular region and fracture-block formation when $y=1$. Equation (2.26) is transformed respectively to Laplace forms as:

$$\frac{\partial^2 \bar{z}_1}{\partial y^2} = \frac{\eta_2}{\lambda_1} (p\bar{z}_2 - z_2(y, 0)) + \frac{\eta_1}{\lambda_1} (p\bar{z}_1 - z_1(y, 0)) \quad (2.46)$$

Applying initial conditions given in equations (2.29) and (2.30) for blocks and fractures to equation (2.46) yields:

$$\frac{\partial^2 \bar{z}_1}{\partial y^2} = \frac{\eta_2}{\lambda_1} p\bar{z}_2 + \frac{\eta_1}{\lambda_1} p\bar{z}_1 \quad (2.47)$$

where

\bar{z}_2 is the dimensionless piezometric head of the blocks in Laplace parameters.

Similarly, Laplace transform is applied to equation (2.27) as:

$$p\bar{z}_2 - z_2(y, 0) = \delta_2 (\bar{z}_1 - \bar{z}_2) \quad (2.48)$$

Substitution of initial condition in (2.30) to equation (2.48) yields:

$$\bar{z}_2 = \frac{\delta_2}{p + \delta_2} \bar{z}_1 \quad (2.49)$$

Combining equations (2.49) and (2.47) yields an expression for \bar{z}_1 as:

$$\frac{\partial^2 \bar{z}_1}{\partial y^2} - \left(\frac{\eta_2}{\lambda_1} \frac{\delta_2}{p + \delta_2} p + \frac{\eta_1}{\lambda_1} p \right) \bar{z}_1 = 0 \quad (2.50)$$

General solution for differential equation (2.50) is given as:

$$\bar{z}_1 = C e^{-\sqrt{\frac{\eta_2}{\lambda_1} \frac{\delta_2}{p + \delta_2} p + \frac{\eta_1}{\lambda_1} p} y} + D e^{\sqrt{\frac{\eta_2}{\lambda_1} \frac{\delta_2}{p + \delta_2} p + \frac{\eta_1}{\lambda_1} p} y} \quad (2.51)$$

where

C and D are coefficients of integration.

Applying boundary condition in equation (2.34) to (2.51) returns D=0 as y goes to infinity and expression given in (2.51) yields:

$$\bar{z}_1 = C e^{-\sqrt{\frac{\eta_2}{\lambda_1} \frac{\delta_2}{p + \delta_2} p + \frac{\eta_1}{\lambda_1} p} y} \quad (2.52)$$

Combination of equations (2.49) and (2.52) yields a general expression for \bar{z}_2

$$\bar{z}_2 = \frac{p}{p + \delta_2} C e^{-\sqrt{\frac{\eta_2}{\lambda_1} \frac{\delta_2}{p + \delta_2} p + \frac{\eta_1}{\lambda_1} p} y} \quad (2.53)$$

To evaluate constant C in equation (2.52), boundary conditions given in equations (2.41), (2.42) and the derivative given by (2.43) at the interface for \bar{z}_1 are needed. Equating equation (2.39), the general expression for \bar{z}_0 and equation (2.52), the general expression for \bar{z}_1 at the interface $y=1$ as given in equation (2.41) return:

$$A e^{-\sqrt{p}} + B e^{\sqrt{p}} = C e^{-\sqrt{\frac{\eta_2}{\lambda_1} \frac{\delta_2}{p + \delta_2} p + \frac{\eta_1}{\lambda_1} p}} \quad (2.54)$$

Boundary condition at the interface $y=1$ is given in equation (2.42). To evaluate this equation, derivative of \bar{z}_1 with respect to y is obtained from equation (2.52) as:

$$\frac{\partial \bar{z}_1}{\partial y} = -C \sqrt{\frac{\eta_2}{\lambda_1} \frac{\delta_2}{p + \delta_2} p + \frac{\eta_1}{\lambda_1}} p e^{-\sqrt{\frac{\eta_2}{\lambda_1} \frac{\delta_2}{p + \delta_2} p + \frac{\eta_1}{\lambda_1}} p y} \quad (2.55)$$

Using the derivative of \bar{z}_0 given in equation (2.43) and equation (2.55) in the boundary condition (2.42), at $y=1$, yield:

$$A e^{-\sqrt{p}} - B e^{\sqrt{p}} = -C \lambda_1 \sqrt{\frac{\eta_2}{\lambda_1} \frac{\delta_2}{p + \delta_2} p + \frac{\eta_1}{\lambda_1}} p e^{-\sqrt{\frac{\eta_2}{\lambda_1} \frac{\delta_2}{p + \delta_2} p + \frac{\eta_1}{\lambda_1}} p} \quad (2.56)$$

Substitution of equation (2.54) to the right side of equation (2.56) for the term

$C e^{-\sqrt{\left(\frac{\eta_2}{\lambda_1} \frac{\delta_2}{p + \delta_2} + \frac{\eta_1}{\lambda_1}\right) p}}$ returns the relation between coefficients A and B as:

$$A = B e^{2\sqrt{p}} \frac{1 + \sqrt{\eta_2 \frac{\delta_2}{p + \delta_2} \lambda_1 + \eta_1 \lambda_1}}{1 - \sqrt{\eta_2 \frac{\delta_2}{p + \delta_2} \lambda_1 + \eta_1 \lambda_1}} \quad (2.57)$$

Equation (2.57) is put in the equation (2.44) to obtain an expression for coefficient B and this operation results:

$$B = \frac{\frac{Q_b}{p\sqrt{p}}}{-1 + e^{2\sqrt{p}} \frac{1 + \sqrt{\eta_2 \frac{\delta_2}{p + \delta_2} \lambda_1 + \eta_1 \lambda_1}}{1 - \sqrt{\eta_2 \frac{\delta_2}{p + \delta_2} \lambda_1 + \eta_1 \lambda_1}}} \quad (2.58)$$

In order to find the relation between coefficients of integration B and C, equation (2.58) is inserted into equation (2.56) and this substitution yields:

$$A = \frac{Q_b}{p\sqrt{p}} e^{2\sqrt{p}} \frac{1 + \sqrt{\eta_2 \frac{\delta_2}{p + \delta_2} \lambda_1 + \eta_1 \lambda_1}}{\sqrt{\eta_2 \frac{\delta_2}{p + \delta_2} \lambda_1 + \eta_1 \lambda_1 (e^{2\sqrt{p}} + 1) + e^{2\sqrt{p}} - 1}} \quad (2.59)$$

$$C = e^{-\sqrt{p}} e^{\sqrt{\frac{\eta_2}{\lambda_1} \frac{\delta_2}{p + \delta_2} p + \frac{\eta_1}{\lambda_1} p}} \left(\frac{Q_b}{p\sqrt{p}} + B(1 + e^{2\sqrt{p}}) \right) \quad (2.60)$$

Substitution of equation (2.58) into (2.60) returns coefficient C as:

$$C = 2 \frac{Q_b}{p\sqrt{p}} e^{\sqrt{p}} \frac{e^{\sqrt{\left(\frac{\eta_2}{\lambda_1} \frac{\delta_2}{p + \delta_2} + \frac{\eta_1}{\lambda_1}\right) p}}}{-1 + e^{2\sqrt{p}} + \left(\eta_2 \frac{\delta_2}{p + \delta_2} \lambda_1 + \eta_1 \lambda_1\right) (1 + e^{2\sqrt{p}})} \quad (2.61)$$

Equations (2.58), (2.59) and (2.61) are inserted to expressions of piezometric heads in Laplace parameters for \bar{z}_0 , \bar{z}_1 and \bar{z}_2 given in general forms with differential equations (2.39), (2.52), (2.53) respectively. These substitutions yield:

$$\bar{z}_0 = \frac{Q_b}{p\sqrt{p}} e^{2\sqrt{p}} \frac{(1 + \sqrt{\eta_2 \frac{\delta_2}{p + \delta_2} \lambda_1 + \eta_1 \lambda_1}) e^{-p\sqrt{y}}}{\sqrt{\eta_2 \frac{\delta_2}{p + \delta_2} \lambda_1 + \eta_1 \lambda_1 (e^{2\sqrt{p}} + 1) + e^{2\sqrt{p}} - 1}} + \frac{e^{p\sqrt{y}} \frac{Q_b}{p\sqrt{p}}}{-1 + e^{2\sqrt{p}} \frac{1 + \sqrt{\eta_2 \frac{\delta_2}{p + \delta_2} \lambda_1 + \eta_1 \lambda_1}}{1 - \sqrt{\eta_2 \frac{\delta_2}{p + \delta_2} \lambda_1 + \eta_1 \lambda_1}}} \quad (2.62)$$

$$\bar{z}_1 = 2 \frac{Q_b}{p\sqrt{p}} e^{\sqrt{p}} \frac{e^{\sqrt{\left(\frac{\eta_2}{\lambda_1} \frac{\delta_2}{p + \delta_2} + \frac{\eta_1}{\lambda_1}\right) p}}}{-1 + e^{2\sqrt{p}} + \left(\eta_2 \frac{\delta_2}{p + \delta_2} \lambda_1 + \eta_1 \lambda_1\right) (1 + e^{2\sqrt{p}})} e^{-\sqrt{\frac{\eta_2}{\lambda_1} \frac{\delta_2}{p + \delta_2} p + \frac{\eta_1}{\lambda_1} p} y} \quad (2.63)$$

$$\bar{z}_2 = 2 \frac{Q_b}{p\sqrt{p}} e^{\sqrt{p}} \frac{\delta_2}{p + \delta_2} \frac{e^{\sqrt{\left(\frac{\eta_2}{\lambda_1} \frac{\delta_2}{p + \delta_2} + \frac{\eta_1}{\lambda_1}\right) p}}}{-1 + e^{2\sqrt{p}} + \left(\eta_2 \frac{\delta_2}{p + \delta_2} \lambda_1 + \eta_1 \lambda_1\right) (1 + e^{2\sqrt{p}})} e^{-\sqrt{\frac{\eta_2}{\lambda_1} \frac{\delta_2}{p + \delta_2} p + \frac{\eta_1}{\lambda_1} p} y} \quad (2.64)$$

2.5 Stehfest Algorithm for Numerical Inversion

Unsteady flow equations of groundwater flow have been simplified by Laplace transforms where the time derivatives due to transient flow conditions are eliminated and concern is given only to space derivative component. This results

in a set of coupled ordinary differential equations which are solved in the Laplace domain. In order to invert Laplace solutions of groundwater equations to real time domain, numerical inversion techniques are utilized as an effective and rather simple method than complex integration requiring advanced mathematical operations.

For this purpose, one of the best known and applied numerical inversion techniques, Stehfest algorithm (Stehfest, 1970) is utilized in this thesis. Mathematical models of Stehfest algorithm are based on Laplace transforms $F(p)$ of groundwater function, $f(t)$. (Moench and Ogata, 1982). Hence, for prescribed Laplace transform $\bar{u}(x, p)$, its inverse $u(x, t)$ is computed from:

$$u_n(x, t) \approx \frac{\ln 2}{t} \sum_{i=1}^N V_i \bar{u}\left(x, i \frac{\ln 2}{t}\right) \quad (2.65)$$

where

i is the summation index.

Subscript n of $u_n(x, t)$ indicates that the inverse transformation is achieved by numerical method introduced by Stehfest (1970).

Laplace parameter, p is replaced by $i \frac{\ln 2}{t}$. Coefficient V_i is expressed in summation notation as:

where

$$V_i = (-1)^{i + \frac{N}{2}} \sum_{k=\text{Int}(\frac{i+1}{2})}^{\min(i, \frac{N}{2})} \frac{k^{\frac{N}{2}} (2k)!}{(\frac{N}{2} - k)! k! (k-1)! (i-k)! (2k-1)!} \quad (2.66)$$

N is the number of terms in Stehfest algorithm.

k is the integer part of $\frac{i+1}{2}$.

Theory states that the larger terms of N returns the more accurate solutions. In practice, rounding errors gives unsatisfactory results for large N values due to greater absolute values of V_i (Stehfest, 1970). As the significant figures used in the computation, accuracy increases for given N . Rate of convergence and results should be checked for different values of N when accuracy is fixed and computation should be continued until satisfactory results are obtained with smooth convergence to solution. No accurate results are obtained if $u(t)$ has discontinuity near t .

In this thesis, different trials for N are executed and results of each trial are compared to exact solutions of sample problem to check the closeness of numerical solution for given N with the analytical solution and appropriate number value, N , is selected after this comparison.

In order to invert Laplace transform solutions for dimensionless head of granular aquifer, fractures and blocks, equations (2.62), (2.63) and (2.64) are substituted respectively into Stehfest algorithm in equation (2.65) and formulations for dimensionless head in real time domain are obtained as:

$$z_0(y, \theta) \approx \frac{\ln 2}{\theta} \sum_{i=1}^N V_i \bar{z}_0(y, i \frac{\ln 2}{\theta}) \quad (2.67)$$

$$z_1(y, \theta) \approx \frac{\ln 2}{\theta} \sum_{i=1}^N V_i \bar{z}_1(y, i \frac{\ln 2}{\theta}) \quad (2.68)$$

$$z_2(y, \theta) \approx \frac{\ln 2}{\theta} \sum_{i=1}^N V_i \bar{z}_2(y, i \frac{\ln 2}{\theta}) \quad (2.69)$$

CHAPTER 3

TEST OF STEHFEST ALGORITHM IN GROUNDWATER PROBLEMS

3.1 Introductory Remarks

The purpose of this chapter is to verify and test the application of Stehfest's numerical inversion technique in groundwater flow problems. The exact analytical solution for one dimensional transient flow in a semi-infinite homogeneous aquifer under constant discharge is available in the literature and the case is also solved by using Stehfest algorithm. Comparison between these two is made to validate the accuracy of numerical solution by Stehfest algorithm. The objective also includes the determination of the best value for N, the number of terms in Stehfest algorithm.

3.2 One Dimensional Transient Flow in a Semi-Infinite Homogeneous Aquifer under Constant Discharge

Groundwater flow equation for one dimensional unsteady flow in a homogeneous aquifer is already given in equation (2.1). In a slightly different form it may be expressed as (Bear, 1979):

$$\frac{\partial^2 h}{\partial x^2} = \frac{1}{v} \frac{\partial h}{\partial t} \quad (3.1)$$

where

h is the piezometric head measured from the initial water surface in the stream.

ν is the hydraulic diffusivity and it is defined as:

$$\nu = \frac{T}{S}$$

where

T is the transmissivity coefficient.

S is the storage coefficient.

Initial condition is given as:

$$h = 0, t=0 \tag{3.2}$$

Boundary conditions for this case are stated as follows:

$$\frac{\partial h}{\partial x} = -\frac{Q}{2T}, x=0 \tag{3.3}$$

$$h = 0, x \rightarrow \infty \tag{3.4}$$

Governing differential equation, initial condition and boundary conditions are transformed to Laplace to eliminate time derivative as carried out in the previous chapter. Laplace transform of equation (3.1) is:

$$\frac{\partial^2 \bar{h}}{\partial x^2} = \frac{p\bar{h}}{\nu} - \frac{h(x,0)}{\nu} \tag{3.5}$$

where

\bar{h} is the piezometric head in Laplace domain.

and

$$\bar{h} = \bar{h}(x, p)$$

Inserting initial condition (3.2) into (3.5) results:

$$\frac{\partial^2 \bar{h}}{\partial x^2} = \frac{p\bar{h}}{v} \quad (3.6)$$

General solution for equation (3.6) is given as:

$$\bar{h}(x, p) = Me^{-\sqrt{\frac{p}{v}}x} + Ne^{\sqrt{\frac{p}{v}}x} \quad (3.7)$$

where

M and N are coefficients of integration.

In order to find coefficients M and N in equation (3.7), boundary conditions given in equations (3.3) and (3.4) are transformed to Laplace domain as:

$$\frac{\partial \bar{h}}{\partial x} = -\frac{Q}{2Tp}, x=0 \quad (3.8)$$

where

Q is the volumetric discharge rate per unit length of stream-aquifer boundary.

$$\bar{h} = 0, x \rightarrow \infty \quad (3.9)$$

Equations (3.8) and (3.9) are substituted into equation (3.7) and coefficients are found as:

$$M = \frac{Q_d v^{0.5}}{2p^{1.5}} \quad (3.10)$$

$$N = 0 \quad (3.11)$$

Q_d is dimensionless discharge defined as:

$$Q_d = \frac{Q}{T}$$

With coefficients M and N given in equations (3.10) and (3.11) respectively, equation (3.7), the solution for piezometric head in Laplace domain, is expressed as:

$$\bar{h}(x, p) = \frac{Q_d v^{0.5}}{2p^{1.5}} e^{-\sqrt{\frac{p}{v}}x} \quad (3.12)$$

Numerical inversion method, the Stehfest algorithm is applied to Laplace domain solution for piezometric head given in equation (3.12) and converted to real time domain. This conversion to Stehfest algorithm is given as:

$$h_n(x, t) \approx \frac{\ln 2}{t} \sum_{i=1}^N V_i \bar{h}(x, i \frac{\ln 2}{t}) \quad (3.13)$$

where

h_n is real time solution for piezometric head.

In the literature, analytical solution for one dimensional transient flow in homogeneous semi-infinite aquifer under constant prescribed discharge is given as (Carslaw and Jaeger, 1959):

$$h_a(x, t) = \frac{Q_d}{2} \left\{ -x + \sqrt{\frac{4tv}{\pi}} e^{-\frac{x^2}{4tv}} + x \operatorname{erf} \left(\sqrt{\frac{x^2}{4tv}} \right) \right\} \quad (3.14)$$

where

h_a is the analytical solution for piezometric head.

Table 3.1 provides the expression for the piezometric head. As stated earlier, the objective in this chapter is to compare $h_a(x, t)$ and $h_n(x, t)$.

Table 3.1: Summary of equations used in the analysis of flow in semi-infinite homogeneous aquifer under constant discharge.

	Symbols for piezometric head	Equations of piezometric head
Analytical solution for piezometric head	$h_a(x, t)$	$h_a(x, t) = \frac{Q_d}{2} \left\{ \sqrt{\frac{4tv}{\pi}} e^{-\frac{x^2}{4tv}} + \text{xerf} \left(\sqrt{\frac{x^2}{4tv}} \right) - x \right\}$
Solution on Laplace domain for piezometric head	$\bar{h}_n(x, p)$	$\bar{h}(x, p) = \frac{Q_d v^{0.5}}{2p^{1.5}} e^{-\sqrt{\frac{p}{v}} x}$
Numerical inversion of Laplace transform for piezometric head	$h_n(x, t)$	$h_n(x, t) \approx \frac{\ln 2}{t} \sum_{i=1}^N V_i \bar{h}(x, i \frac{\ln 2}{t})$

3.3 Sensivity Analysis of N Values on the Numerical Solution

In equation (3.13), question about finding correct N value arises. For this reason, several runs by Stehfest algorithm are performed using different values of N. Table 3.2 below illustrates results when $\nu = 0.2$, $Q_d = 0.05$, $x = 300\text{m}$, $t = 500000$ seconds. As it is obvious from the results, for values N=8 to N=26 numerical inversion method by Stehfest algorithm gives nearly close values to exact analytical solutions verifying that methodology of Stehfest algorithm is sufficiently accurate for the groundwater problem described above.

In the literature, there are numerous examples for the application of Stehfest algorithm to groundwater problems such as Moench (1984), Chen (1985), Chen et al. (1993) and Dündar (2005).

Table 3.2: Outputs of exact analytical solution vs. numerical solution using Stehfest algorithm for different values of N for $\nu = 0.2$, $Q_d = 0.05$ $x = 300\text{m}$, $t = 500000$ seconds (139 hours).

Analytical Solution, h_a (m)	Numerical Solution, h_n (m) Using Stehfest Algorithm	
$h_a = 3.355748\text{ m}$	n=2	6.421130
	n=4	3.480190
	n=6	3.362071
	n=8	3.354915
	n=10	3.354329
	n=12	3.354357
	n=20	3.354369
	n=26	3.357080
	n=28	2.873333
	n=30	4.215606
	n=48	-3412268127712.720000

Value of N is selected as 8 due to the closeness of numerical solution at this value, however various runs demonstrate that up to N=26, the values obtained

by this method give acceptable results in 0.001 precision as can be seen in Table 3.2. As it can be observed from Figure 3.1 through and Figure 3.4, outputs for smaller N values than N=8 are deviating from analytical solution and therefore they are not considered acceptable due to the fact that accuracy increases as N increases however, as illustrated in Figure 3.3 and Figure 3.4, for N=26 and larger values deviations from analytical solutions again start and outputs of

Stehfest algorithm becomes unrealistic due to truncation errors in computation. Subroutine in VBA Excel to solve Stehfest algorithm for semi infinite homogeneous aquifers under constant discharge is given in Appendix A.

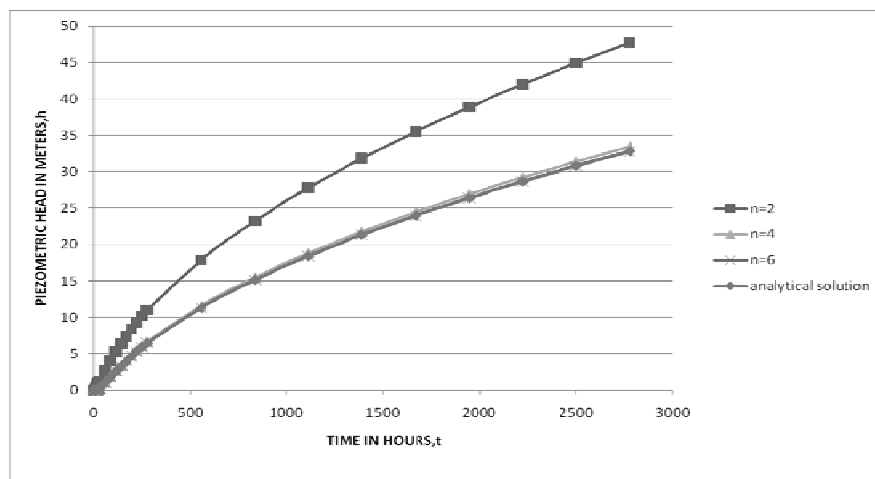


Figure 3.1: Piezometric head vs. time at $x=300$ m for values of N up to 6

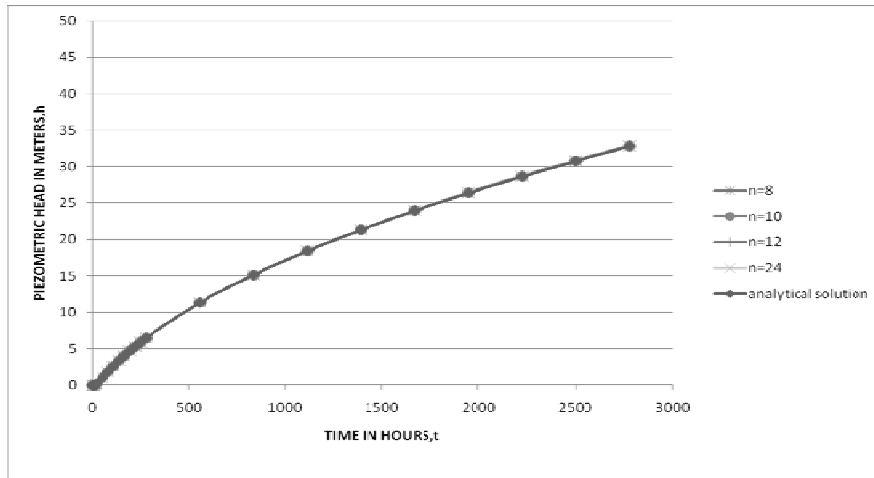


Figure 3.2: Piezometric head vs. time at $x=300$ m for values of $N = 8, 10, 12, 24$

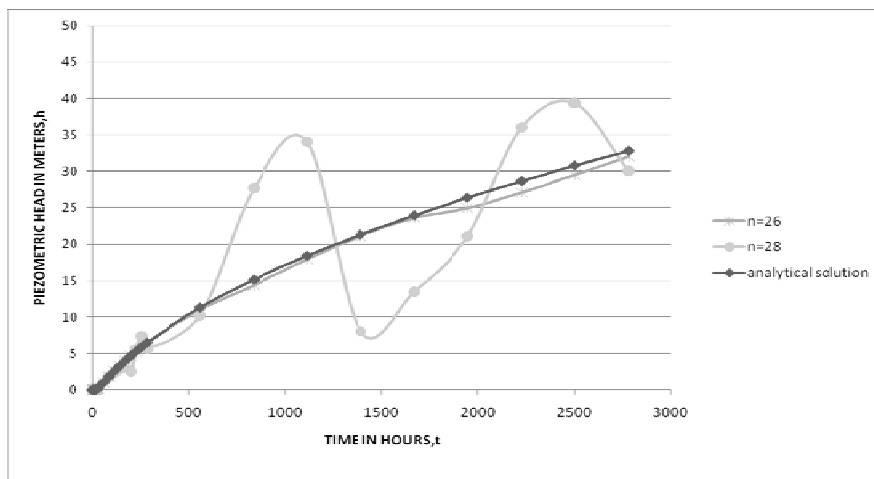


Figure 3.3: Piezometric head vs. time at $x=300$ m for values of $N=26$ and $N=28$

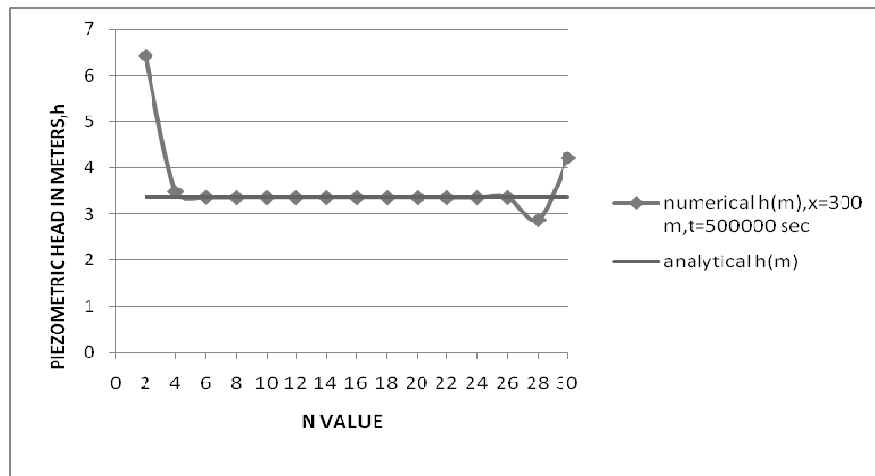


Figure 3.4: Piezometric head of numerical and analytical solutions vs. N at $x=300$ m, $t=500000$ secs (139 hrs)

3.4 Analytical and Numerical Solutions for Piezometric Head

3.4.1 Variation of piezometric head with time

From Figure 3.5 to Figure 3.7, the variations of piezometric head with time are presented for a series of distance. Figure 3.5 illustrates the time variation of piezometric head obtained by numerical solution proposed by Stehfest (1970) whereas Figure 3.6 illustrates the analytical solution of piezometric head variation with time. In Figure 3.7, these two solution methods are compared at $x=300$ m.

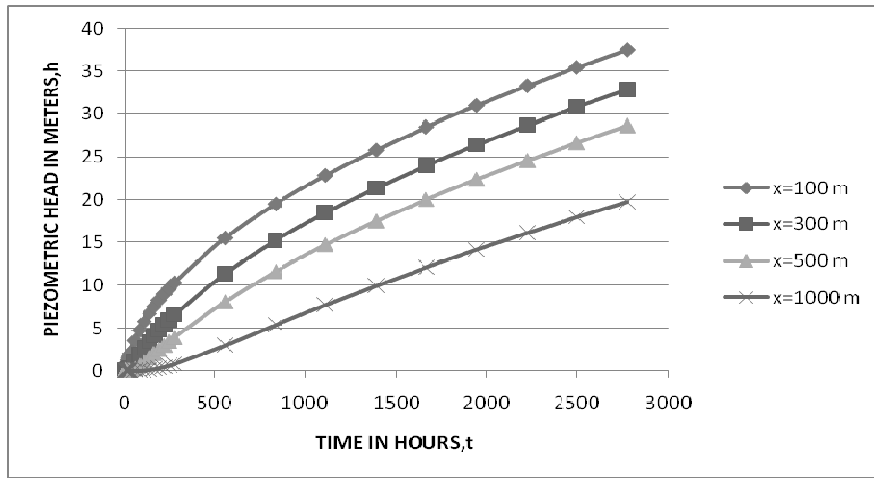


Figure 3.5: Numerical solution of piezometric head vs. time for different values of distance.

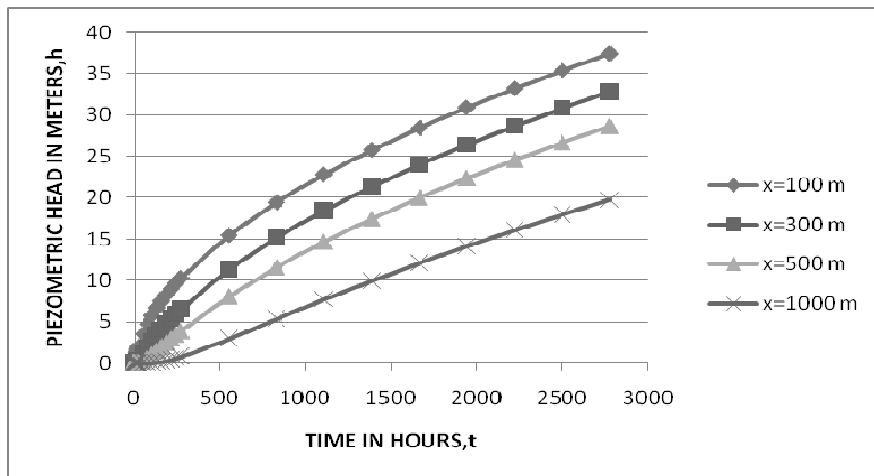


Figure 3.6: Analytical solution of piezometric head vs. time for different values of distance.

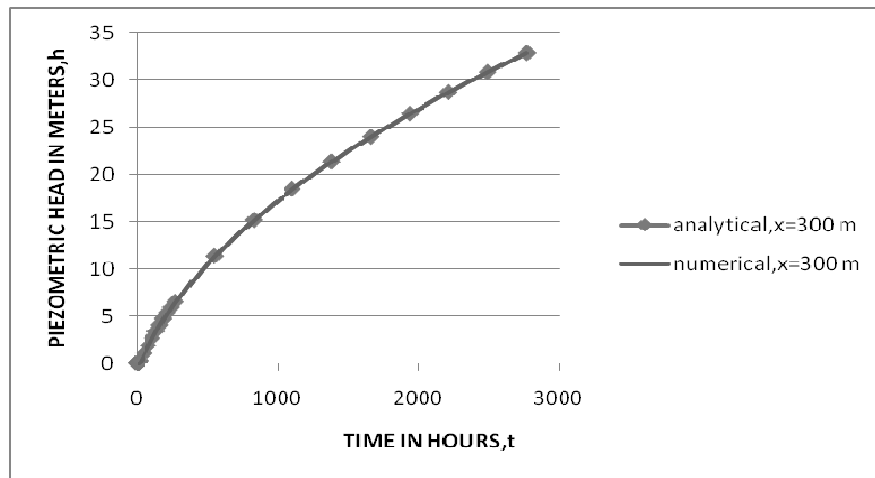


Figure 3.7: Numerical and analytical solutions of piezometric head vs. time at $x=300$ m.

3.4.2 Variation of piezometric head with time

From Figure 3.8 to Figure 3.10, the variations of piezometric head with distance are presented for a series of time. Figure 3.8 illustrates the distance variation of piezometric head obtained by numerical solution proposed by Stehfest (1970) whereas Figure 3.9 illustrates the analytical solution of piezometric head variation with distance. In Figure 3.10, these two solution methods are compared at $t=90000$ sec (25 hrs).

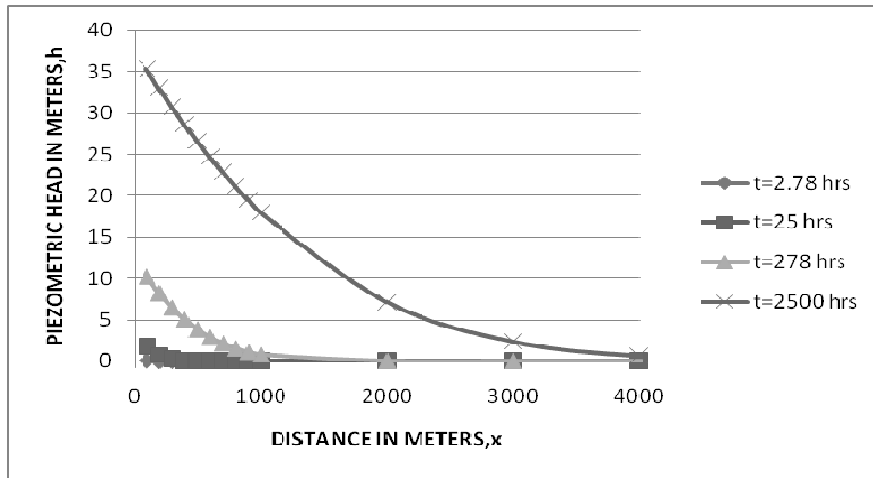


Figure 3.8: Numerical solution of piezometric head vs. distance in meters for different values of time.

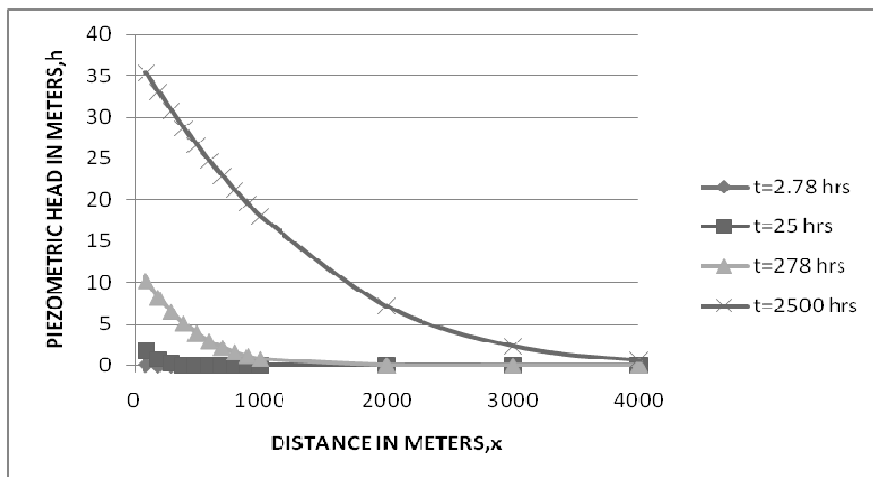


Figure 3.9: Analytical solution of piezometric head vs. distance in meters for different values of time.

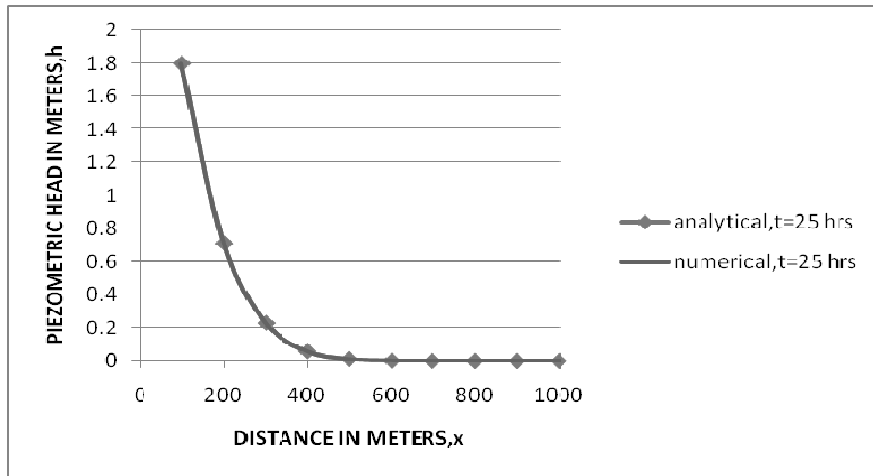


Figure 3.10: Numerical and analytical solutions of piezometric head vs. distance in meters at $t=90000$ sec.

3.5 Concluding Remarks

From Figure 3.7 and Figure 3.10, it can be inferred that outputs of Stehfest algorithm for piezometric head are identical to analytical solutions. The results prove that this numerical inversion method provides a powerful tool to compute groundwater equations.

CHAPTER 4

APPLICATION OF STEHFEST ALGORITHM TO COMPOSITE AQUIFERS

4.1 Application Methodology

Groundwater flow equations with corresponding initial and boundary conditions for granular aquifer, fractures and blocks are derived and converted to non dimensional forms in order to represent outputs in graphical forms independent of system characteristics of each problem. Laplace domain solutions are transformed by an appropriate numerical inversion method, Stehfest algorithm to obtain real time solutions for piezometric head of granular aquifer, fractures and blocks as explained in equations (2.67), (2.68) and (2.69). In order to transform solutions of dimensionless piezometric head from Laplace domain to real dimensionless time domain, a numerical simulator based on Stehfest's inverse Laplace transformation is developed using VBA in Excel (Jahan and Jelmert, 2008) and applied to composite aquifers. Subroutines in VBA computing dimensionless piezometric heads of granular aquifer, fractures and blocks are developed for each media and given in Appendices B, C and D respectively.

4.2 Variation of Dimensionless Piezometric Head

As given in dimensionless Laplace equations for piezometric head of granular aquifer, fractures and blocks in equations (2.62), (2.63) and (2.64), solutions depend on ratios of transmissivity and storage coefficients rather than transmissivity and storage of each region itself. With this methodology, comments can be made on the interaction between each region, flow rate and drawdown at any time and at any distance from stream regardless of aquifer parameters of each region. Definitions of aquifer parameter and flow properties used in the equations are summarized in the Table 4.1 and Table 4.2.

Table 4.1: Dimensional and dimensionless piezometric head symbols used in the equations of groundwater flow

	DEPENDENT VARIABLES (PIEZOMETRIC HEADS)		INDEPENDENT VARIABLES	
DIMENSIONAL	Granular Aquifer	h_0	Distance	x
	Fractures	h_1		
	Blocks	h_2	Time	t
DIMENSIONLESS	Granular Aquifer	z_0	Distance	y
	Fractures	z_1		
	Blocks	z_2	Time	θ

Table 4.2: Flow and aquifer parameters in groundwater equations

AQUIFER PARAMETERS (INPUT PARAMETERS)	
DIMENSIONAL	DIMENSIONLESS
$b, [L]$	$Q_b = \frac{QL}{2T_0H_0}$
$H_0, [L]$	
$L, [L]$	$\lambda_1 = T_1/T_0$
$Q, [L^2T^{-1}]$	$\lambda_2 = T_2/T_0$
$T_0, [L^2T^{-1}]$	$\eta_1 = S_1/S_0$
$S_0, [-]$	$\eta_2 = S_2/S_0$
$K_0, [LT^{-1}]$	$\delta_2 = \varepsilon L^2 \frac{\lambda_2}{\eta_2}$
$T_1, [L^2T^{-1}]$	
$S_1, [-]$	
$K_1, [LT^{-1}]$	
$T_2, [L^2T^{-1}]$	
$S_2, [-]$	
$K_2, [LT^{-1}]$	
$\varepsilon, [L^{-2}]$	

Related aquifer parameters; storage coefficient, transmissivity and conductivity are selected according to values derived from literature illustrating ranges for storage, hydraulic conductivity and transmissivity coefficient.

Table 4.3: Ranges of storage coefficient for different types of aquifer (Hall, 1996)

Storage Coefficient, S (-)	Confined and leaky aquifer	10^{-5} - 10^{-3}
	Unconfined aquifer	0.05-0.3

Table 4.4: Hydraulic conductivity ranges for different representative materials (USBR of Reclamation, 1997)

K (m/day)	Clean Gravel	Clean Sand and Gravel	Fine Sand	Silt, Clay and mixed	Massive Clay
	Very High	High	Moderate	Low	Very Low
	10^3 - 10^4	10^1 - 10^3	10^{-1} - 10^1	10^{-4} - 10^{-1}	10^{-5} - 10^{-4}

Table 4.5: Transmissivity ranges for different properties and use (USBR of Reclamation, 1997)

	Irrigation Use					Domestic Use			
T (m ² /d)	Unlikely	Very Good	Good	Fair	Poor	Good	Fair	Poor	Infeasible
		10 ⁶	10 ⁴ - 10 ⁶	10 ³ - 10 ⁴	10 ² - 10 ³	50- 10 ²	10- 50	1- 10	0.1- 1

To illustrate the application and use of the proposed solution, a hypothetical composite aquifer is selected. Charts illustrating flow pattern of the aquifer are developed using these numerical values. Aquifer parameters and flow properties for this aquifer are:

$$\lambda_1 = 15, \lambda_2 = 0.01, \eta_1 = 0.2, \eta_2 = 2, Q_b = 0.06, \delta_2 = 0.5$$

4.2.1 Variation of Dimensionless Piezometric Head in Granular Aquifer

Using aquifer parameters given in Chapter 4.2 above, the variation of dimensionless piezometric head in granular aquifer with time is plotted in Figure 4.1 for series of dimensionless distance. Likewise the variation of dimensionless piezometric head in granular aquifer with distance is illustrated in Figure 4.2 for a series of dimensionless time.

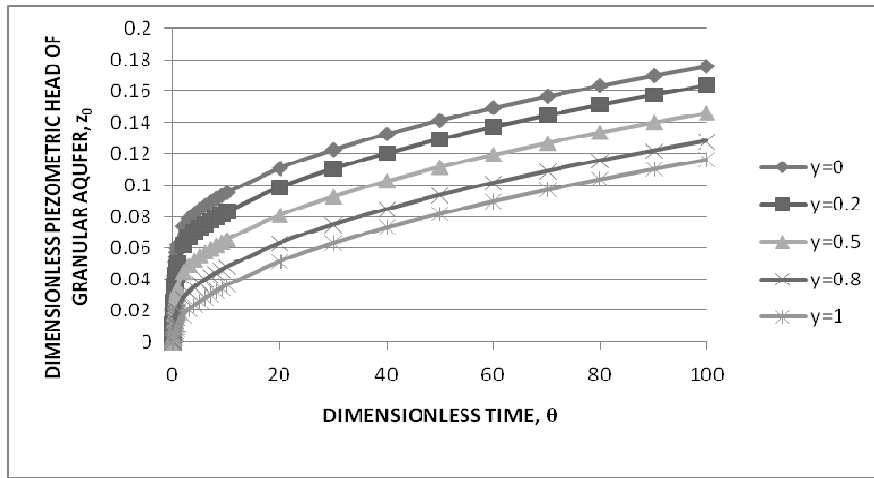


Figure 4.1: Dimensionless piezometric head of granular aquifer z_0 vs. dimensionless time θ for different values of dimensionless distance γ

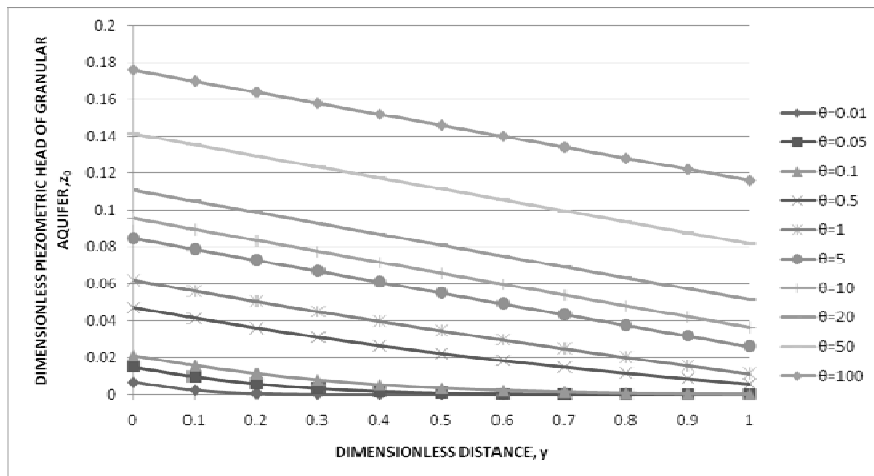


Figure 4.2: Dimensionless piezometric head of granular aquifer z_0 vs. dimensionless distance γ for different dimensionless time θ

As can be seen from Figure 4.2, flow in finite granular aquifer becomes steady when it approaches large θ ($\theta \geq 1$). For smaller values of θ , transient flow conditions exist.

4.2.2 Variation of Dimensionless Piezometric Head in Fractures

Dimensionless piezometric head variation in fractures with time is given in Figure 4.3 for a series of dimensionless distance. Figure 4.4 illustrates the variation of dimensionless piezometric head in fractures with distance for a series of dimensionless time.

As can be seen in Figure 4.4, transient flow conditions are valid even for time series corresponding to late times $\theta=100$ unlike nearly steady state flow condition in granular aquifer at $\theta=100$ as shown in Figure 4.2.

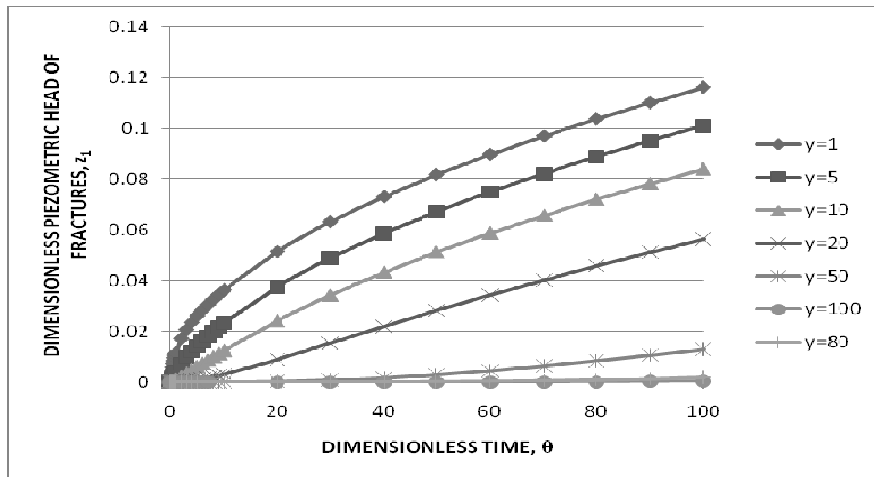


Figure 4.3: Dimensionless piezometric head of fractures z_1 vs. dimensionless time θ for different values of dimensionless distance y

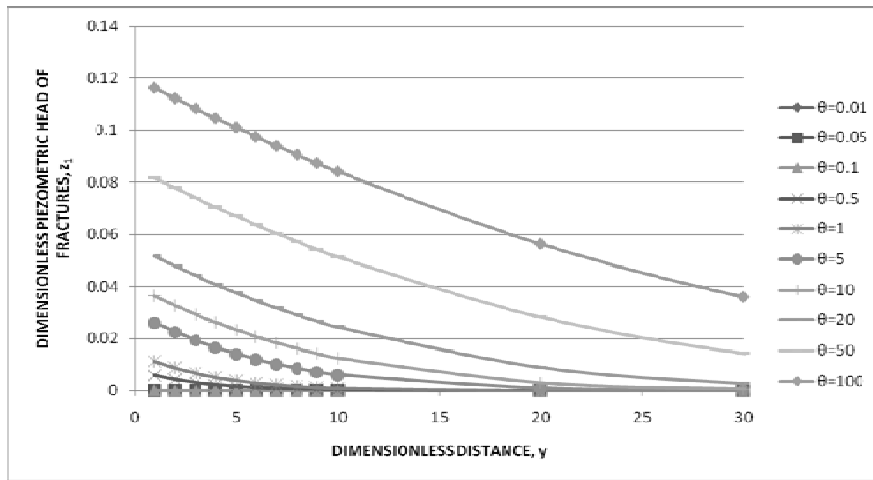


Figure 4.4: Dimensionless piezometric head of fractures z_1 vs. dimensionless distance y for different values of dimensionless time θ

4.2.3 Variation of Dimensionless Piezometric Head in Blocks

Figure 4.5 illustrates the time variation of dimensionless piezometric head for given aquifer parameters with a series of dimensionless distance. Likewise, Figure 4.6 illustrates the distance variation of dimensionless piezometric head with a series of dimensionless time. Similar to flow pattern in fractures shown in Figure 4.4, unsteady flow conditions remain in blocks even at $\theta=100$.

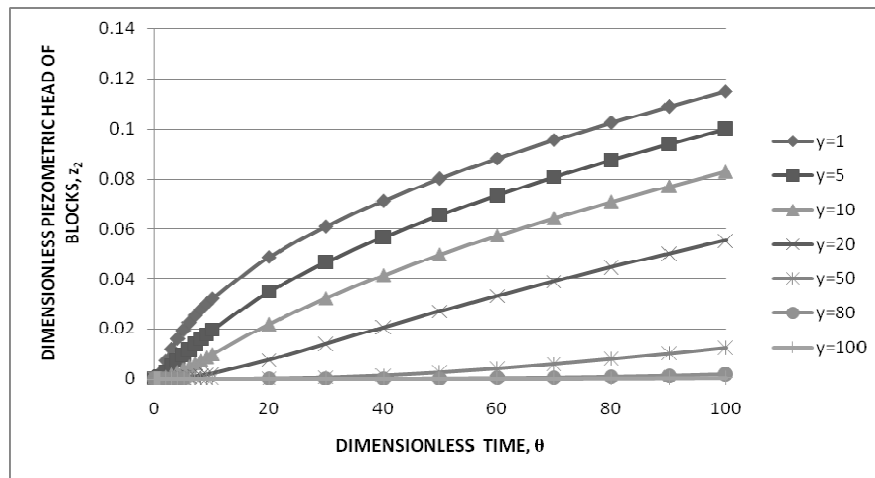


Figure 4.5: Dimensionless piezometric head of blocks z_2 vs. dimensionless time θ for different values of dimensionless distance γ .

As it is evident from Figure 4.3, Figure 4.5 and Figure 4.6 for dimensionless piezometric head of fractures and blocks tends to approach zero as distance goes to infinity proving the boundary conditions $z_1 = 0$ and $z_2 = 0$ as γ goes to infinity for fractures and blocks.

Analyzing Figure 4.1 to Figure 4.6, it can be figured out that flow in granular region having finite length, semi infinite fractured rock composed of fractures and blocks follow the similar pattern both in time and distance.

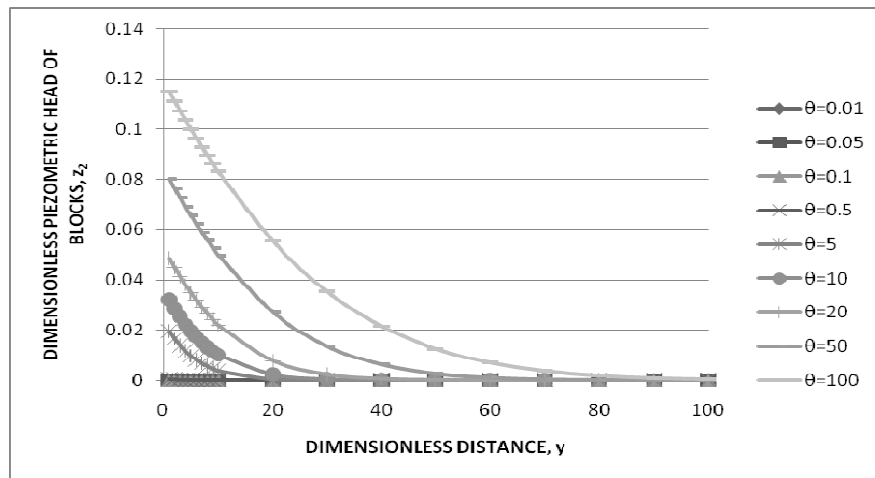


Figure 4.6: Dimensionless piezometric head of blocks z_2 vs. dimensionless distance y for different values of dimensionless time θ .

4.2.4 Variation of Dimensionless Piezometric Head for Granular Aquifer-Fractures Interface

Figure 4.7 is the verification of boundary condition that piezometric head of granular region and fractures are equal at the interface $y=1$. As it is obvious from Figure 4.7, flow pattern and piezometric head are exactly the same for each case.

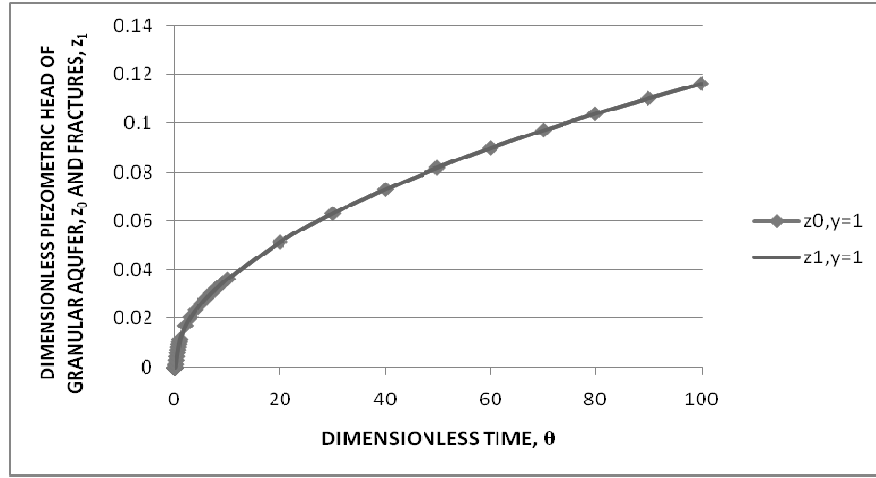


Figure 4.7: Dimensionless piezometric head of granular aquifer z_0 and fractures z_1 vs. dimensionless time θ at the intersection, $y=1$.

At $y=1$, granular aquifer-fractured rock interface groundwater flows from granular aquifer to fractures at the same rate. Recalling from chapter 2, flow boundary condition for confined aquifer at $y=1$ is given as:

$$K_0 \frac{\partial h_0}{\partial x} = K_1 \frac{\partial h_1}{\partial x}, \quad x=L, \quad t>0 \quad (2.14)$$

Above equation (2.14) for confined aquifer in dimensionless form can be written as:

$$\frac{\partial z_0}{\partial y} = \lambda_1 \frac{\partial z_1}{\partial y}, \quad y=1, \quad \theta>0 \quad (2.33)$$

From above equation (2.33), it can be derived that at the interface transmissivity ratio of fractures to granular aquifer is equal to the space gradient of piezometric head of granular aquifer to fractures. For this hypothetical aquifer, λ_1 is taken 15; therefore the granular head gradient and slope of flow pattern for granular aquifer is greater than fractures as shown in Figure 4.8.

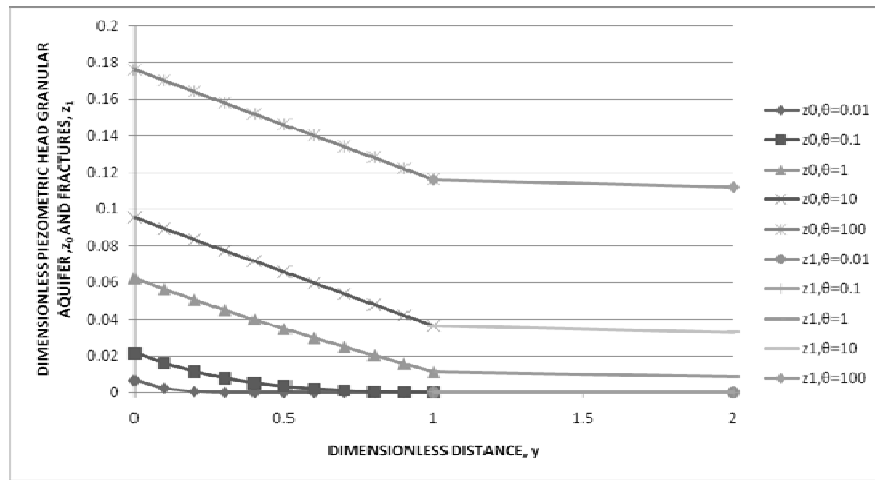


Figure 4.8: Dimensionless piezometric head of granular aquifer z_0 and fractures z_1 vs. dimensionless distance y for different values of dimensionless time θ

4.2.5 Comparison between Dimensionless Piezometric Head of Fractures and Blocks

In fracture network and block matrices, groundwater flow takes place at fractures and this flow is transferred to blocks having much higher storage capacity than fractures. The amount of flow from fractures to blocks depends on the pressure difference between two faces. At earlier times of continuous discharging from stream, head difference between fractures and blocks has reached a peak value that can be seen from Figure 4.10 due to flow from blocks to fracture and blocks cannot respond this excitation at that time period. As it can be interpreted from Figure 4.9, Figure 4.10 and Figure 4.11, the piezometric head of fractures and blocks tend to approach each other as time passes; exchange of flow from fractures to blocks decreases and equilibrium state between fractures and blocks is reached.

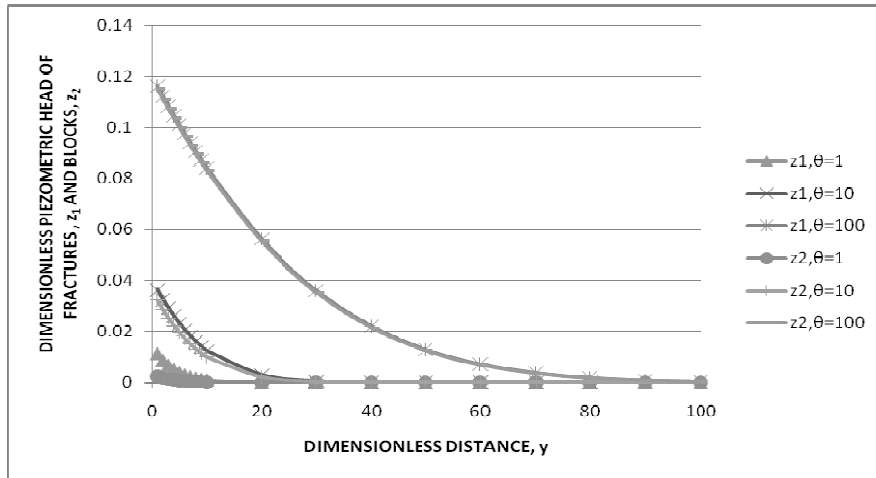


Figure 4.9: Dimensionless piezometric head of fractures z_1 and blocks z_2 vs. dimensionless distance y for different values of dimensionless time θ

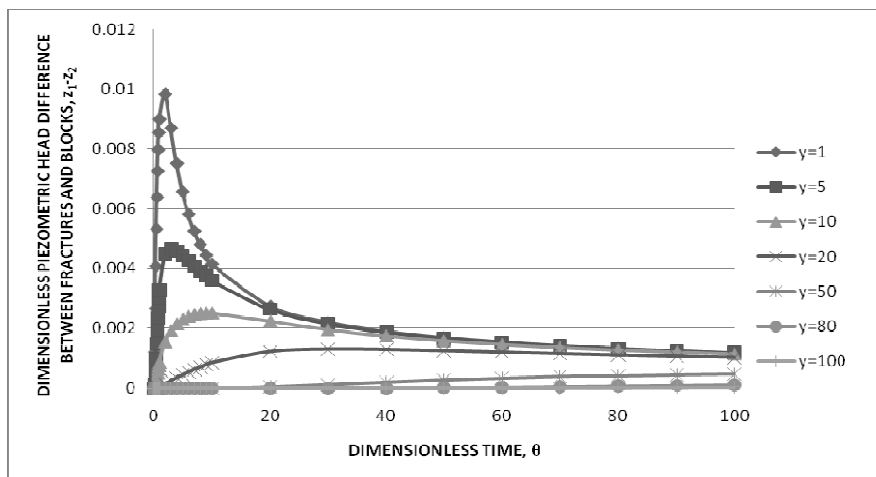


Figure 4.10: Dimensionless piezometric head difference between fractures z_1 and blocks z_2 vs. dimensionless time θ for different values of dimensionless distance y

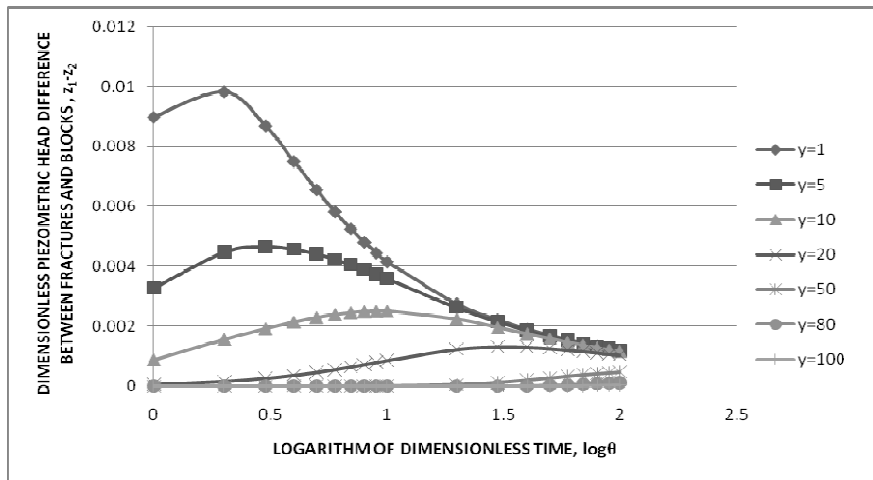


Figure 4.11: Dimensionless piezometric head difference between fractures z_1 and blocks z_2 vs. logarithm of dimensionless time θ for different values of dimensionless distance γ

4.3 Sensivity Analysis of Aquifer Characteristics

4.3.1 Effect of λ_1 on the Flow through Composite Aquifer

The dimensionless parameter λ_1 reflects the contrast between the transmissivities of granular aquifer and fractures system. In this section, the influence of this parameter on the flow behavior is investigated. The effect of λ_1 on the piezometric heads of granular aquifer, fractures and blocks is presented in the following sub-sections.

4.3.1.1 Effect of λ_1 on the dimensionless head of granular aquifer

Figure 4.12 illustrates the effect of different λ_1 values in the dimensionless piezometric head of granular aquifer and the variation of dimensionless head

with time is illustrated. As λ_1 increases accounting for smaller transmissivity of granular aquifer, flow from stream is maintained in the granular aquifer and head in granular aquifer is greater for smaller λ_1 .

Figure 4.13 illustrates the variation of dimensionless piezometric head of granular aquifer with distance for a series of λ_1 at $\theta=0.5$, corresponding to earlier times of flow. Similar flow pattern is shown in Figure 4.14 for $\theta=10$, corresponding to later times of flow. As it can be seen from Figure 4.14, the flow pattern has almost reached steady state conditions for different λ_1 values.

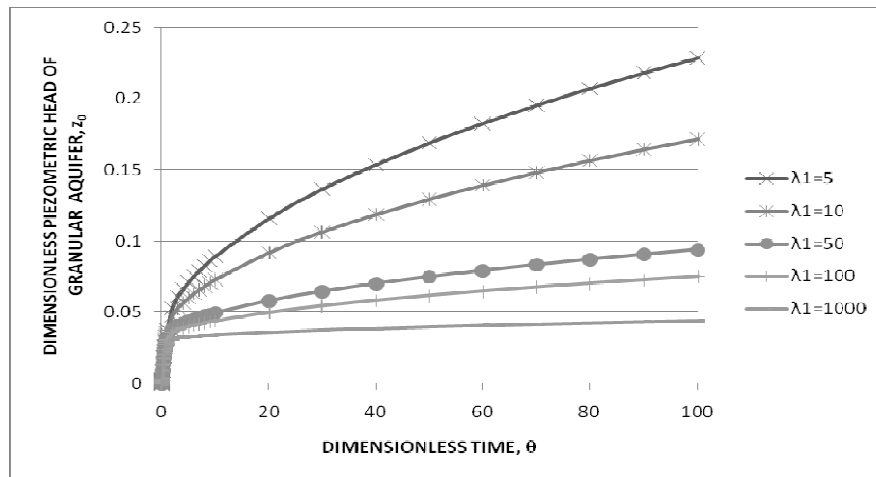


Figure 4.12: Dimensionless piezometric head of granular aquifer z_0 vs. dimensionless time θ for different values of λ_1 at $\gamma=0.5$.

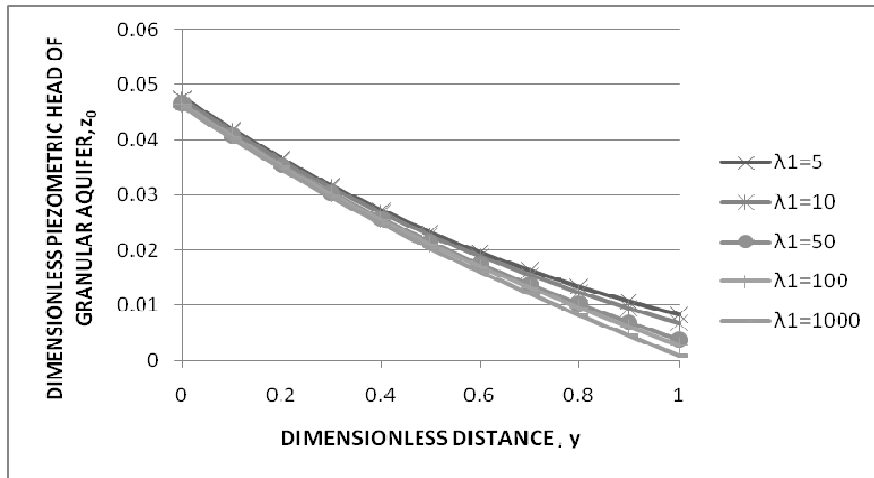


Figure 4.13: Dimensionless piezometric head of granular aquifer z_0 vs. dimensionless distance y for different values of λ_1 at $\theta = 0.5$.

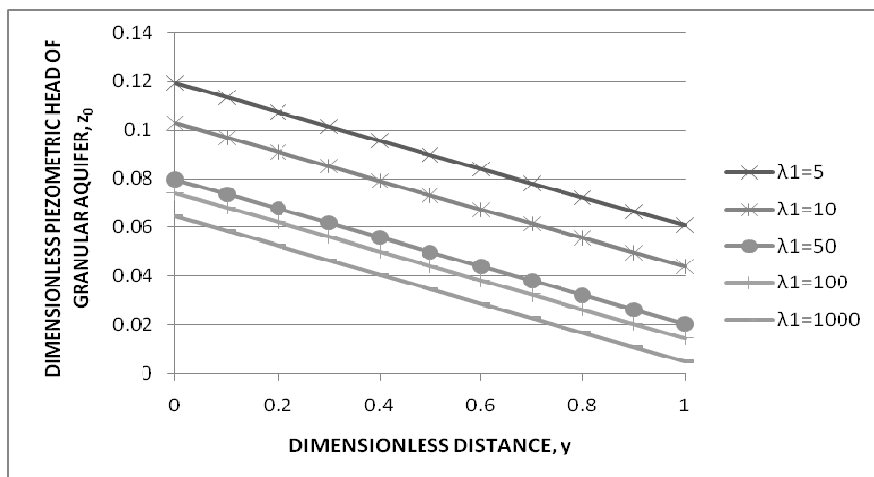


Figure 4.14: Dimensionless piezometric head of granular aquifer z_0 vs. dimensionless distance y for different values of λ_1 at $\theta = 10$

4.3.1.2 Effect of λ_1 on the dimensionless head of fractures

λ_1 is interpreted as flow resistance of fractures since flow from stream follows granular region first and then comes to fracture system. In nature, the transmissivity of fractures is more likely than granular part. Drawdown of fractures decrease due to increasing transmissivity contrast between fractures and granular aquifer as can be seen from Figure 4.15. The variation of dimensionless piezometric head in fractures with dimensionless distance at $\theta=0.5$ for a series of λ_1 is illustrated in Figure 4.16.

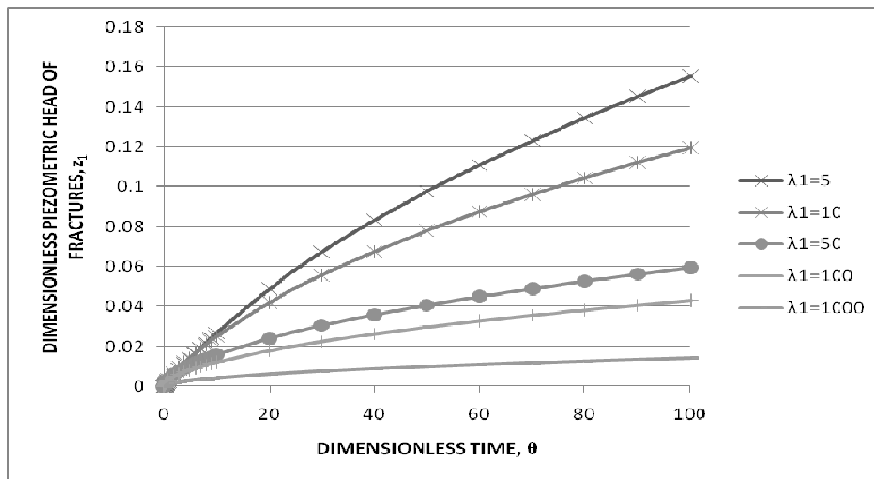


Figure 4.15: Dimensionless piezometric head of fractures z_1 vs. dimensionless time θ for different values of λ_1 at $y=5$

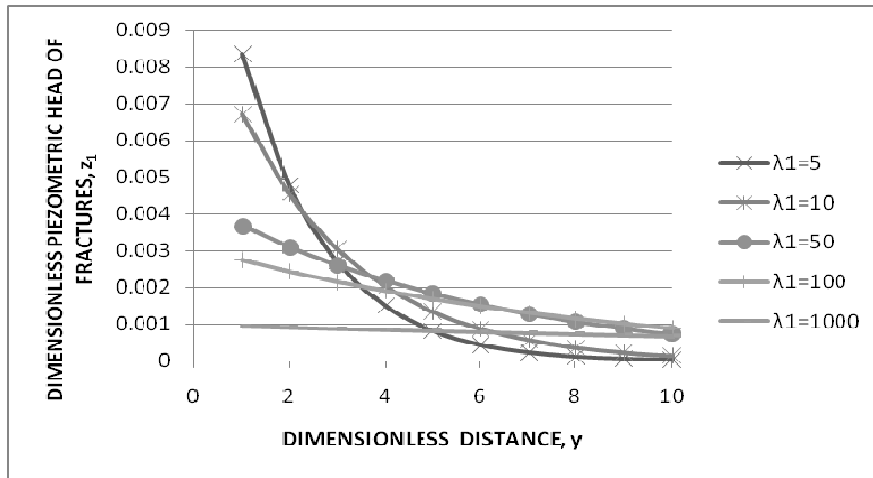


Figure 4.16: Dimensionless piezometric head of fractures z_1 vs. dimensionless distance γ for different values of λ_1 at $\theta = 0.5$

4.3.1.3 Effect of λ_1 on the dimensionless head of blocks

Flow pattern showing the variation of dimensionless head of blocks with dimensionless time for a series of λ_1 at $\gamma=5$ is similar to flow pattern for fractures illustrated in Figure 4.15. In the similar manner as in Figure 4.16 for fractures, Figure 4.17 illustrates the variation of dimensionless piezometric head of blocks with dimensionless distance for a series of λ_1 at $\theta=0.5$.

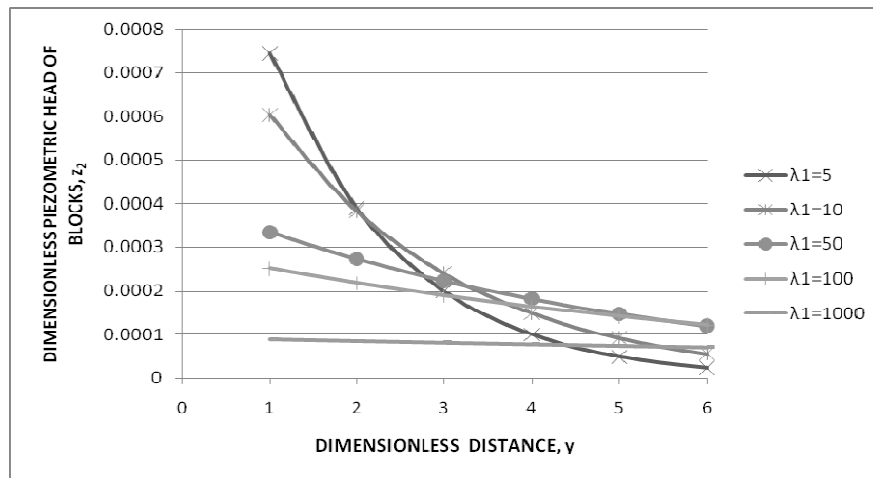


Figure 4.17: Dimensionless piezometric head of blocks z_2 vs. dimensionless distance y for different values of λ_1 at $\theta = 0.5$.

4.3.1.4 Effect of λ_1 on the dimensionless head on the interface

Dimensionless form of boundary condition stating the flow rate equality between granular aquifer and fractures at the interface, $y=1$ is given in equation (2.33). This equation at the interface relates the gradient of piezometric head with the transmissivity ratio λ_1 which is an indication of flow transfer at that point. From the equation and results of the analysis illustrated in Figure 4.18. If λ_1 is smaller than unity, the gradient of granular aquifer is smaller than the gradient of fractures since flow through high transmissivity zone is smoother and relatively easier. If λ_1 is greater than unity, aquifer, the gradient of granular aquifer is greater than the gradient of fractures. The same slope for equal transmissivity is achieved, that is when λ_1 is unity.

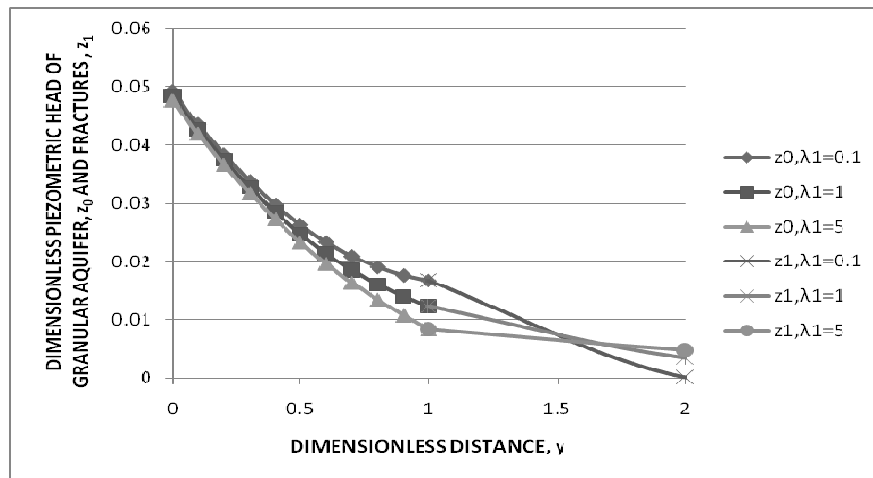


Figure 4.18: Dimensionless piezometric heads of granular aquifer and fractures vs. dimensionless distance at $\theta=0.5$ for different values of λ_1 .

4.3.2 Effect of λ_2 on the Flow through Composite Aquifer

The dimensionless parameter λ_2 reflects the contrast between the transmissivities of granular aquifer and blocks. In this section, the influence of this parameter on the flow behavior is investigated. The effect of λ_2 on the piezometric heads of granular aquifer, fractures and blocks is presented in the following sub-sections.

4.3.2.1 Effect of λ_2 on the dimensionless head of granular aquifer

Figure 4.19 illustrates the effect of different λ_2 values in the dimensionless piezometric head of granular aquifer and the variation of dimensionless head with time at $y=0.5$ is illustrated.

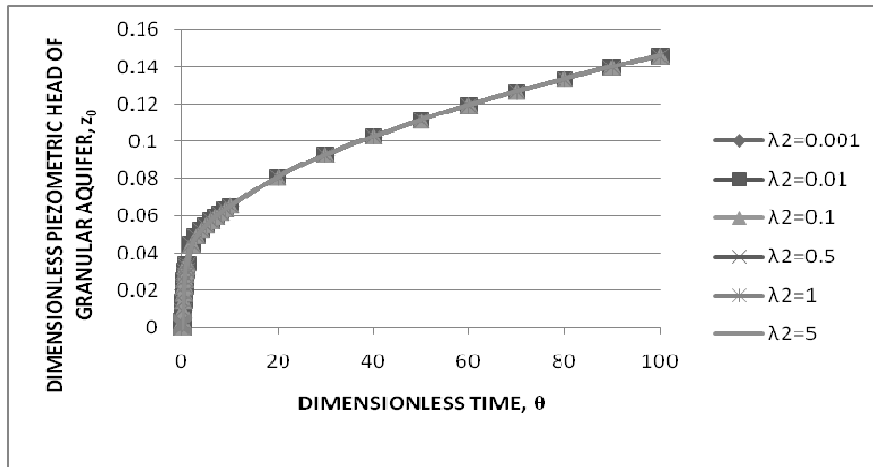


Figure 4.19: Dimensionless piezometric head of granular aquifer z_0 vs. dimensionless time θ for different values of λ_2 at $\gamma=0.5$.

Figure 4.20 illustrates the variation of dimensionless piezometric head of granular aquifer with distance for a series of λ_2 at $\theta=0.5$. As it can be seen from Figure 4.21, the flow pattern has almost reached steady state conditions at $\theta=10$.

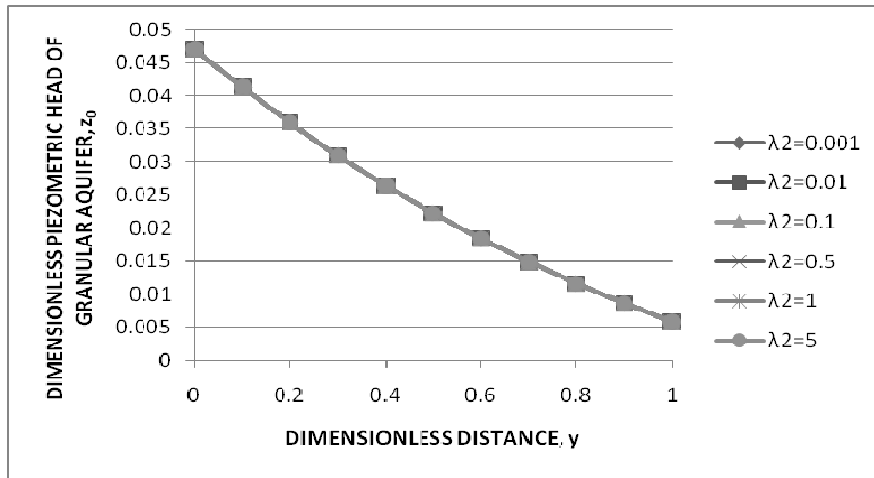


Figure 4.20: Dimensionless piezometric head of granular aquifer z_0 vs. dimensionless distance y for different values of λ_2 at $\theta = 0.5$

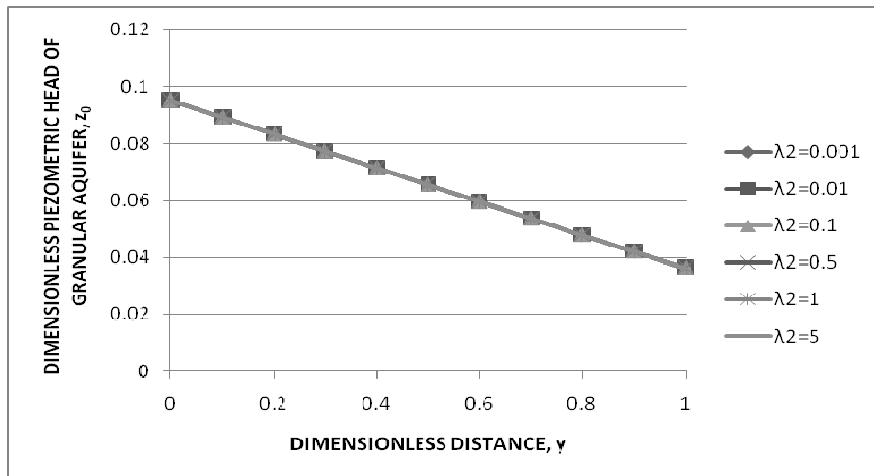


Figure 4.21: Dimensionless piezometric head of granular aquifer z_0 vs. dimensionless distance y for different values of λ_2 at $\theta = 10$.

4.3.2.2 Effect of λ_2 on the dimensionless head of fractures

The variation of dimensionless piezometric head of fractures with dimensionless time for a series of λ_2 values at $y=5$ is illustrated in Figure 4.22. In Figure 4.23, the variation of dimensionless piezometric head of fractures with distance for a series of λ_2 values at $\theta=0.5$ is shown.

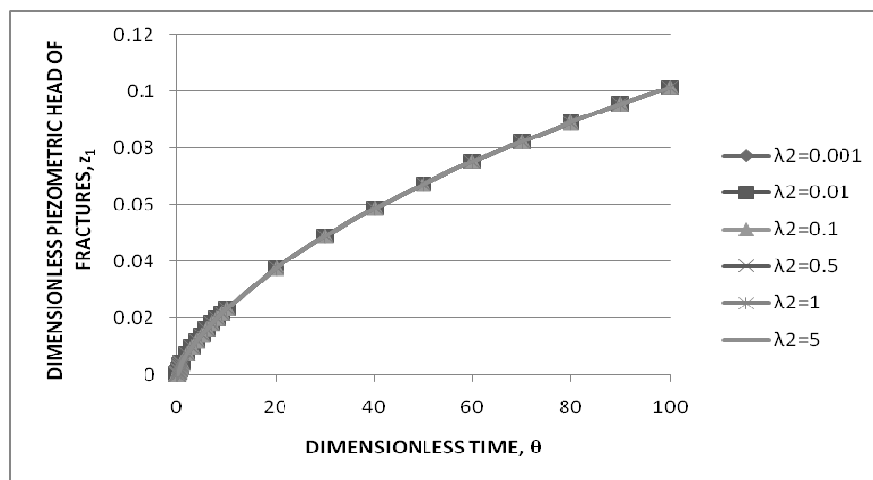


Figure 4.22: Dimensionless piezometric head of fractures z_1 vs. dimensionless time θ for different values of λ_2 at $y=5$.

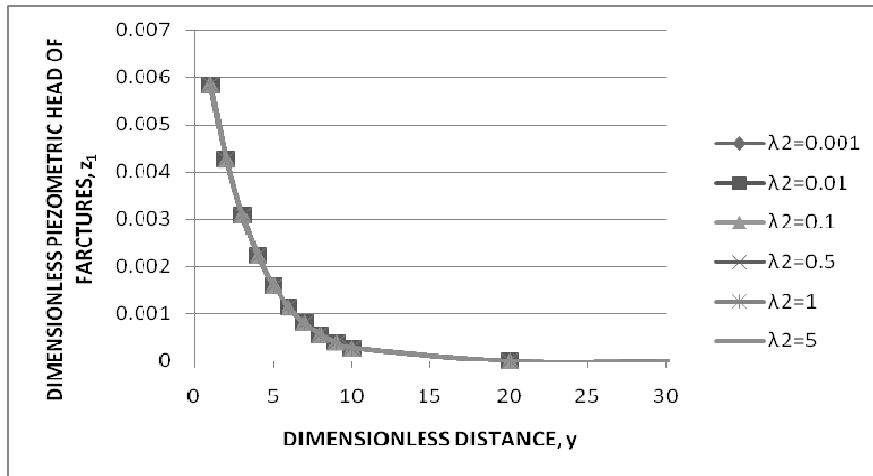


Figure 4.23: Dimensionless piezometric head of fractures z_1 vs. dimensionless distance y for different values of λ_2 at $\theta = 0.5$.

4.3.2.3 Effect of λ_2 on the dimensionless head of blocks

The variation of dimensionless piezometric head of blocks with dimensionless time for a series of λ_2 values at $y=5$ is illustrated in Figure 4.24. In Figure 4.25, the variation of dimensionless piezometric head of blocks with distance for a series of λ_2 values at $\theta=0.5$ is shown.

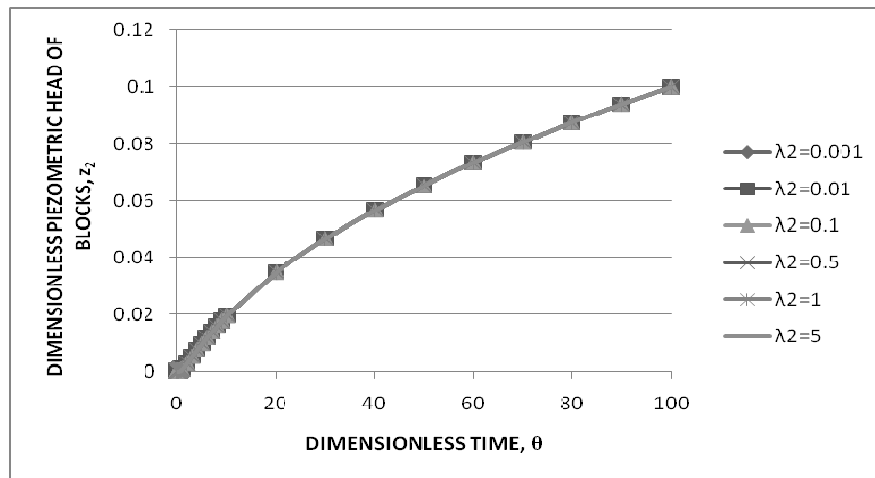


Figure 4.24: Dimensionless piezometric head of blocks z_2 vs. dimensionless time θ for different values of λ_2 at $\gamma=5$.

As it can be seen from Figure 4.19 to Figure 4.25 that groundwater flow behavior is independent of λ_2 . The conducting property of blocks is ignored in double-porosity model and equations of piezometric head are derived with this assumption. For this reason, λ_2 has no influence on the flow behavior.

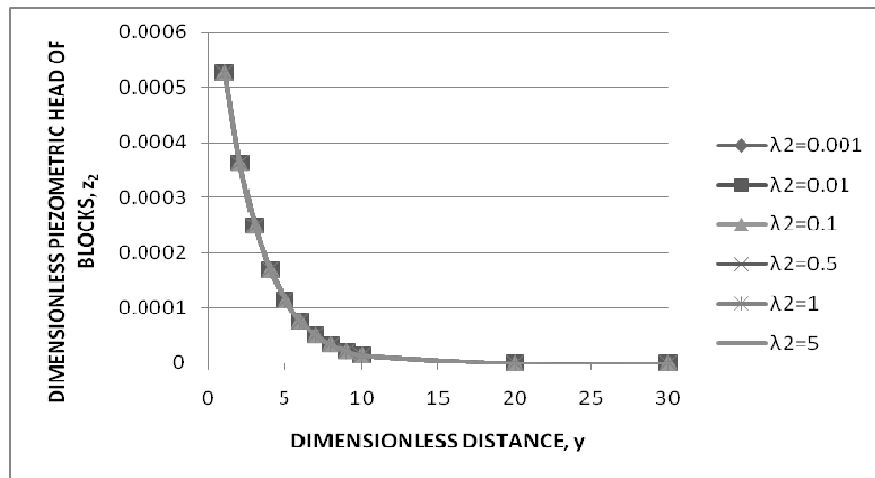


Figure 4.25: Dimensionless piezometric head of blocks z_2 vs. dimensionless distance y for different values of λ_2 at $\theta = 0.5$.

4.3.3 Effect of η_1 on the Flow through Composite Aquifer

The dimensionless parameter η_1 reflects the contrast between the storage coefficients of granular aquifer and fractures system. In this section, the influence of this parameter on the flow behavior is investigated. The effect of η_1 on the piezometric heads of granular aquifer, fractures and blocks is presented in the following sub-sections.

4.3.3.1 Effect of η_1 on the dimensionless head of granular aquifer

Figure 4.26 illustrates the effect of different η_1 values in the dimensionless piezometric head of granular aquifer and the variation of dimensionless head with time at $y=0.5$ is illustrated.

Figure 4.27 illustrates the variation of dimensionless piezometric head of granular aquifer with distance for a series of η_1 at $\theta=0.5$. Similar flow pattern is shown in

Figure 4.28 for $\theta=10$. As it can be seen from Figure 4.28, the flow pattern has almost reached steady state conditions for different η_1 values and flow pattern is almost linear.

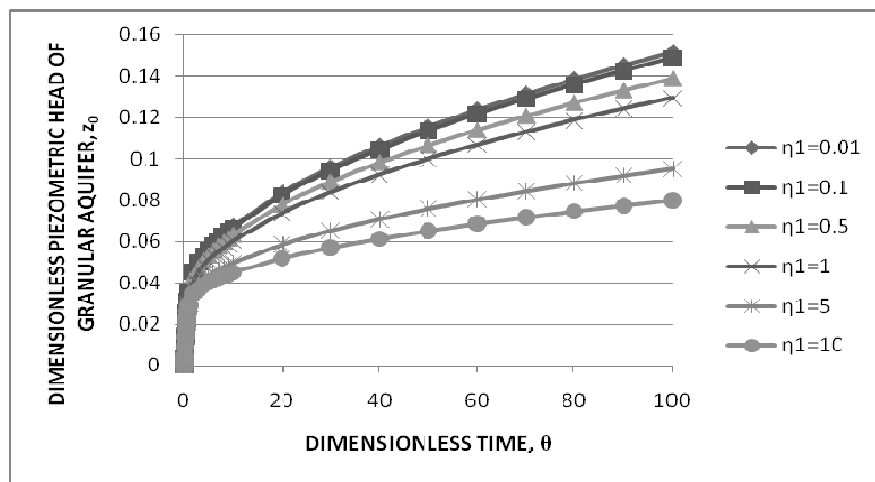


Figure 4.26: Dimensionless piezometric head of granular aquifer z_0 vs. dimensionless time θ for different values of η_1 at $\gamma=0.5$

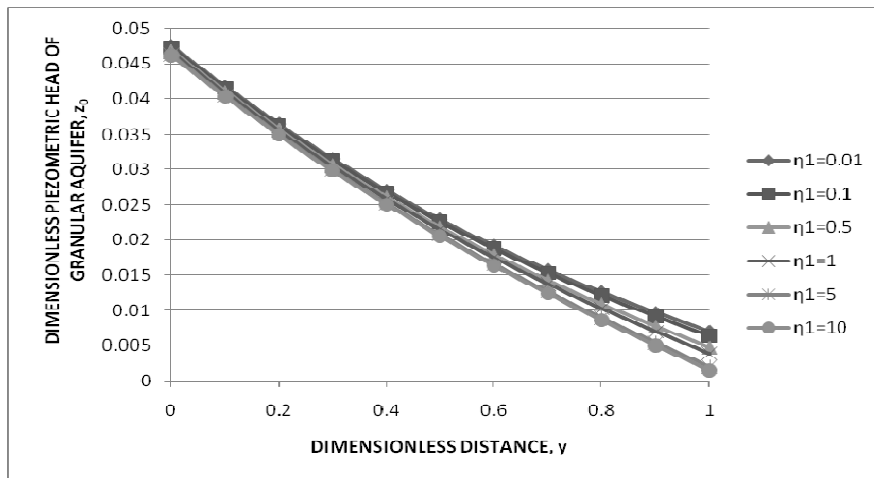


Figure 4.27: Dimensionless piezometric head of granular aquifer z_0 vs. dimensionless distance y for different values of η_1 at $\theta = 0.5$

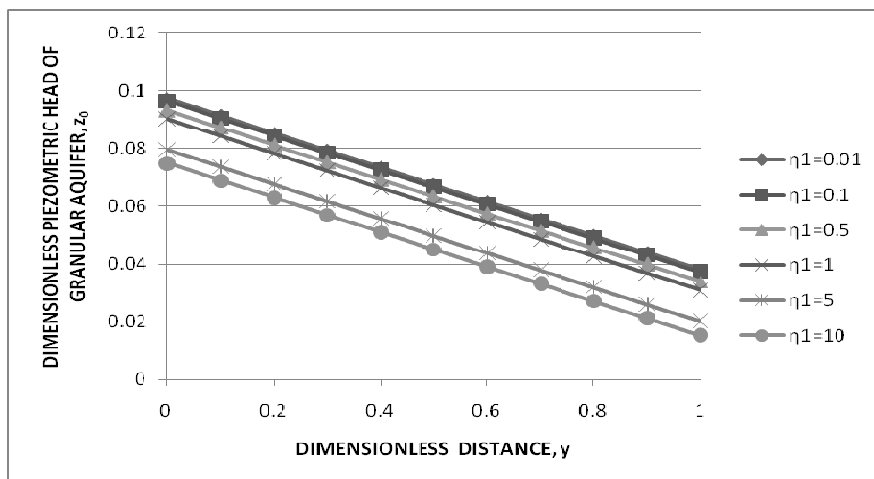


Figure 4.28: Dimensionless piezometric head of granular aquifer z_0 vs. dimensionless distance y for different values of η_1 at $\theta = 10$

4.3.3.2 Effect of η_1 on the dimensionless head of fractures

In Figure 4.29, the variation of dimensionless piezometric head of fractures with dimensionless time at $\gamma=5$ for a series of η_1 is illustrated. Since storativity or storage coefficient is defined as the value of water released or taken into storage per unit surface area of the aquifer, per unit change in the component of head normal to that surface (Hall, 1996). Higher values of storage coefficient return smaller amounts of drawdown and dimensionless piezometric head with respect to time decreases. Similar flow patterns for granular region are shown in Figure 4.26, Figure 4.27 and Figure 4.28. Figure 4.30 illustrates the variation of dimensionless piezometric head of fractures with dimensionless distance at $\theta=0.5$ for a series of η_1 .

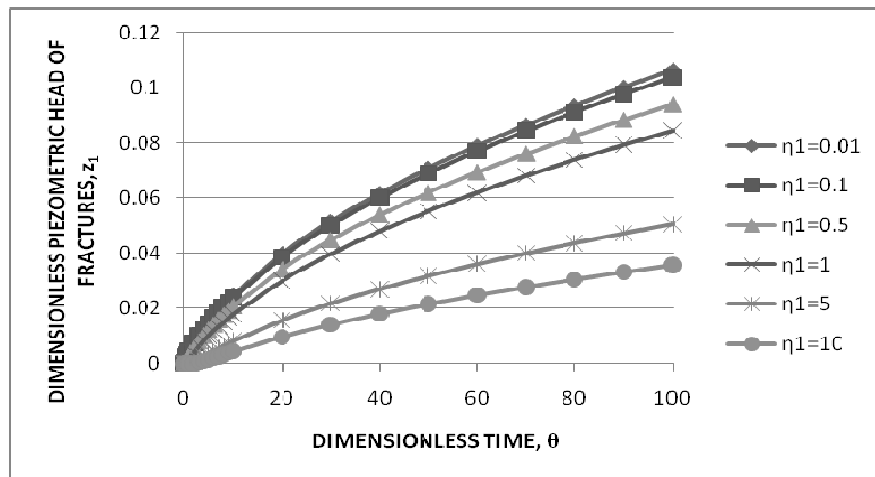


Figure 4.29: Dimensionless piezometric head of fractures z_1 vs. dimensionless time θ for different values of η_1 at $\gamma=5$

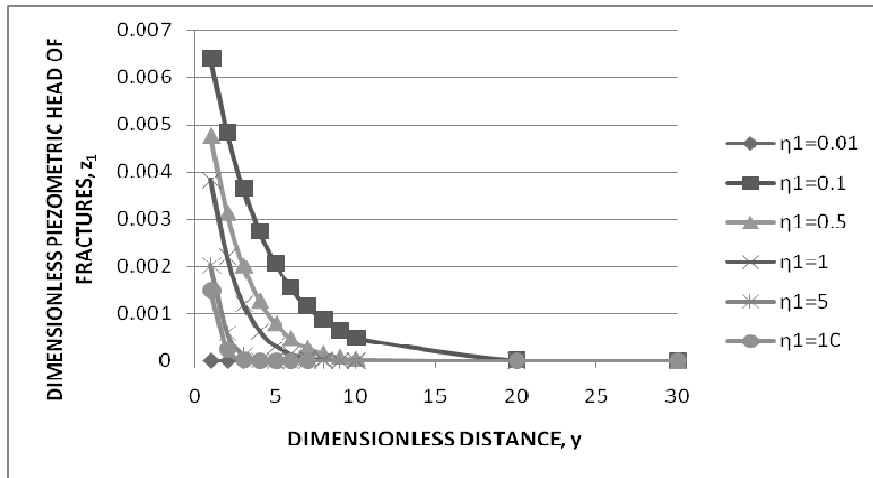


Figure 4.30: Dimensionless piezometric head of fractures z_1 vs. dimensionless distance y for different values of η_1 at $\theta = 0.5$

4.3.3.3 Effect of η_1 on the dimensionless head of blocks

Figure 4.31 shows the variation of dimensionless piezometric head of blocks with dimensionless time at $y=5$ for a series of η_1 . Flow pattern for blocks is similar to the case for fractures shown in Figure 4.29. Likewise, flow pattern in Figure 4.32 showing the variation of head in blocks with dimensionless distance at $\theta=0.5$ is the same as Figure 4.30.

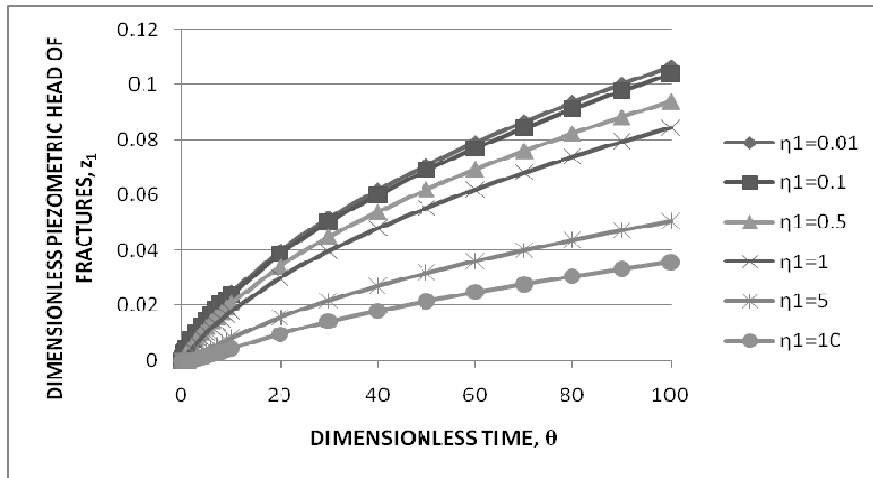


Figure 4.31: Dimensionless piezometric head of blocks z_2 vs. dimensionless time θ for different values of η_1 at $y=5$

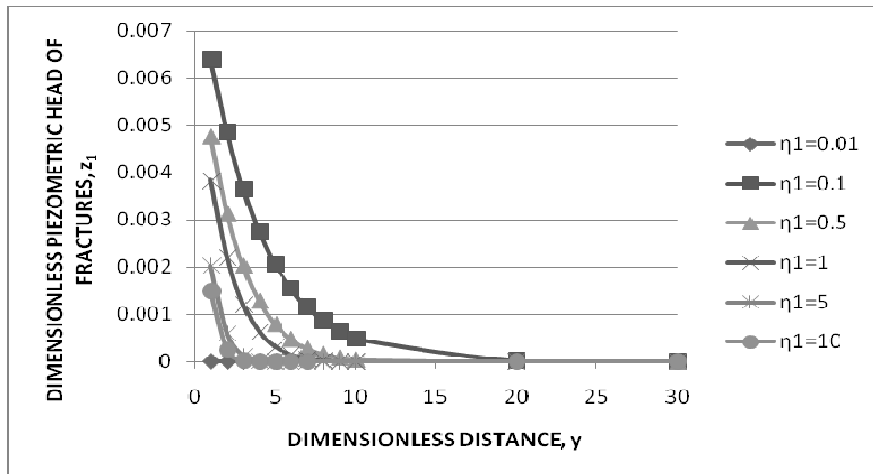


Figure 4.32: Dimensionless piezometric head of blocks z_2 vs. dimensionless distance γ for different values of η_1 at $\theta = 0.5$

4.3.4 Effect of η_2 on the Flow through Composite Aquifer

The dimensionless parameter η_2 reflects the contrast between the storage coefficients of granular aquifer and blocks system. In this section, the influence of this parameter on the flow behavior is investigated. The effect of η_2 on the piezometric heads of granular aquifer, fractures and blocks is presented in the following sub-sections.

4.3.4.1 Effect of η_2 on the dimensionless head of granular aquifer

Figure 4.33 illustrates the effect of different η_2 values in the dimensionless piezometric head of granular aquifer and the variation of dimensionless head with time at $\gamma=0.5$ is illustrated.

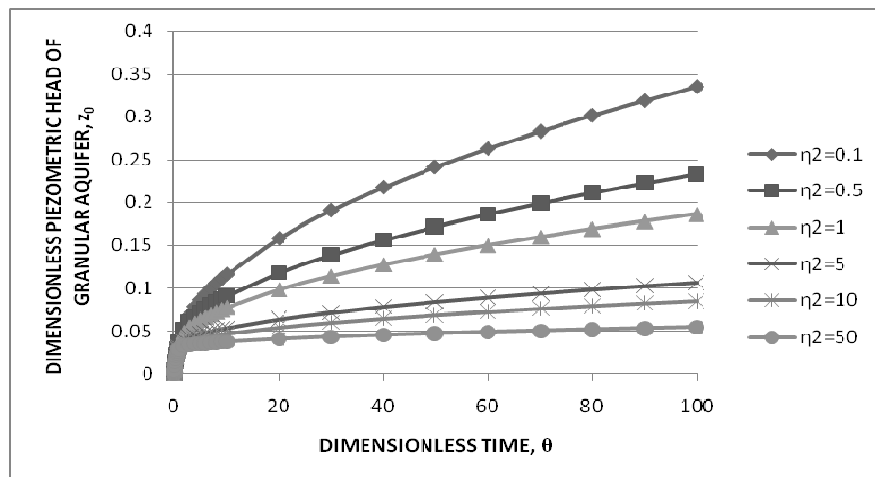


Figure 4.33: Dimensionless piezometric head of granular aquifer z_0 vs. dimensionless time θ for different values of η_2 at $\gamma=0.5$.

Figure 4.34 illustrates the variation of dimensionless piezometric head of granular aquifer with distance for a series of η_2 at $\theta=0.5$. Similar flow pattern is shown in Figure 4.35 for $\theta=10$. As it can be seen from Figure 4.35, the flow pattern has almost reached steady state conditions for different η_2 values and flow pattern is almost linear.

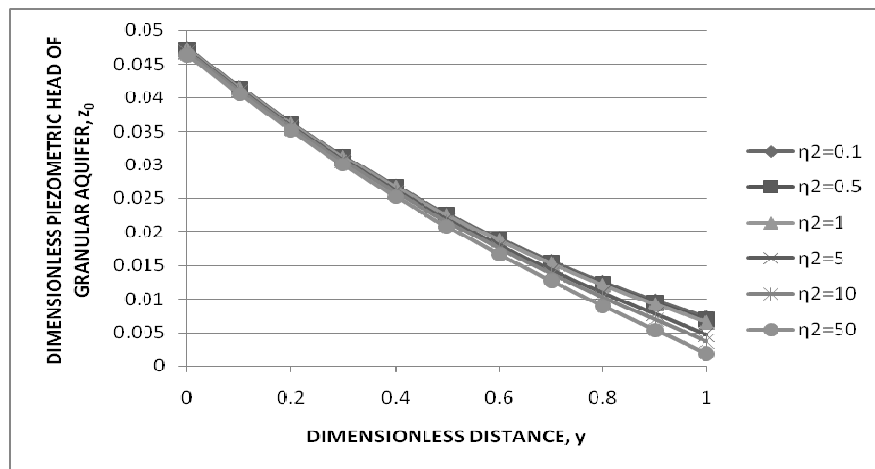


Figure 4.34: Dimensionless piezometric head of granular aquifer z_0 vs. dimensionless distance y for different values of η_2 at $\theta = 0.5$

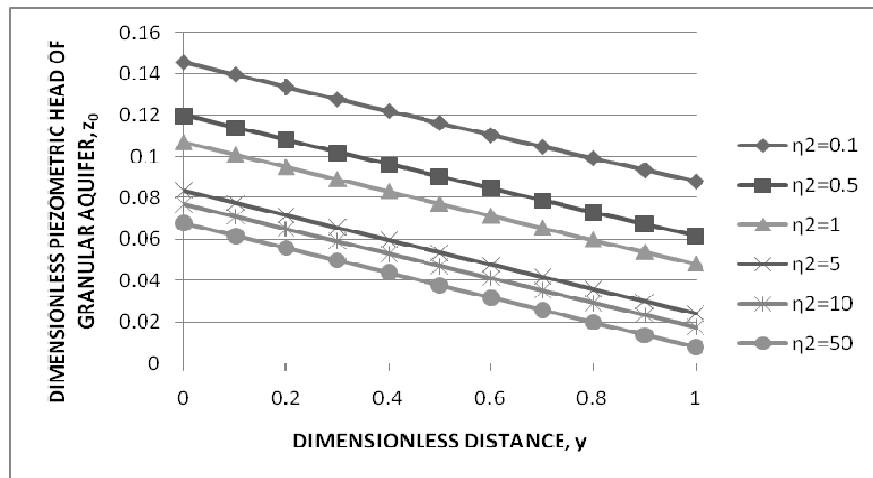


Figure 4.35: Dimensionless piezometric head of granular aquifer z_0 vs. dimensionless distance y for different values of η_2 at $\theta = 10$

4.3.4.2 Effect of η_2 on the dimensionless head of fractures

In Figure 4.36, the variation of dimensionless piezometric head of fractures with dimensionless time at $y=5$ for a series of η_2 is illustrated. Higher values of storage coefficient return smaller amounts of drawdown. Similar flow patterns for granular region are shown in Figure 4.33, Figure 4.34, and Figure 4.35. Figure 4.37 illustrates the variation of dimensionless piezometric head of fractures with dimensionless distance at $\theta=0.5$ for a series of η_2 .

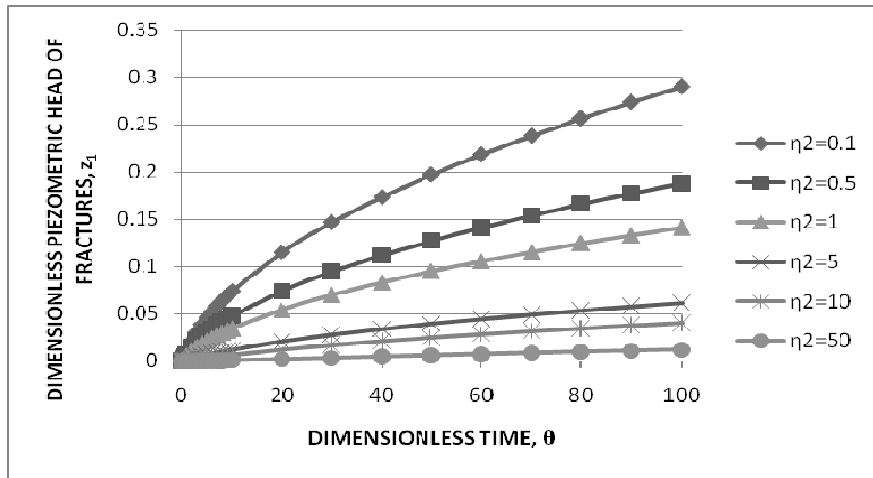


Figure 4.36: Dimensionless piezometric head of fractures z_1 vs. dimensionless time θ for different values of η_2 at $\gamma=5$.

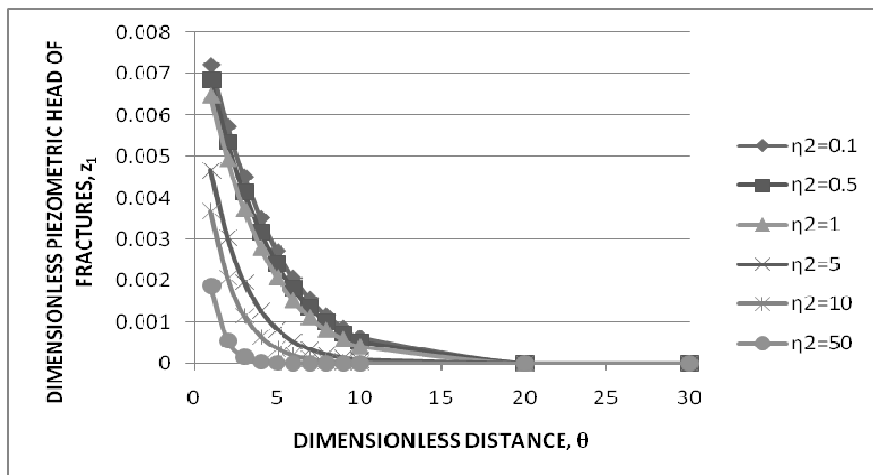


Figure 4.37: Dimensionless piezometric head of fractures z_1 vs. dimensionless distance γ for different values of η_2 at $\theta=0.5$.

4.3.4.3 Effect of η_2 on the dimensionless head of blocks

Figure 4.38 shows the variation of dimensionless piezometric head of blocks with dimensionless time at $y=5$ for a series of η_2 . Flow pattern for blocks is similar to the case for fractures shown in Figure 4.36. Likewise, flow pattern in Figure 4.39 showing the variation of head in blocks with dimensionless distance at $\theta=0.5$ is the same as Figure 4.37.

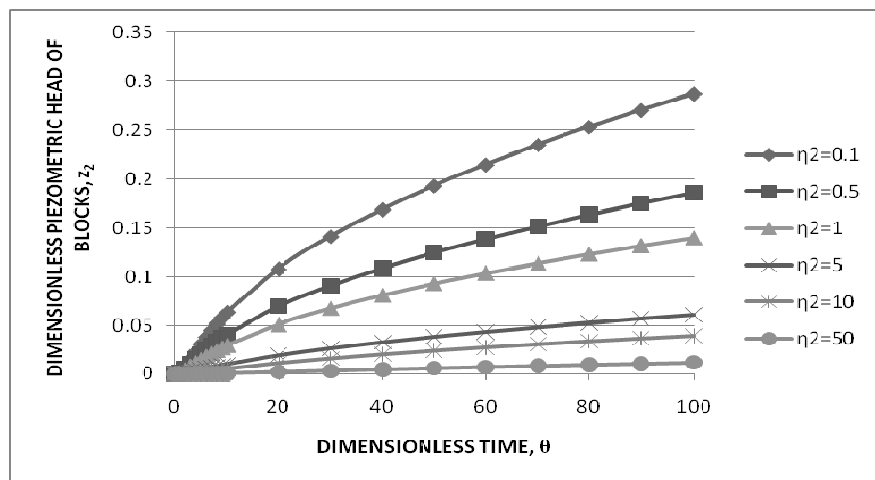


Figure 4.38: Dimensionless piezometric head of blocks z_2 vs. dimensionless time θ for different values of η_2 at $y=5$.

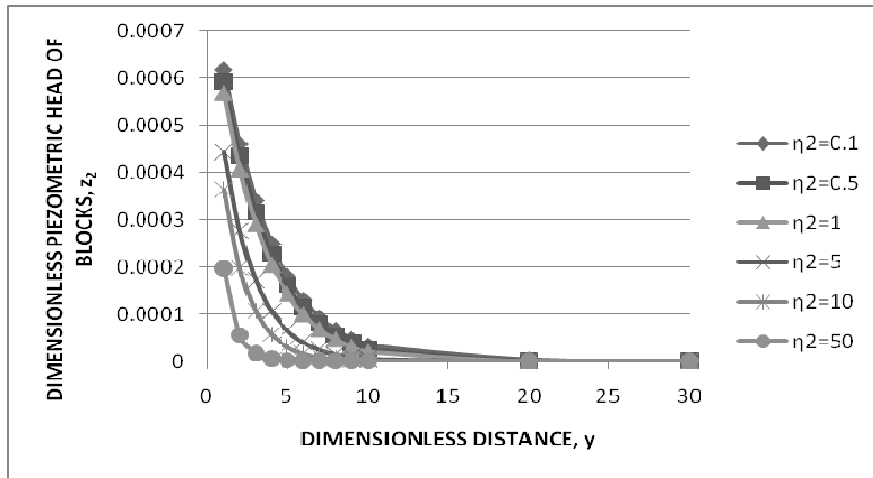


Figure 4.39: Dimensionless piezometric head of blocks z_2 vs. dimensionless distance y for different values of η_2 at $\theta = 0.5$

4.3.5 Effect of δ_2 on the Flow through Composite Aquifer

The dimensionless parameter δ_2 reflects the effect of fractured rock shape which depends on the geometry of rock. δ_2 also depends on the length of granular aquifer, transmissivity ratio of blocks to granular aquifer λ_2 and transmissivity ratio of blocks to granular aquifer η_2 as given in equation (2.24):

$$\delta_2 = \varepsilon L^2 \frac{\lambda_2}{\eta_2} \quad (2.24)$$

In this section, parameters other than shape factor are assumed to be constant and effect of δ_2 on the piezometric heads only accounts for the shape factor change. The effect of δ_2 on the piezometric heads of granular aquifer, fractures and blocks is presented in the following sub-sections.

4.3.5.1 Effect of δ_2 on dimensionless head of granular aquifer

Figure 4.40 illustrates the effect of different δ_2 values in the dimensionless piezometric head of granular aquifer and the variation of dimensionless head with time at $y=0.5$ is illustrated.

Figure 4.41 illustrates the variation of dimensionless piezometric head of granular aquifer with distance for a series of η_2 at $\theta=0.5$. Similar flow pattern is shown in Figure 4.42 for $\theta=10$. As it can be seen from Figure 4.42, the flow pattern has almost reached steady state conditions for different η_2 values and flow pattern is almost linear.

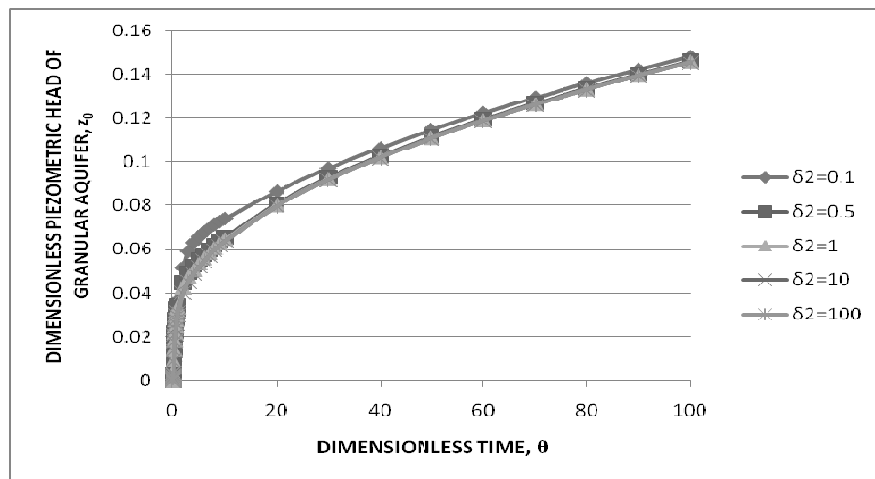


Figure 4.40: Dimensionless piezometric head of granular aquifer z_0 vs. dimensionless time θ for different values of δ_2 at $y=0.5$

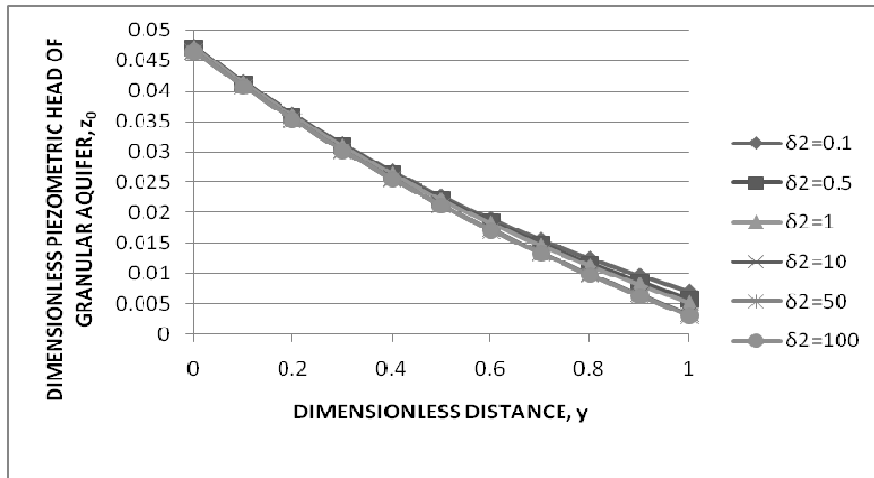


Figure 4.41: Dimensionless piezometric head of granular aquifer z_0 vs. dimensionless distance y for different values of δ_2 at $\theta = 0.5$

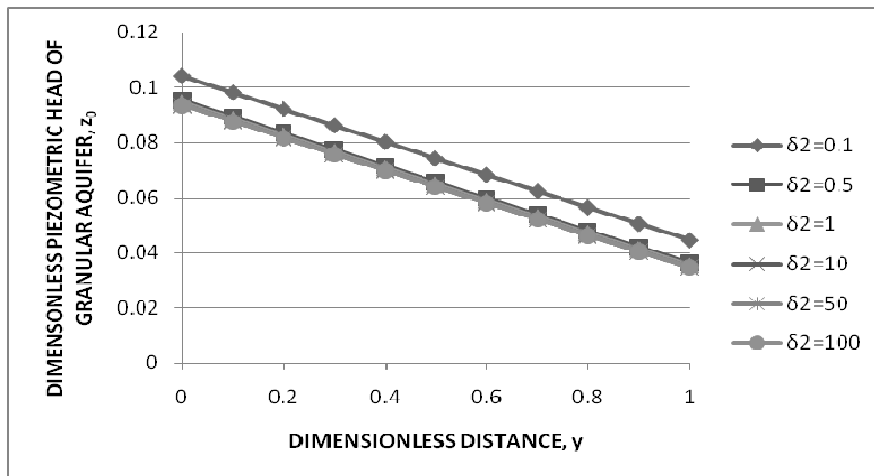


Figure 4.42: Dimensionless piezometric head of granular aquifer z_0 vs. dimensionless distance y for different values of δ_2 at $\theta = 10$

4.3.5.2 Effect of δ_2 on the dimensionless head of fractures

The flow mechanism in fractures is formulated in equation (2.2) as:

$$T_1 \frac{\partial^2 h_1}{\partial x^2} = S_1 \frac{\partial h_1}{\partial t} + v, L < x < \infty, t > 0 \quad (2.2)$$

The volume of water exchange from blocks to fractures, v is presented in equation (2.4) as:

$$v = \varepsilon T_2 (h_1 - h_2), L < x < \infty, t > 0 \quad (2.4)$$

Coefficient δ_2 is assumed to be only related with shape factor, ε keeping all other parameters constant. Increasing shape factor yields larger δ_2 and larger volume of flow, v passes to fractures and filled with water. Rate of piezometric head of fractures with time is smaller in turn for larger δ_2 and ε as can be seen from Figure 4.43.

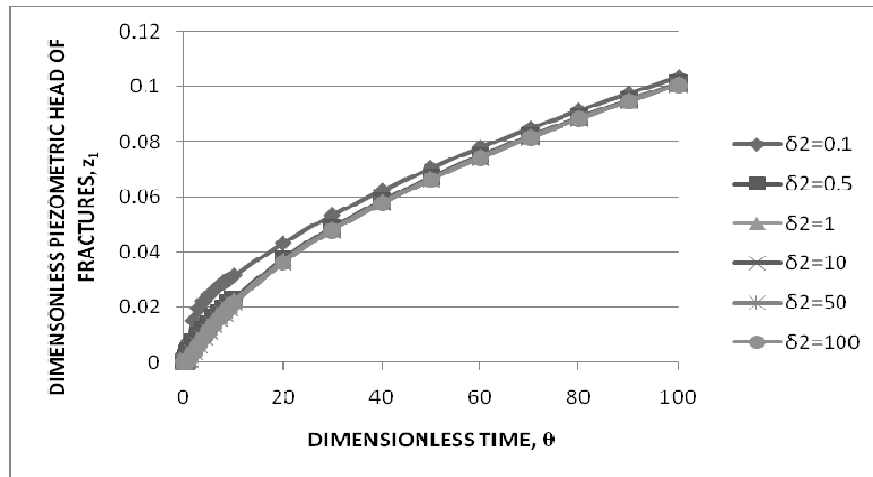


Figure 4.43: Dimensionless piezometric head of fractures z_1 vs. dimensionless time θ for different values of δ_2 at $\gamma=5$

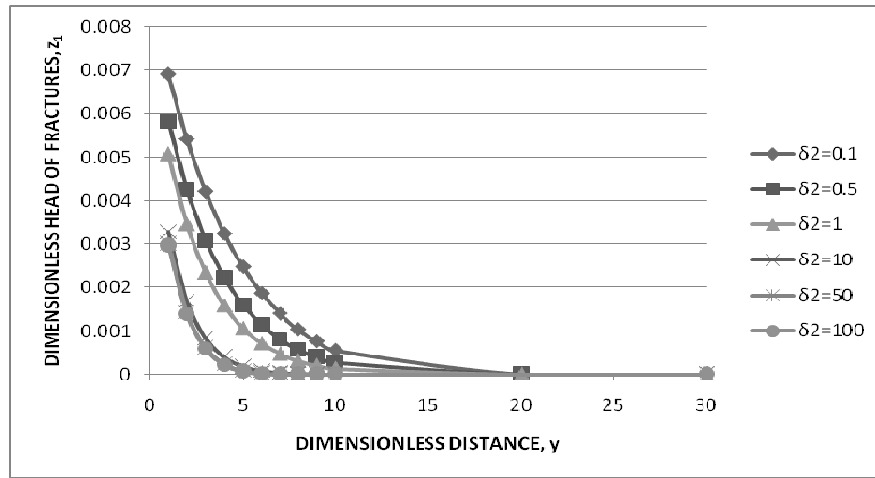


Figure 4.44: Dimensionless piezometric head of fractures z_1 vs. dimensionless distance y for different values of δ_2 at $\theta = 0.5$

4.3.5.3 Effect of δ_2 on the dimensionless head of blocks

Flow mechanism for blocks by neglecting transmissivity is formulated in equation (2.5) as:

$$S_2 \frac{\partial h_2}{\partial t} = \varepsilon T_2 (h_1 - h_2), \quad L < x < \infty, \quad t > 0 \quad (2.5)$$

Larger shape factor ε yields larger δ_2 and volume from blocks to fractures increases in turn resulting a higher rate of piezometric head of blocks with respect to time as can be seen from Figure 4.45.

In these analyses from Figure 4.40 to Figure 4.46, different values of δ_2 is used to account for the change in shape factor of aquifer geometry keeping η_2 and λ_2 constant for given length of aquifer. The shape factor of aquifer depends on the number of fractures and characteristic dimension of matrix block. If fracture number increases, the shape factor increases. For larger block matrix, the shape factor becomes smaller.

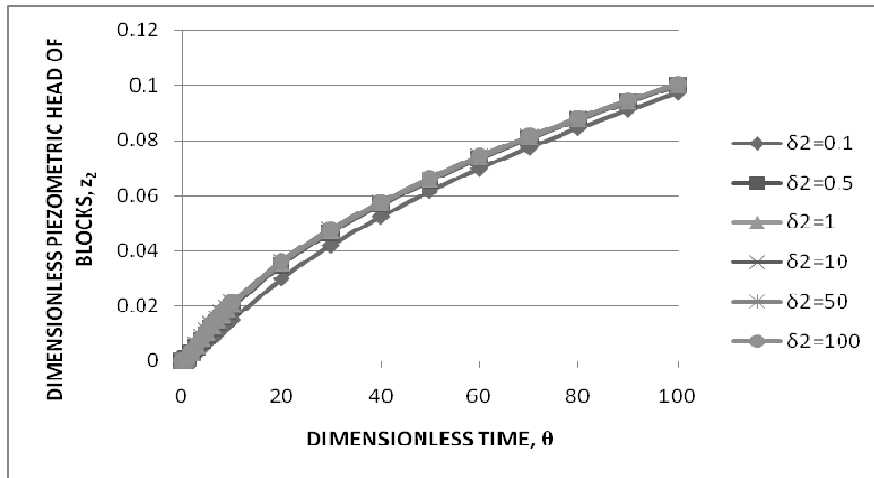


Figure 4.45: Dimensionless piezometric head of blocks z_2 vs. dimensionless time θ for different values of δ_2 at $\gamma=5$

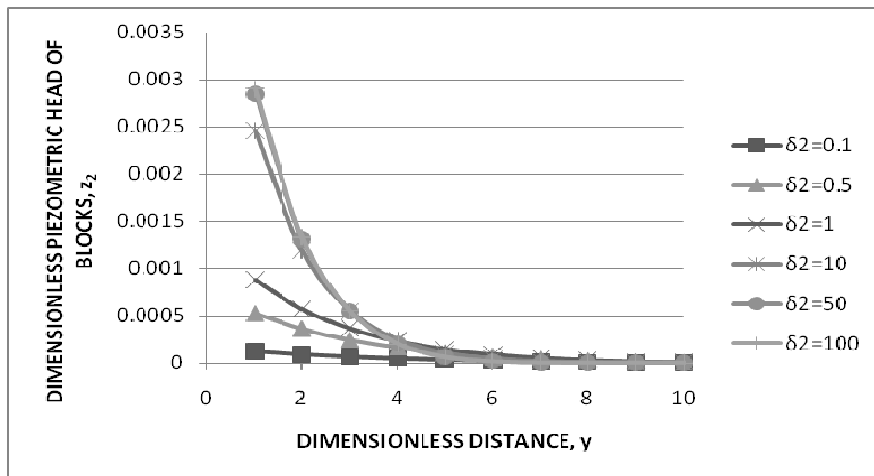


Figure 4.46: Dimensionless piezometric head of blocks z_2 vs. dimensionless distance γ for different values of δ_2 at $\theta = 0.5$

4.4 Concluding Remarks

Results of graphs illustrate the behavior of flow pattern in each medium. Equations of composite aquifer can be further simplified to equations of finite, semi-infinite aquifer by changing boundary conditions and aquifer parameters. The results of composite aquifer with altered aquifer parameters can then be compared to equations of finite and semi-infinite aquifer. Next chapter exemplifies such special cases and compares the results of composite aquifer solution method.

CHAPTER 5

FURTHER EVALUATION AND DISCUSSION OF PROPOSED SOLUTION: APPLICATION TO SPECIAL CASES

5.1 Introduction

The objective of this chapter is to investigate the possibility of application of the proposed semi-analytical solution to simplified problems which may be considered as special cases of the composite aquifer considered in this research work. In that context, groundwater problems for finite aquifer with impervious boundary and recharge boundary on the right hand side are considered and solved in Laplace domain with prescribed initial and boundary conditions. In both cases, solutions are inverted numerically by Stehfest algorithm and these results are compared with the results of Stehfest algorithm developed for composite aquifer with extreme inputs for transmissivity coefficients of fractures and blocks.

5.2 One Dimensional Transient Flow in a Finite Aquifer with Impervious Boundary under Constant Discharge

The idealized cross section of a finite confined aquifer with impervious boundary on the right hand side is shown in Figure 5.1. Flow in this finite confined aquifer depends on time and space. As in the case of composite aquifer, for mathematical simplification, partial differential equation of groundwater flow is

converted to ordinary differential equation by Laplace transform and it is solved for piezometric head with known initial and boundary conditions.

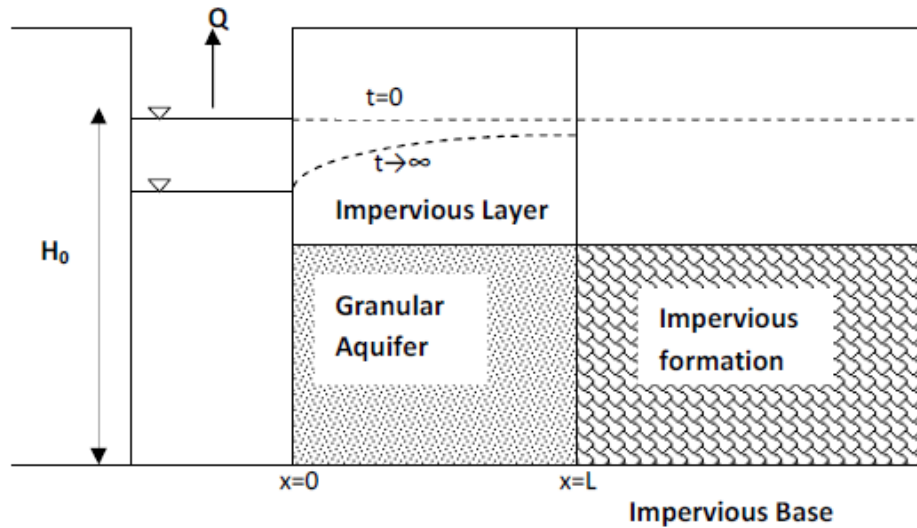


Figure 5.1: One dimensional transient flow in a finite aquifer with impervious boundary under constant discharge.

Governing differential equation for finite aquifer is given in equation (2.1) and initial condition for this case is stated in equation (2.7). Boundary condition at the stream-aquifer interface is the same as equation (2.10). At the impervious boundary of finite aquifer, condition may be written as:

$$\lim_{x \rightarrow L} \frac{\partial h_0}{\partial x} = 0, \quad x=L, \quad t>0 \quad (5.1)$$

Non-dimensional forms of governing differential equation (2.1), initial condition in equation (2.7), boundary condition at the stream-aquifer interface in equation (2.10) are derived in equations (2.25), (2.28) and (2.31) respectively.

Boundary condition for impervious end of granular finite aquifer is given as:

$$\lim_{y \rightarrow 1} \frac{\partial z_0}{\partial y} = 0, y=1, \theta > 0 \quad (5.2)$$

Dimensionless partial differential equation with initial and boundary conditions are transformed to Laplace domain and general solution for \bar{z}_0 is the same as the expression given in equation (2.39). Laplace form of boundary condition at stream-aquifer interface is the same as equation (2.40) and Laplace transform of equation (5.2) is given as:

$$\lim_{y \rightarrow 1} \frac{\partial z_0}{\partial y} = 0, y = 1, \theta > 0 \quad (5.3)$$

Using boundary condition in equation (2.40), relation between constants of integration, A and B, given in equation (2.39) is derived as:

$$A = B e^{2\sqrt{p}} \quad (5.4)$$

By using boundary condition in equation (5.3) and substitution of relation given in equation (5.4), B is obtained as:

$$B = \frac{Q_b}{(e^{2\sqrt{p}} - 1)\sqrt{p}} \quad (5.5)$$

Then, constant B is inserted to equation (5.4) and A is obtained as:

$$A = \frac{Q_b}{(e^{2\sqrt{p}} - 1)\sqrt{p}} e^{2\sqrt{p}} \quad (5.6)$$

Laplace domain solution for one dimensional transient flow in finite aquifer with impervious boundary under constant discharge is obtained by the substitution of (5.5) and (5.6) into equation (2.39) as:

$$\bar{z}_0 = \frac{Q_b e^{2\sqrt{p}}}{(e^{2\sqrt{p}} - 1)\sqrt{p}} e^{-\sqrt{p}y} + \frac{Q_b}{(e^{2\sqrt{p}} - 1)\sqrt{p}} e^{\sqrt{p}y} \quad (5.7)$$

Equation (5.7) is the Laplace form of piezometric head of finite granular aquifer. To get the results in real time domain, equation (5.7) is inserted into equation (2.67) and numerical inversion is applied by Stehfest algorithm.

Subroutine computing dimensionless piezometric head in finite granular aquifer with impervious boundary in real time domain by Stehfest algorithm is given in Appendix E. The results obtained by equation (2.67) are compared with the results of composite aquifer solution by Stehfest algorithm for small transmissivity values of fractures and blocks in the semi-infinite fractured rock region. For very small values of fracture and block transmissivity, semi-infinite fractured rock acts as if it is impervious and then the system solution is expected to approach to the solution of finite granular aquifer with impervious boundary. For small transmissivity values of fractures and blocks, λ_1 , λ_2 and δ_2 become small in turn. Following aquifer values and parameters are considered for this hypothetical aquifer to demonstrate the impervious behavior of strata.

$$\lambda_1 = 10^{-8}, \lambda_2 = 10^{-8}, \eta_1 = 0.2, \eta_2 = 2, Q_b = 0.06, \delta_2 = 5 \times 10^{-7}$$

Figure 5.2 illustrates the comparison between dimensionless piezometric head of finite aquifer with impervious boundary on the right hand side and dimensionless piezometric head obtained by composite aquifer solution with very small transmissivity values for a series of dimensionless distance. Figure 5.3 illustrates the same comparison as in Figure 5.2. The results are plotted on the same chart as in Figure 5.4 and Figure 5.5. Figure 5.4 illustrates the variation of dimensionless piezometric head with dimensionless distance at $\theta=0.05$ for finite aquifer with impervious boundary on the right hand side and composite aquifer solution. The variation of dimensionless piezometric head with dimensionless time at $y=0.5$ is shown in Figure 5.5.

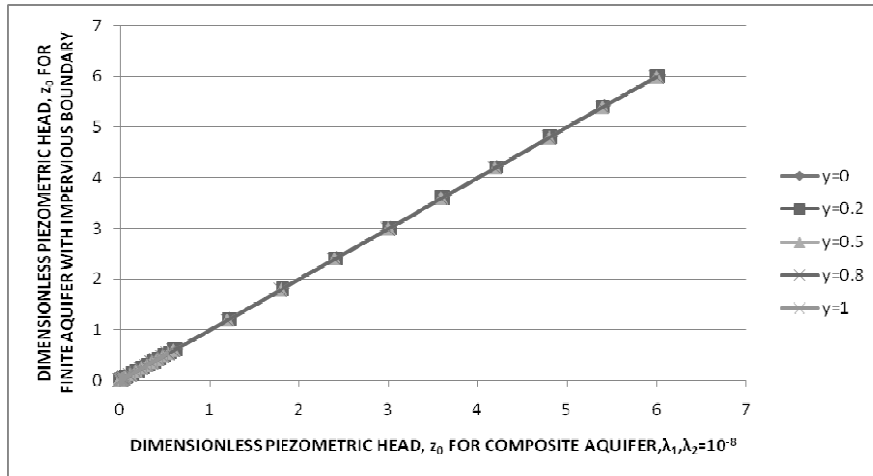


Figure 5.2: Dimensionless piezometric head for finite aquifer with impervious boundary solution vs. dimensionless piezometric head for composite aquifer solution when $\lambda_1 = 10^{-8}$, $\lambda_2 = 10^{-8}$ for different values of dimensionless distance

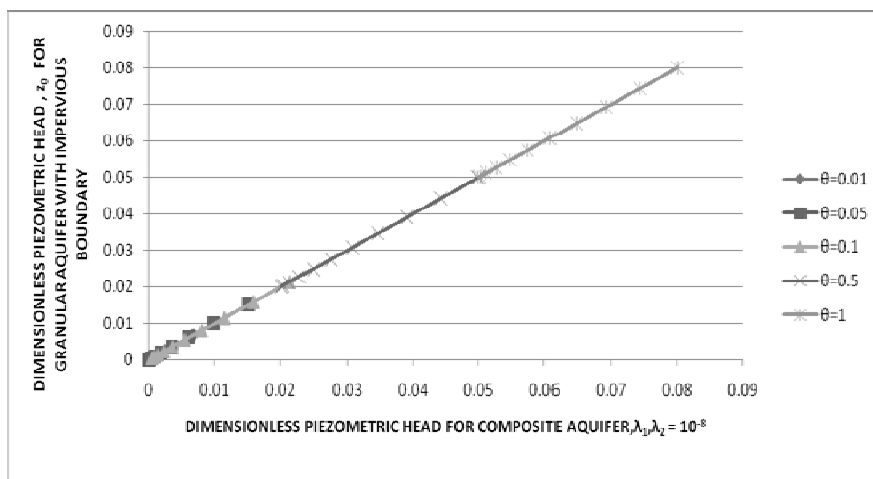


Figure 5.3: Dimensionless piezometric head for finite aquifer with impervious boundary solution vs. dimensionless piezometric head for composite aquifer solution when $\lambda_1 = 10^{-8}$, $\lambda_2 = 10^{-8}$ for different values of dimensionless time.

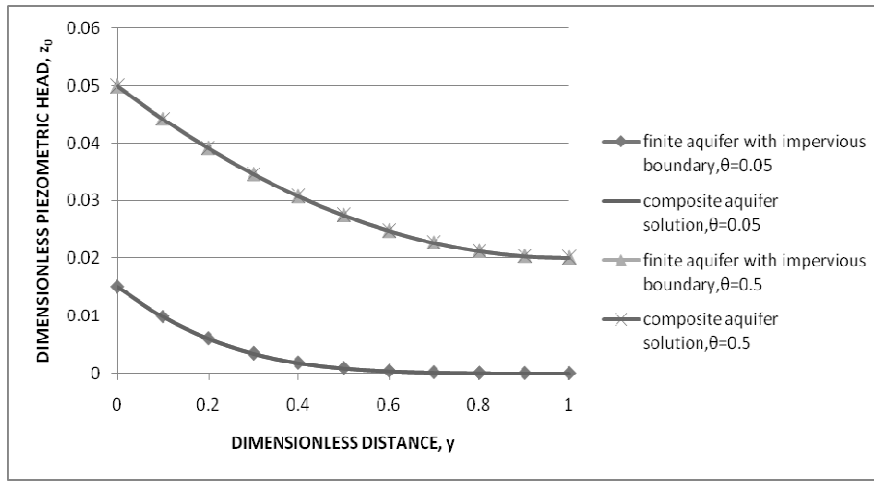


Figure 5.4: Dimensionless piezometric head vs. dimensionless distance at $\theta=0.05$ and $\theta=0.5$

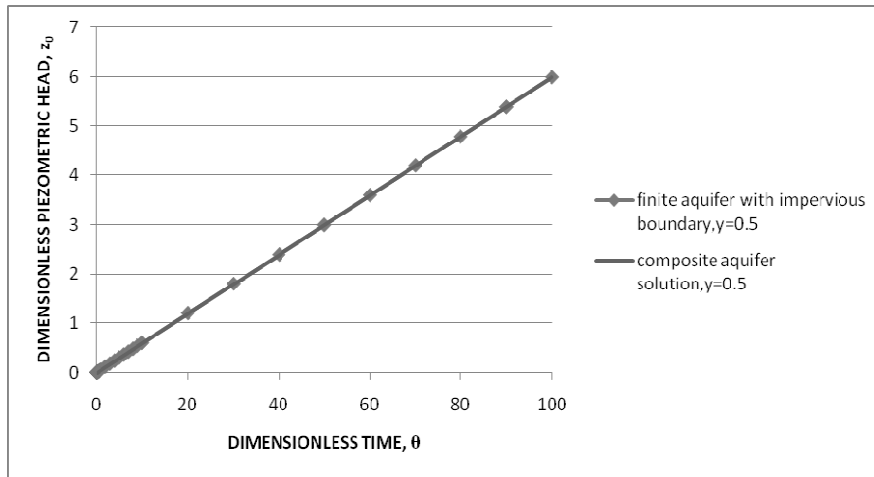


Figure 5.5: Dimensionless piezometric head vs. dimensionless time at $y=0.5$

As expected, the results of composite aquifer obtained by inserting very small transmissivity ratios for fractures and blocks, λ_1 and λ_2 is exactly the same as the solution derived for finite aquifer with impervious boundary. This

comparison proves the correctness and precision of the proposed methodology for composite aquifer. It also shows further the accuracy of the Stehfest's methodology for numerical inversion.

5.3 One Dimensional Transient Flow in a Finite Aquifer with Recharge Boundary under Constant Discharge

The idealized cross section of a finite confined aquifer bounded by stream on the right hand side is shown in Figure 5.6. Finite aquifer is bounded by streams at both ends and water is continuously discharged at one side. It is assumed that no fluctuations in the water level on the right hand side occur.

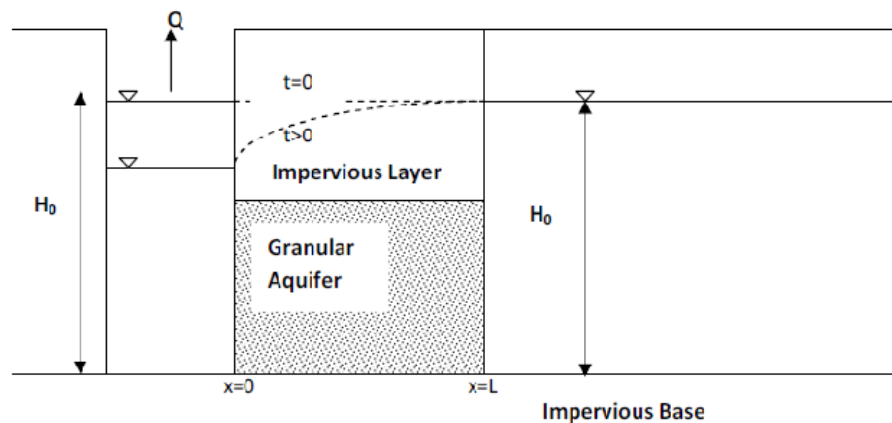


Figure 5.6: One dimensional transient flow in a finite aquifer with recharge boundary under constant discharge

Equation (2.1) is the governing one dimensional partial differential equation for this case too. The only difference is the boundary condition on the right hand side boundary:

$$h_0 = H_0, x = L, t > 0 \quad (5.8)$$

Initial condition for this case is the same as equation (2.7).

Boundary condition given in equation (5.8) is converted to dimensionless form as:

$$z_0 = 0, y=1, \theta > 0 \quad (5.9)$$

These conditions are transferred to Laplace domain in order to eliminate the complexity due to time derivative such that partial differential equation is simplified to ordinary differential equation. General expression for Laplace solution of dimensionless piezometric head for finite aquifer with recharge boundary is the same as equation (2.39) derived for composite aquifer and finite aquifer with impervious boundary.

Boundary condition in Laplace domain at the stream-aquifer interface is the same as equation (2.40). The Laplace form of equation (5.9) is:

$$\bar{z}_0 = 0, y=1, \theta > 0 \quad (5.10)$$

Using boundary condition in equation (5.10), relation between constants of integration, A and B, in equation (2.39) is found as:

$$A = -Be^{2\sqrt{p}} \quad (5.11)$$

Equation (5.11) is inserted to boundary condition in (2.40) and B is obtained as:

$$B = -\frac{Q_b}{(e^{2\sqrt{p}} + 1)\sqrt{p}} \quad (5.12)$$

With known coefficient B, A is obtained by substituting equation (5.12) into equation (5.11) as:

$$A = \frac{Q_b}{(e^{2\sqrt{p}} + 1)\sqrt{p}} e^{2\sqrt{p}} \quad (5.13)$$

Inserting coefficients A and B given in equations (5.13) and (5.12) respectively into (2.39), dimensionless Laplace domain solution for piezometric head in finite aquifer with recharge boundary is obtained as:

$$\frac{-}{z_0} = \frac{Q_b e^{2\sqrt{p}}}{(e^{2\sqrt{p}} + 1)\sqrt{p}} e^{-\sqrt{p}y} - \frac{Q_b}{(e^{2\sqrt{p}} + 1)\sqrt{p}} e^{\sqrt{p}y} \quad (5.14)$$

As in the case of finite aquifer with impervious boundary, dimensionless Laplace form of piezometric head in finite aquifer with recharge boundary is converted to real time domain by equation (2.67). Subroutine computing dimensionless piezometric head in finite granular aquifer with recharge boundary in real time domain by Stehfest algorithm is given in Appendix F. The results obtained by equation (2.67) are compared with the results of composite aquifer solution by Stehfest algorithm for large transmissivity values of fractures and blocks in the semi-infinite fractured rock region. For very large values of fracture and block transmissivity, semi-infinite fractured rock acts as if it is lake of semi-infinite length and then the system solution is expected to approach to the solution of finite granular aquifer with recharge boundary. For large transmissivity values of fractures and blocks, λ_1 , λ_2 and δ_2 become large in turn. Following aquifer values and parameters are considered for this hypothetical aquifer to demonstrate the groundwater flow behavior.

$$\lambda_1 = 10^8, \lambda_2 = 10^8, \eta_1 = 0.2, \eta_2 = 2, Q_b = 0.06, \delta_2 = 5 \times 10^9$$

Figure 5.7 illustrates the comparison between dimensionless piezometric head of finite aquifer with recharge boundary on the right hand side and dimensionless piezometric head obtained by composite aquifer solution with very large transmissivity values for a series of dimensionless distance. Figure 5.8 illustrates the same comparison as in Figure 5.7.

The results are plotted on the same chart as in Figure 5.9 and Figure 5.10. Figure 5.9 illustrates the variation of dimensionless piezometric head with dimensionless distance at $\theta=0.05$ for finite aquifer with recharge boundary on the right hand side and composite aquifer solution. The variation of dimensionless piezometric head with dimensionless time at $\gamma=0.5$ is shown in Figure 5.10.

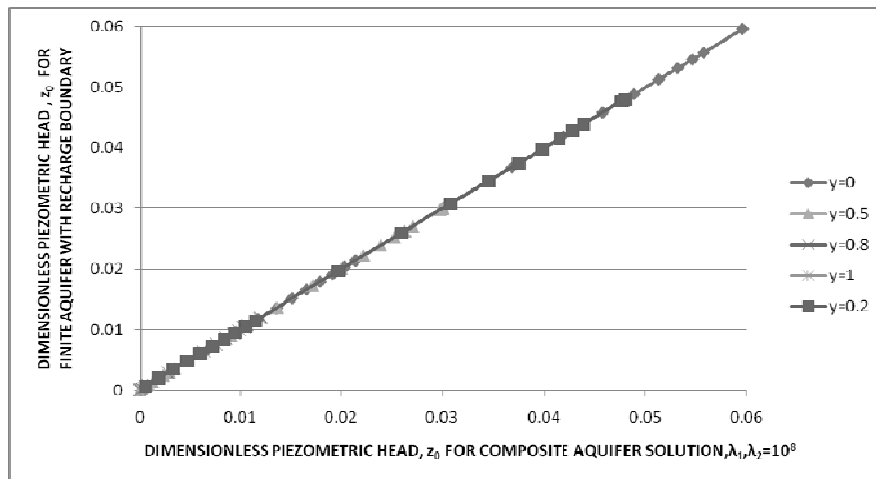


Figure 5.7: Dimensionless piezometric head for finite aquifer with recharge boundary solution vs. dimensionless piezometric head for composite aquifer solution when $\lambda_1=10^8, \lambda_2=10^8$ for different values of dimensionless distance

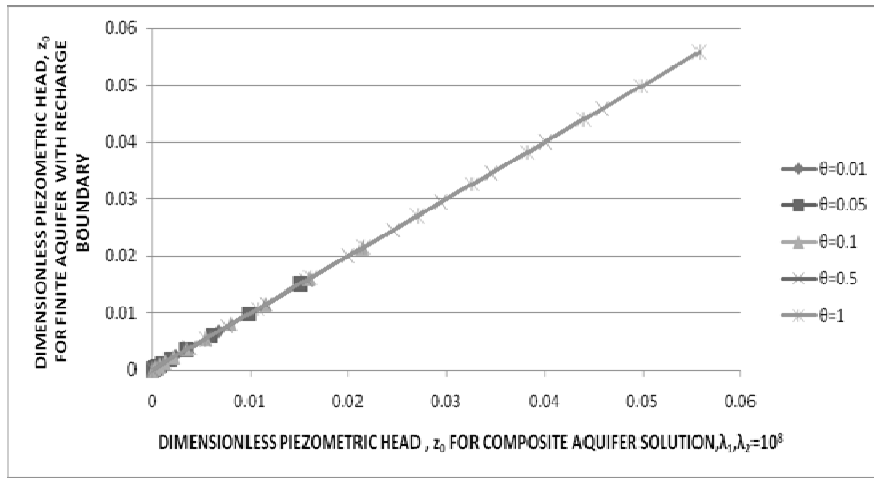


Figure 5.8: Dimensionless piezometric head for finite aquifer with recharge boundary solution vs. dimensionless piezometric head for composite aquifer solution when $\lambda_1=10^8, \lambda_2=10^8$ for different values of dimensionless time

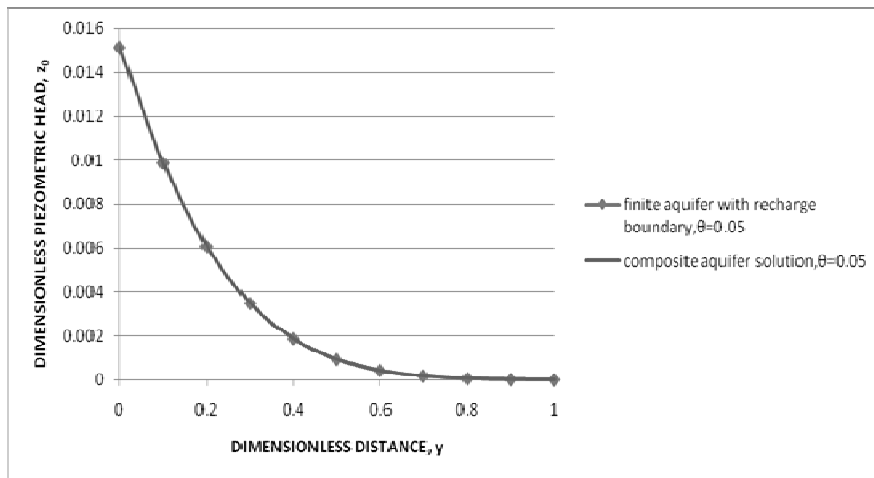


Figure 5.9: Dimensionless piezometric head vs. dimensionless distance at $\theta=0.05$

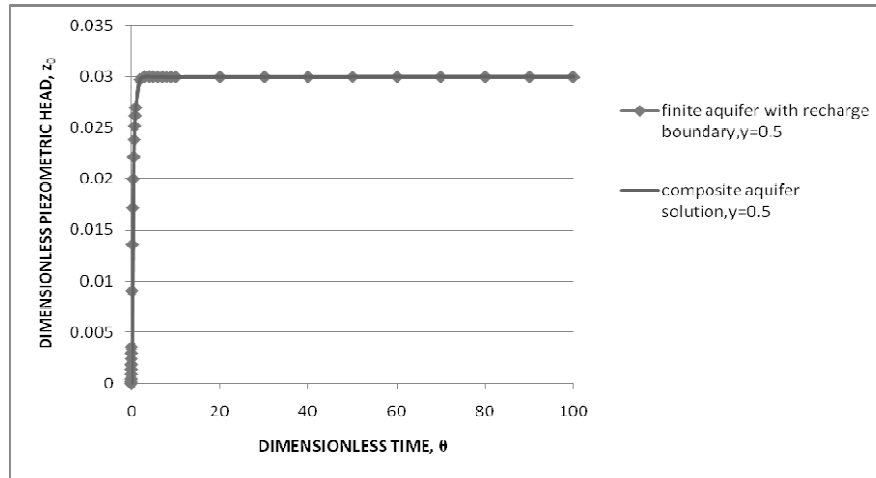


Figure 5.10: Dimensionless piezometric head vs dimensionless time at $y=0.5$

5.3.1 Steady State Condition

Figure 5.10 illustrates the behavior of finite aquifer with recharge boundary and it is evident from the figure that after a relatively short time from discharge excitation from stream, steady state condition is reached on both streams and re-equilibrium state is established in a short time period. For steady-state condition in finite aquifer with recharge boundary, the equation of groundwater flow is rather simplified to:

$$\frac{\partial^2 z_0}{\partial y^2} = 0, \quad 0 < y < 1, \quad \theta > 0 \quad (5.15)$$

with boundary conditions same as equations given in (2.31) and (5.9). Expression for z_0 is obtained as:

$$z_0 = C_1 y + C_2 \quad (5.16)$$

where C_1 and C_2 are coefficients of integration and obtained from substitution of boundary conditions as:

$$C_1 = -Q_b \quad (5.17)$$

$$C_2 = Q_b \quad (5.18)$$

By substitution of equations (5.17) and (5.18) into (5.16), z_0 is obtained as:

$$z_0 = -Q_b y + Q_b \quad (5.19)$$

Results of steady state conditions are compared with the solutions of transient composite aquifer conditions with large transmissivity and finite homogeneous aquifer by Laplace transformation.

From Figure 5.12, it can be seen that steady state condition intersects transient flow conditions at $\theta=2$ after start of pumping indicating steady flow conditions reached. As can be seen from Figure 5.11, at $\theta=10$ steady state flow conditions have already been reached.

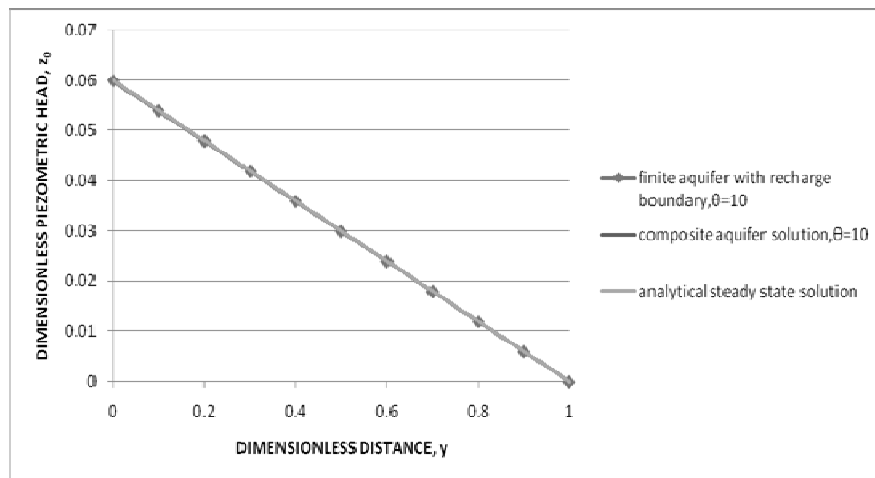


Figure 5.11: Dimensionless piezometric head vs. dimensionless distance and steady state condition at $\theta=10$

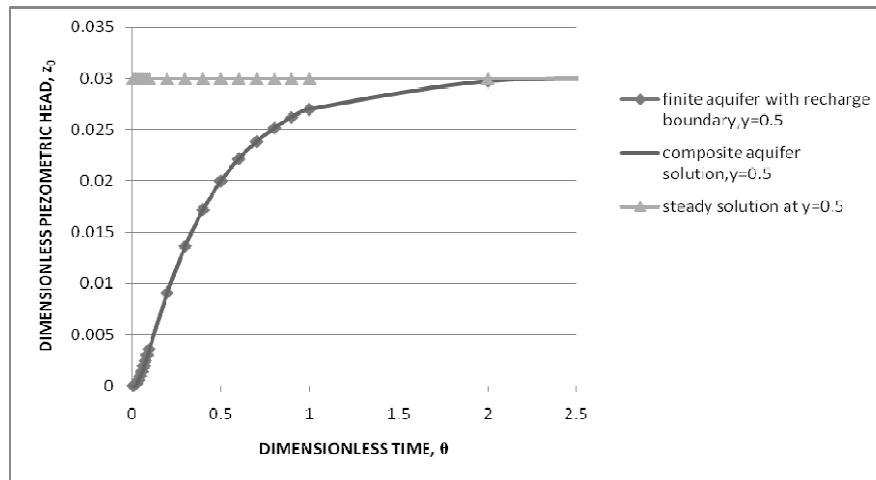


Figure 5.12: Dimensionless piezometric head vs. dimensionless time and steady state condition at $y=0.5$

5.4 Concluding Remarks

As can be seen from charts, the results of composite aquifer solution with small and large transmissivity values are exactly the same as the results of finite aquifer with impervious boundary and recharge boundary on the right hand side, respectively. With the application of semi-analytical proposed method to these special cases, correctness of Stehfest Algorithm is further verified.

CHAPTER 6

SUMMARY AND CONCLUSION

In this, one dimensional transient flow under constant discharge from stream adjacent to composite aquifer is considered. The aim is to utilize groundwater reserve in composite aquifer, which is a typical formation in arid regions, composed of semi-infinite fractured rock and finite alluvial deposit. For this purpose, flow in such formations is analyzed by the determinations of piezometric heads in the parts comprising composite aquifer; the granular aquifer, fractures and blocks respectively. The equations of flow in the parts of the composite aquifer are the equations of continuity (conservation of mass) combined with the Darcy's Law. For the interporosity flow in fractured rock, the double porosity conceptual approach, with pseudo steady state flow assumption, is considered to account water exchange between fractures and rocks.

In order to obtain independent solutions from discharge, piezometric head, and other parameter specific to the problem, the equations are converted to non-dimensional forms. The mathematical simplifications have been made by eliminating time component using Laplace transforms. With these eliminations, the partial differential equations are simplified to ordinary differential equations and become easier to handle. However, the inversion of semi-analytical Laplace domain solutions for piezometric heads in groundwater flow applications is difficult due to analytical complex integration and it requires advanced mathematical techniques. Real time forms of Laplace solutions are obtained by

Stehfest's numerical inversion method. In order to validate the correctness of the results, analytically available groundwater problems are solved by Stehfest method, number of terms is tested and results of the numerical solution methods are compared with the analytical solutions. The results of each cases yield exactly the same results and the method is verified.

Stehfest algorithm is evaluated by subroutines in VBA by suitable data of aquifer parameters taken from literature and a hypothetical aquifer is considered accordingly. Results show that, for finite granular aquifer, flow conditions remain at the earlier times of disturbance, $\theta=0.05$. However flow behavior of granular aquifer approach to almost steady case at $\theta=10$. For semi-infinite fractured rock, flow conditions remain transient even at the very late times such as $\theta=100$. Initial and boundary conditions are checked whether the results of algorithm are correct. The equality of piezometric head and flux equality between fractures and granular aquifer are checked at the interface. In addition, the gradient of flow with respect to space for granular aquifer and fractures depend on the transmissivity contrast λ_1 , in between. Due to exchange of water flow exchange between blocks and fractures, the similar flow pattern of fractures and blocks are obtained. The difference of piezometric head has reached the peak value at earlier times from the start of pumping. Flow from blocks to fractures occurs at the instant of pumping and blocks has not yet reflect the excitation of the system. Equilibrium between fractures and blocks is established and flow exchange is reduced in time.

Sensitivity analyses are carried out to illustrate the effect of dimensionless aquifer parameters that reflect the geometry, transmissivity contrast and storage contrast of the parts of aquifer rather than individual aquifer characteristics. Hydraulic gradients at the granular aquifer and fractured rock interface are dependent on transmissivity ratio, λ_1 . In nature, since the transmissivity of fractures is greater than granular aquifer, this ratio is greater than the unity.

As the transmissivity contrast between granular aquifer and fractures increases, the drawdown for all parts of the aquifer decreases.

The transmissivity contrast between blocks and granular aquifer λ_2 does not alter the results since block transmissivity is neglected in the analysis.

Drawdown is less for higher storage contrast between granular aquifer and fractures; η_1 . Similar patterns of flow are obtained for η_2 , storage contrast between granular aquifer and blocks.

The aquifer parameter δ_2 accounts for the change in shape coefficient ε by keeping all other parameters constant. For fractures, as ε increases volume of water transfer increases and rate of piezometric head with time decreases in turn for larger δ_2 . For blocks, pattern is reversed due to flow exchange; that is for larger δ_2 , the rate of piezometric head with time increases.

Evaluations on proposed semi-analytical method to simplified forms of composite aquifer are obtained by altering fracture and block transmissivity values. Comparison is made between composite aquifer with small transmissivity values for fractured and finite aquifer with impervious boundary on the right hand side. Likewise, another comparison case is between composite aquifer with large transmissivity values for fractured and finite aquifer with recharge boundary on the right hand side. Subroutines are developed for finite aquifer under constant discharge with impervious boundary and recharge boundary in order to compare the subroutine of composite aquifer solutions with extreme transmissivity values of fractures and blocks. The results of composite aquifer with fracture and block transmissivity values 10^{-8} approaches to the solution of finite aquifer with impervious boundary and the results of composite aquifer with fracture and block transmissivity values 10^8 approach to the solution of finite aquifer with recharge boundary. The steady state of flow in finite aquifer with recharge boundary on the right hand side is reached at earlier stage of excitation, $\theta=2$.

These exact matches further verify the correctness of Stehfest Algorithm and proves the applicability of the method in groundwater problems.

REFERENCES

Bai, M., Elsworth, D., and Roegiers, J.-C., (1993),Multiporosity/Permeability Approach to the Simulation of Naturally Fractured Reservoirs. Water Resources Research, Vol.29, No.6, p.1621-1633.

Barenblatt, G., U.P., Zheltov, and G.H., Kochina, (1960).Basic concepts in the theory of seepage of homogeneous liquids in fractured rocks (strata). J.Appl.Math.Mech.Engl.Transl.v.24. pp.1286-1303.

Bear, J., (1972).Dynamics of Fluids in Porous Media, American Elsevier, New York, 1-26,785 pp.

Bear, J., (1979).Hydraulics of Groundwater. McGraw Hill Book Comp. New York.

Bear, J., Tsang, C.F., and de Marsily, G. (1993). Flow and contaminant transport in fractured rock. Academic Press, San Diego, USA.

Budd, D., and Vacher, H., (2004),Matrix permeability of the confined Floridan Aquifer, Florida, USA. Hydrogeology Journal, v.12, no 5., p.531-549(19).

Bureau of Reclamation (1997), Ground Water Manual. U.S, Government Printing Office, Washington D.C.

Carslaw, H.S. and Jaeger, J.C.,(1959).Conduction of Heat in Solids.2nd Ed., Oxford University Press, London, England.

Chen, C-W., Chen, J-S., Liu, C-W., and Yeh, H-D.,(1996).A Laplace transform for tracer tests in a radially convergent flow field with upstream dispersion, Journal of Hydrology v.183,263-275.

Delleur, W.J., (2006).Handbook of Groundwater Engineering. Second Edition. CRC Press, Taylor and Francis Group,LLC, Boca Raton, FL.

Dündar, S.,(2005). Solution of One-Dimensional Transient Flow in Fractured Aquifers by Numerical Laplace Transform Inversion, MS Thesis METU, Ankara, Turkey.

Dündar, S., and Önder, H.(2006).One dimensional Transient Flow in a Semi-Infinite Fractured Aquifer under Constant Discharge Condition. Proceedings, Seventh International Congress on Advances in Civil Engineering, October 11-13, 2006, İstanbul, Turkey.

Edwards, C.H. and Penney, E.D (2004).Differential Equations, Computing and Modeling: New Jersey, Pearson Prentice Hall Education, INC.

Engelder,T., Fiscer, M.P., and Gross, M.R.(1993).Geological Aspects of Fracture Mechanics, A Short Course Manual. Geological Society of America, 281 pp.

Ferris, J.G, Knowles, D.B., Brown, R.H., and Stallman, R.W.,(1962),Theory of Aquifer Tests. U.S. Geol .Survey Water-Supply Paper 1536-E, p 69-174

Hall, P.; computer programs by Chen. J. (1996). Water Wells and Aquifer Test Analysis. Water Resources Publications, LLC, Highlands Ranch, Colorado, USA.

Hunt, B., (2005).Visual Basic Programs for Spreadsheet Analysis. GROUND WATER., vol.43, no.1, pp 138-141.

Huyakorn, P.S., and Pinder, G.F., (1983), Computational Methods in Subsurface Flow. Academic Press, New York.

Jahan, N. and Jelmer,T.,(2008). A New Approach of Well Test Simulator Development: Stehfest Algorithm in VBA (Excel). In: Proceedings of International Conference on Chemical Engineering 2008 ICChE2008, 29-30 December, Dhaka, Bangladesh.

Kazemi, H., (1969). Pressure transient analysis of naturally fractured reservoirs with uniform fracture distribution, Soc. Pet. Eng .J. Trans. AIME, v.246, pp. 451-462.

Kazemi , H., Seth, M.S. and Thomas, G.W. (1969). The interpretation of interference tests in naturally fractured reservoirs with uniform fracture distribution, Soc.Pet.Engng. J.9, 463-472.

Liu , J., Bodvarsson, G.S., Wu, Y-S, (2003).Analysis of flow behavior in fractured lithophysal reservoirs. Journal of Contaminant Hydrology,vol.62-63,pp 189-211.

Lohman, S.W., (1972) Geological Survey Professional Paper 708.Groundwater Hydraulics.US Government Printing Office,Washington,1972,40-41

Moench, A.F., (1984).Double porosity models for a fissured groundwater reservoir with fracture skin. Water Resources. Res., v.20, no.7, pp. 831-846.

Moench, A. and Ogata, A.(1982),Analysis of constant discharge wells by numerical inversion of Laplace transform solutions. in Rosenshein, J.S. and Bennett, G.D., EDS., Groundwater Hydraulics: Water Resources Monograph 9,American Geophysical Union, Washington D.C.,p.146-170.

Najurieta, H.L., (1980).A Theory for pressure transient analysis in naturally fractured reservoirs, J.Petrol.Tech., pp 1241-1250

Önder, H., (1989). Analysis of groundwater flow in a composite aquifer. Progress Report submitted to King Abdulaziz University

Önder, H., (1997).Analysis of one-dimensional groundwater flow in a non-uniform aquifer. Journal of Hydraulic Engineering, August 1997, 732-736.

Önder, H. (1998). One dimensional transient flow in a finite fractured aquifer. Hydrological Sciences-Journal des Sciences Hydrologiques, 43(2) April 1998, 243-260.

Stehfest, H., (1970).Numerical Inversion of Laplace Transforms. Communications of the ACM, 13(1)

Streltsova, T.D., (1975), Unsteady unconfined flow into a surface reservoir. Journal of Hydrology, v.27, 95-110.

Streltsova, T.D., (1976). Hydrodynamics of groundwater flow in a fractured formation, Wat. Resources. Res. 12(3), 405-414.

Streltsova, T.D.,(1988).Well Testing in Heterogeneous formations. John Wiley, New York, USA.

Walton, W.C.,(2007). Aquifer Test Modeling. CRC Press, Taylor and Francis Group, LLC, Boca Raton, FL.

Warren, J.E and Root, P.J., (1963).The behavior of naturally fractured reservoirs. Soc.Pet.Eng J.3, 245-255.

Zimmerman, R.W., Chen, G., Hodger, T. and Bodversson , G.S.(1993).A numerical dual-porosity model with semi-analytical treatment of fracture/matrix flow, Water Resources Res.vol 29,pp 2127-37.

APPENDIX A

SUBROUTINE IN VBA EXCEL TO SOLVE STEHFEST ALGORITHM FOR SEMI-INFINITE HOMOGENEOUS AQUIFER UNDER CONSTANT DISCHARGE

The numerical inversion method proposed by Stehfest to find real time solution for the piezometric head in semi-infinite homogeneous aquifer is:

$$h_n(x, t) \approx \frac{\ln 2}{t} \sum_{i=1}^N V_i \bar{h}(x, i \frac{\ln 2}{t}) \quad (3.13)$$

$$V_i = (-1)^{i+\frac{N}{2}} \sum_{k=\text{int}(\frac{i+1}{2})}^{\min(i, \frac{N}{2})} \frac{k^{\frac{N}{2}} (2k)!}{(\frac{N}{2} - k)! k! (k-1)! (i-k)! (2k-1)!} \quad (2.66)$$

where

h is the real time solution for the piezometric head in semi-infinite homogeneous aquifer.

\bar{h} is the analytical solution obtained by Laplace transform for the piezometric head in semi-infinite homogeneous aquifer and it is given below as:

$$\bar{h}(x, p) = \frac{Q_d v^{0.5}}{2p^{1.5}} e^{-\sqrt{\frac{p}{v}}x} \quad (3.12)$$

Subroutine in VBA is executed to compute $h(x, t)$ from $\bar{h}(x, p)$ is given below as:

Function pdt_semi_infinite(n, nu, Qd, t, x) As Double

'x indicates distance

't indicates time

Dim i, k, kbg, knd, nh, sn As Integer

Dim v(1 To 50), g(1 To 50), h(1 To 25) As Double

Dim d, r As Double

Dim L, pds_semi_infinite, a, p As Double

Const ln2 = 0.693414718105599

r = n Mod 2

If r = 1 Then

 MsgBox "Error: n must be even"

ElseIf n > 50 Then

 MsgBox "Error:n must be less than 50"

Else

 g(1) = 1

 nh = Int(n / 2)

 d = nh Mod 2

 sn = 2 * d - g(1)

For i = 1 To n

 g(i + 1) = i * g(i)

Next i

h(1) = 2 / g(nh)

```

For i = 2 To nh
h(i) = (i ^ nh) * g(2 * i + 1) / (g(nh - i + 1) * g(i + 1) * g(i))
Next i
a = ln2 / t
pdt_semi_infinite = 0
For i = 1 To n
kbg = Int((i + 1) / 2)
knd = WorksheetFunction.Min(i, nh)
v(i) = 0
For k = kbg To knd
v(i) = v(i) + h(k) / (g(i - k + 1) * g(2 * k - i + 1))
Next k
v(i) = sn * v(i)
sn = -sn
p = a * i
pds_semi_infinite = ((Qd * Sqr(nu)) / (2 * (p ^ 1.5))) * Exp(-(p / nu) ^ 0.5) * x
pdt_semi_infinite = pdt_semi_infinite + v(i) * pds_semi_infinite
Next i
pdt_semi_infinite = a * pdt_semi_infinite
End If
End Function
Sub semi_infinite_aquifer()
Dim number_of_elements, diffusivity, dim_discharge, time, distance As Double
Dim m, j As Integer
number_of_elements = CDbI(InputBox("even number value", "number of elements",
"Enter an even number for elements in calculation smaller than 50.))
diffusivity = CDbI(InputBox("diffusivity coefficient", "diffusivity coefficient", "enter
diffusivity coefficient in m2/sec.))

```

```

dim_discharge = CDbI (InputBox ("dim_discharge", "dimensionless discharge ", "enter
dim_discharge"))

Cells(1, 1) = "nu= " + "" + CStr(diffusivity) + ", " + "Qd= " + CStr(dim_discharge)

time = 100

distance = 100

m = 2

j = 2

Do While distance < 1000

If distance > 1000 Then Exit Do

Cells(1, j) = distance

Do While time < 1000

If time > 1000 Then Exit Do

Cells(m, 1) = time

Cells(m, j) = pdt_semi_infinite(number_of_elements, diffusivity, dim_discharge, time,
distance)

m = m + 1

time = time + 100

Loop

Do While 1000 < time < 10000

If time > 10000 Then Exit Do

Cells(m, 1) = time

Cells(m, j) = pdt_semi_infinite(number_of_elements, diffusivity, dim_discharge, time,
distance)

m = m + 1

time = time + 1000

Loop

time = time - 1000

Do While 10000 < time < 100000

If time > 100000 Then Exit Do

```

```

Cells(m, 1) = time
Cells(m, j) = pdt_semi_infinite(number_of_elements, diffusivity, dim_discharge, time,
distance)
m = m + 1
time = time + 10000
Loop
time = time - 10000
Do While 100000 < time < 1000000
If time > 1000000 Then Exit Do
Cells(m, 1) = time
Cells(m, j) = pdt_semi_infinite(number_of_elements, diffusivity, dim_discharge, time,
distance)
m = m + 1
time = time + 100000
Loop
time = time - 100000
Do While 1000000 < time < 10000000
If time > 10000000 Then Exit Do
Cells(m, 1) = time
Cells(m, j) = pdt_semi_infinite(number_of_elements, diffusivity, dim_discharge, time,
distance)
m = m + 1
time = time + 1000000
Loop
time = 100
m = 2
j = j + 1
distance = distance + 100
Loop

```

```

Do While 1000 < distance < 10000
If distance > 10000 Then Exit Do
Cells(1, j) = distance
Do While time < 1000
If time > 1000 Then Exit Do
Cells(m, 1) = time
Cells(m, j) = pdt_semi_infinite(number_of_elements, diffusivity, dim_discharge, time,
distance)
m = m + 1
time = time + 100
Loop
Do While 1000 < time < 10000
If time > 10000 Then Exit Do
Cells(m, 1) = time
Cells(m, j) = pdt_semi_infinite(number_of_elements, diffusivity, dim_discharge, time,
distance)
m = m + 1
time = time + 1000
Loop
time = time - 1000
Do While 10000 < time < 100000
If time > 100000 Then Exit Do
Cells(m, 1) = time
Cells(m, j) = pdt_semi_infinite(number_of_elements, diffusivity, dim_discharge, time,
distance)
m = m + 1
time = time + 10000
Loop
time = time - 10000

```

```

Do While 100000 < time < 1000000
If time > 1000000 Then Exit Do
Cells(m, 1) = time
Cells(m, j) = pdt_semi_infinite(number_of_elements, diffusivity, dim_discharge, time,
distance)
m = m + 1
time = time + 100000
Loop
time = time - 100000
Do While 1000000 < time < 10000000
If time > 10000000 Then Exit Do
Cells(m, 1) = time
Cells(m, j) = pdt_semi_infinite(number_of_elements, diffusivity, dim_discharge, time,
distance)
m = m + 1
time = time + 1000000
Loop
time = 100
m = 2
j = j + 1
distance = distance + 1000
Loop
End Sub

```

Table A.1: Analytical solution for semi-infinite homogeneous aquifer under constant discharge for $\nu=0.2$, $Q_d=0.05$

t (sec)	x (m)																			
	100	200	300	400	500	600	700	800	900	1000	2000	3000	4000	5000	6000	7000	8000	9000	10000	
100	0	0	0	0	0	0	0	0	0	0	0	0	0	0	0	0	0	0	0	0
200	0	0	0	0	0	0	0	0	0	0	0	0	0	0	0	0	0	0	0	0
300	0	0	0	0	0	0	0	0	0	0	0	0	0	0	0	0	0	0	0	0
400	0	0	0	0	0	0	0	0	0	0	0	0	0	0	0	0	0	0	0	0
500	7E-14	0	0	0	0	0	0	0	0	0	0	0	0	0	0	0	0	0	0	0
600	6E-12	0	0	0	0	0	0	0	0	0	0	0	0	0	0	0	0	0	0	0
700	2E-10	0	0	0	0	0	0	0	0	0	0	0	0	0	0	0	0	0	0	0
800	2E-09	0	0	0	0	0	0	0	0	0	0	0	0	0	0	0	0	0	0	0
900	1E-08	0	0	0	0	0	0	0	0	0	0	0	0	0	0	0	0	0	0	0
1000	5E-08	0	0	0	0	0	0	0	0	0	0	0	0	0	0	0	0	0	0	0
2000	7E-05	1E-13	0	0	0	0	0	0	0	0	0	0	0	0	0	0	0	0	0	0
3000	0.001	1E-09	0	0	0	0	0	0	0	0	0	0	0	0	0	0	0	0	0	0
4000	0.004	1E-07	9E-15	0	0	0	0	0	0	0	0	0	0	0	0	0	0	0	0	0
5000	0.0099	2E-06	3E-12	0	0	0	0	0	0	0	0	0	0	0	0	0	0	0	0	0
6000	0.0186	1E-05	2E-10	0	0	0	0	0	0	0	0	0	0	0	0	0	0	0	0	0
7000	0.03	5E-05	3E-09	7E-15	0	0	0	0	0	0	0	0	0	0	0	0	0	0	0	0
8000	0.0438	0.0001	3E-08	3E-13	0	0	0	0	0	0	0	0	0	0	0	0	0	0	0	0
9000	0.0595	0.0003	2E-07	6E-12	0	0	0	0	0	0	0	0	0	0	0	0	0	0	0	0
10000	0.0768	0.0007	6E-07	6E-11	1E-15	0	0	0	0	0	0	0	0	0	0	0	0	0	0	0
20000	0.2961	0.0197	0.0005	4E-06	9E-09	6E-12	0	0	0	0	0	0	0	0	0	0	0	0	0	0
30000	0.5372	0.0733	0.0051	0.0002	3E-06	2E-08	7E-11	1E-13	0	0	0	0	0	0	0	0	0	0	0	0
40000	0.773	0.1537	0.0187	0.0013	6E-05	1E-06	2E-08	1E-10	5E-13	3E-15	0	0	0	0	0	0	0	0	0	0
50000	0.9982	0.2513	0.0431	0.0049	0.0004	2E-05	5E-07	9E-09	1E-10	7E-13	0	0	0	0	0	0	0	0	0	0
60000	1.2125	0.3595	0.0778	0.012	0.0013	1E-04	5E-06	2E-07	4E-09	6E-11	0	0	0	0	0	0	0	0	0	0
70000	1.4167	0.474	0.1216	0.0234	0.0033	0.0003	3E-05	1E-06	5E-08	2E-09	0	0	0	0	0	0	0	0	0	0
80000	1.6117	0.5922	0.1729	0.0394	0.0069	0.0009	9E-05	7E-06	4E-07	2E-08	0	0	0	0	0	0	0	0	0	0
90000	1.7985	0.7123	0.2305	0.06	0.0124	0.002	0.0003	3E-05	2E-06	1E-07	0	0	0	0	0	0	0	0	0	0
100000	1.978	0.8332	0.2931	0.0849	0.02	0.0038	0.0006	7E-05	7E-06	5E-07	0	0	0	0	0	0	0	0	0	0
200000	3.4909	1.9964	1.0483	0.5025	0.2189	0.0862	0.0306	0.0098	0.0028	0.0007	1E-12	0	0	0	0	0	0	0	0	0
300000	4.6958	3.0306	1.8505	1.0655	0.5768	0.2928	0.1391	0.0617	0.0255	0.0098	1E-08	0	0	0	0	0	0	0	0	0
400000	5.7269	3.9559	2.6233	1.6663	1.0117	0.5861	0.3235	0.1698	0.0847	0.0401	1E-06	8E-14	0	0	0	0	0	0	0	0
500000	6.6427	4.7981	3.3557	2.2687	1.4805	0.9312	0.5638	0.3283	0.1836	0.0986	2E-05	3E-11	0	0	0	0	0	0	0	0
600000	7.4749	5.5753	4.0491	2.8598	1.9619	1.3059	0.8426	0.5265	0.3183	0.1861	0.0001	2E-09	0	0	0	0	0	0	0	0
700000	8.2429	6.3001	4.7073	3.4349	2.4455	1.6971	1.1471	0.7547	0.4829	0.3003	0.0005	3E-08	8E-14	0	0	0	0	0	0	0
800000	8.9596	6.9818	5.3344	3.9928	2.9255	2.0966	1.4688	1.0051	0.6715	0.4377	0.0014	3E-07	3E-12	0	0	0	0	0	0	0
900000	9.6341	7.6271	5.9339	4.5336	3.3991	2.4995	1.8014	1.2719	0.8792	0.5948	0.0034	2E-06	6E-11	-2E-14	0	0	0	0	0	0
1E+06	10.273	8.2412	6.5089	5.0579	3.8649	2.9024	2.1409	1.5505	1.102	0.7683	0.0067	6E-06	6E-10	0	0	0	0	0	0	0
2E+06	15.453	13.285	11.336	9.5962	8.0585	6.7115	5.5424	4.5375	3.682	2.9609	0.1971	0.0046	4E-05	9E-08	6E-11	2E-14	0	0	0	0
3E+06	19.442	17.214	15.165	13.292	11.588	10.049	8.6664	7.4321	6.3372	5.3723	0.7327	0.0511	0.0017	3E-05	2E-07	7E-10	1E-12	0	0	0
4E+06	22.81	20.546	18.438	16.482	14.677	13.018	11.499	10.116	8.8616	7.7297	1.5366	0.1873	0.0135	0.0006	1E-05	2E-07	1E-09	5E-12	0	0
5E+06	25.78	23.491	21.342	19.33	17.454	15.711	14.096	12.606	11.237	9.9821	2.5127	0.4311	0.0489	0.0036	0.0002	5E-06	9E-08	1E-09	7E-12	0
6E+06	28.466	26.159	23.98	21.926	19.998	18.191	16.504	14.933	13.475	12.125	3.5946	0.7784	0.1201	0.013	0.001	5E-05	2E-06	4E-08	6E-10	0
7E+06	30.937	28.616	26.413	24.327	22.357	20.501	18.757	17.121	15.593	14.167	4.74	1.2161	0.2342	0.0333	0.0035	0.0003	1E-05	5E-07	2E-08	0
8E+06	33.238	30.905	28.683	26.571	24.567	22.671	20.88	19.192	17.606	16.117	5.9218	1.7294	0.3943	0.0692	0.0093	0.0009	7E-05	4E-06	2E-07	0
9E+06	35.4	33.057	30.819	28.685	26.654	24.724	22.894	21.162	19.527	17.985	7.1228	2.3049	0.5999	0.1241	0.0202	0.0026	0.0003	2E-05	1E-06	0
1E+07	37.444	35.094	32.842	30.689	28.634	26.676	24.813	23.044	21.367	19.78	8.3315	2.9307	0.8491	0.2004	0.0382	0.0058	0.0007	7E-05	5E-06	0

Table A.2: Numerical solution by Stehfest for semi-infinite homogeneous aquifer for $N=8$, $\nu=0.2$, $Q_d=0.05$

t(sec)	x(m)																		
	100	200	300	400	500	600	700	800	900	1000	2000	3000	4000	5000	6000	7000	8000	9000	10000
100	-4E-10	-3E-18	-2E-26	-2E-34	-2E-42	-1E-50	-1E-58	-9E-67	-7E-75	-6E-83	-8E-164	-1E-244	0	0	0	0	0	0	0
200	-1E-07	-2E-13	-4E-19	-8E-25	-2E-30	-3E-36	-6E-42	-1E-47	-2E-53	-4E-59	-3E-116	-2E-173	-1E-230	-8E-288	0	0	0	0	0
300	-9E-07	-4E-11	-8E-16	-2E-20	-4E-25	-8E-30	-2E-34	-3E-39	-7E-44	-2E-48	-3E-95	-7E-142	-1E-188	-3E-235	-6E-282	0	0	0	0
400	-3E-06	-7E-10	-7E-14	-6E-18	-5E-22	-5E-26	-4E-30	-4E-34	-4E-38	-3E-42	-1E-82	-4E-123	-2E-163	-6E-204	-2E-244	-8E-285	0	0	0
500	-4E-06	-6E-09	-1E-12	-3E-16	-8E-20	-2E-23	-5E-27	-1E-30	-3E-34	-7E-38	-5E-74	-3E-110	-2E-146	-2E-182	-1E-218	-7E-255	-5E-291	0	0
600	-2E-06	-2E-08	-1E-11	-7E-15	-3E-18	-2E-21	-9E-25	-4E-28	-2E-31	-1E-34	-1E-67	-1E-100	-1E-133	-9E-167	-9E-200	-9E-233	-9E-266	-8E-299	0
700	3E-06	-8E-08	-8E-11	-7E-14	-6E-17	-5E-20	-5E-23	-4E-26	-4E-29	-3E-32	-9E-63	-2E-93	-7E-124	-2E-154	-5E-185	-1E-215	-4E-246	-1E-276	-3E-307
800	1E-05	-2E-07	-3E-10	-5E-13	-6E-16	-9E-19	-1E-21	-2E-24	-2E-27	-3E-30	-8E-59	-2E-87	-6E-116	-1E-144	-4E-173	-9E-202	-2E-230	-6E-259	-2E-287
900	3E-05	-4E-07	-1E-09	-2E-12	-4E-15	-9E-18	-2E-20	-4E-23	-7E-26	-1E-28	-2E-55	-2E-82	-2E-109	-2E-136	-2E-163	-3E-190	-3E-217	-3E-244	-4E-271
1000	4E-05	-8E-07	-3E-09	-8E-12	-2E-14	-6E-17	-2E-19	-5E-22	-1E-24	-4E-27	-1E-52	-3E-78	-7E-104	-2E-129	-5E-155	-1E-180	-4E-206	-1E-231	-3E-257
2000	0.0001	-8E-06	-6E-07	-1E-08	-2E-10	-3E-12	-4E-14	-7E-16	-1E-17	-2E-19	-1E-37	-1E-55	-9E-74	-8E-92	-6E-110	-5E-128	-4E-146	-4E-164	-3E-182
3000	0.0008	2E-05	-4E-06	-3E-07	-1E-08	-3E-10	-1E-11	-4E-13	-1E-14	-4E-16	-7E-31	-1E-45	-2E-60	-4E-75	-6E-90	-1E-104	-2E-119	-3E-134	-6E-149
4000	0.0037	8E-05	-1E-05	-2E-06	-1E-07	-6E-09	-3E-10	-2E-11	-9E-13	-5E-14	-8E-27	-1E-39	-2E-52	-3E-65	-3E-79	-9E-91	-1E-103	-2E-116	-4E-129
5000	0.0096	0.0002	-1E-05	-5E-06	-5E-07	-4E-08	-3E-09	-2E-10	-2E-11	-1E-12	-4E-24	-2E-35	-6E-47	-2E-58	-8E-70	-3E-81	-1E-92	-4E-104	-1E-115
6000	0.0184	0.0002	3E-06	-9E-06	-1E-06	-2E-07	-2E-08	-2E-09	-1E-10	-1E-11	-5E-22	-2E-32	-6E-43	-2E-53	-8E-64	-3E-74	-1E-84	-4E-95	-1E-105
7000	0.0299	0.0002	3E-05	-1E-05	-3E-06	-5E-07	-6E-08	-7E-09	-7E-10	-8E-11	-2E-20	-4E-30	-8E-40	-2E-49	-4E-59	-8E-69	-2E-78	-4E-88	-8E-98
8000	0.0438	0.0002	8E-05	-2E-05	-6E-06	-1E-06	-2E-07	-2E-08	-3E-09	-4E-10	-3E-19	-3E-28	-3E-37	-2E-46	-2E-55	-2E-64	-2E-73	-2E-82	-2E-91
9000	0.0596	0.0003	0.0001	-1E-05	-1E-05	-2E-06	-4E-07	-6E-08	-9E-09	-1E-09	-4E-18	-1E-26	-3E-35	-1E-43	-3E-52	-9E-61	-3E-69	-8E-78	-2E-86
10000	0.077	0.0005	0.0002	-6E-06	-1E-05	-4E-06	-8E-07	-1E-07	-2E-08	-4E-09	-3E-17	-2E-25	-2E-33	-2E-41	-1E-49	-1E-57	-9E-66	-7E-74	-6E-82
20000	0.2963	0.0192	0.0004	0.0003	7E-05	-2E-05	-2E-05	-9E-06	-3E-06	-1E-06	-2E-12	-4E-18	-8E-24	-2E-29	-3E-35	-6E-41	-1E-46	-2E-52	-4E-58
30000	0.5373	0.0732	0.0044	0.0004	0.0003	0.0001	-1E-05	-3E-05	-2E-05	-9E-06	-4E-10	-8E-15	-2E-19	-4E-24	-8E-29	-2E-33	-3E-38	-7E-43	-2E-47
40000	0.7729	0.154	0.0178	0.001	0.0005	0.0003	0.0001	-1E-05	-4E-05	-3E-05	-7E-09	-7E-13	-6E-17	-5E-21	-5E-25	-4E-29	-4E-33	-4E-37	-3E-41
50000	0.998	0.2518	0.0424	0.0041	0.0005	0.0003	9E-05	-2E-05	-4E-05	-6E-08	-1E-11	-3E-15	-8E-19	-2E-22	-5E-26	-1E-29	-3E-33	-7E-37	
60000	1.2122	0.36	0.0775	0.0109	0.001	0.0006	0.0005	0.0003	6E-05	-2E-05	-2E-07	-1E-10	-7E-14	-3E-17	-2E-20	-9E-24	-4E-27	-2E-30	-1E-33
70000	1.4163	0.4745	0.1216	0.0222	0.0026	0.0006	0.0006	0.0004	0.0002	3E-05	-8E-07	-8E-10	-7E-13	-6E-16	-5E-19	-5E-22	-4E-25	-4E-28	-3E-31
80000	1.6113	0.5926	0.1732	0.0383	0.0058	0.0008	0.0007	0.0006	0.0004	0.0001	-2E-06	-3E-09	-5E-12	-6E-15	-9E-18	-1E-20	-2E-23	-2E-26	-3E-29
90000	1.798	0.7127	0.2309	0.0591	0.0111	0.0015	0.0007	0.0007	0.0005	0.0003	-4E-06	-1E-08	-2E-11	-4E-14	-9E-17	-2E-19	-4E-22	-7E-25	-1E-27
100000	1.9774	0.8334	0.2937	0.0842	0.0186	0.003	0.0007	0.0007	0.0007	0.0004	-8E-06	-3E-08	-8E-11	-2E-13	-6E-16	-2E-18	-5E-21	-1E-23	-4E-26
200000	3.49	1.996	1.0489	0.5035	0.2189	0.0848	0.0286	0.0081	0.0022	0.001	-8E-05	-6E-06	-1E-07	-2E-09	-3E-11	-4E-13	-7E-15	-1E-16	-2E-18
300000	4.6947	3.0297	1.8505	1.0665	0.578	0.293	0.1378	0.0594	0.023	0.008	0.0002	-4E-05	-3E-06	-1E-07	-3E-09	-1E-10	-4E-12	-1E-13	-4E-15
400000	5.7256	3.9548	2.6229	1.6669	1.0131	0.5873	0.3236	0.1685	0.0822	0.0371	0.0008	-1E-04	-2E-05	-1E-06	-6E-08	-3E-09	-2E-10	-9E-12	-5E-13
500000	6.6412	4.7968	3.3549	2.2689	1.4816	0.9328	0.5649	0.3282	0.182	0.0958	0.0015	-1E-04	-5E-05	-5E-06	-4E-07	-3E-08	-2E-09	-2E-10	-1E-11
600000	7.4733	5.5738	4.048	2.8595	1.9627	1.3075	0.8443	0.5274	0.3178	0.1841	0.0018	3E-05	-9E-05	-1E-05	-2E-06	-2E-07	-2E-08	-1E-09	-1E-10
700000	8.2411	6.2984	4.706	3.4343	2.4459	1.6985	1.149	0.7562	0.4834	0.2994	0.0019	0.0003	-1E-04	-3E-05	-5E-06	-6E-07	-7E-08	-7E-09	-8E-10
800000	8.9577	6.98	5.3329	3.9919	2.9256	2.0978	1.4707	1.007	0.6728	0.4377	0.002	0.0008	-2E-04	-6E-05	-1E-05	-2E-06	-2E-07	-3E-08	-4E-09
900000	9.632	7.6251	5.9322	4.5325	3.3989	2.5003	1.8032	1.274	0.881	0.5956	0.0029	0.0013	-1E-04	-1E-04	-2E-05	-4E-06	-6E-07	-9E-08	-1E-08
1E+06	10.271	8.2392	6.5071	5.0566	3.8644	2.9029	2.1425	1.5527	1.1042	0.7698	0.0052	0.0017	-6E-05	-1E-04	-4E-05	-8E-06	-1E-06	-2E-07	-4E-08
2E+06	15.45	13.282	11.333	9.5935	8.0563	6.7098	5.5416	4.5377	3.6833	2.9632	0.1916	0.0042	0.003	0.0007	-2E-04	-2E-04	-9E-05	-3E-05	-1E-05
3E+06	19.438	17.21	15.162	13.288	11.585	10.046	8.6641	7.4306	6.3367	5.3728	0.7318	0.044	0.0038	0.0035	0.0011	-1E-04	-3E-04	-2E-04	-9E-05
4E+06	22.806	20.542	18.433	16.478	14.673	13.014	11.496	10.113	8.8597	7.7287	1.5396	0.1784	0.0103	0.0046	0.0035	0.0011	-1E-04	-4E-04	-3E-04
5E+06	25.775	23.486	21.337	19.326	17.45	15.707	14.092	12.603	11.234	9.9798	2.5176	0.4241	0.0407	0.0051	0.0052	0.0031	0.0009	-2E-04	-4E-04
6E+06	28.461	26.154	23.974	21.921	19.993	18.186	16.499	14.929	13.471	12.122	3.6001	0.7746	0.1089	0.0102	0.0056	0.0051	0.0026	0.0006	-2E-04
7E+06	30.932	28.61	26.407	24.321	22.352	20.496	18.751	17.117	15.588	14.163	4.7452	1.2155	0.2223	0.0261	0.0059	0.0062	0.0044	0.002	0.0003
8E+06	33.232	30.899	28.677	26.565	24.561	22.665	20.874	19.187	17.601	16.113	5.9264	1.7317	0.3832	0.0583	0.0083	0.0065	0.006	0.0036	0.0013
9E+06	35.393	33.05	30.813	28.678	26.647	24.718	22.888	21.156	19.521	17.98	7.1266	2.3093	0.5907	0.1107	0.0155	0.0066	0.007	0.0052	0.0027
1E+07	37.437	35.087	32.835	30.683	28.628	26.67	24.807	23.038	21.361	19.774	8.3344	2.9367	0.8423	0.1857	0.0298	0.0074	0.0074	0.0066	0.0042

APPENDIX B

SUBROUTINE OF COMPOSITE AQUIFER IN VBA EXCEL TO SOLVE STEHFEST ALGORITHM FOR DIMENSIONLESS PIEZOMETRIC HEAD OF GRANULAR AQUIFER UNDER CONSTANT DISCHARGE

The numerical inversion method proposed by Stehfest to find real time solution for the piezometric head in semi-infinite homogeneous aquifer is:

$$z_0(y, \theta) \approx \frac{\ln 2}{\theta} \sum_{i=1}^N V_i \bar{z}_0(y, i \frac{\ln 2}{\theta}) \quad (2.67)$$

$$V_i = (-1)^{i+\frac{N}{2}} \frac{\sum_{k=\text{int}(\frac{i+1}{2})}^{\min(i, \frac{N}{2})} k^{N/2} (2k)!}{(\frac{N}{2} - k)! k! (k-1)! (i-k)! (2k-1)!} \quad (2.66)$$

where

z_0 is the real time solution for dimensionless head in granular aquifer.

\bar{z}_0 is the analytical solution obtained by Laplace transform for dimensionless piezometric head in granular aquifer and it is given below as:

$$\bar{z}_0 = \frac{Q_b}{p\sqrt{p}} \frac{e^{-p\sqrt{y}} (1 + \sqrt{(\eta_2 \frac{\delta_2}{p+\delta_2} \lambda_1 + \eta_1 \lambda_1)}) e^{2\sqrt{p}}}{\sqrt{(\eta_2 \frac{\delta_2}{p+\delta_2} \lambda_1 + \eta_1 \lambda_1) (e^{2\sqrt{p}} + 1) + e^{2\sqrt{p}} - 1}} + \frac{e^{p\sqrt{y}} \frac{Q_b}{p\sqrt{p}}}{-1 + e^{2\sqrt{p}} \frac{1 + \sqrt{(\eta_2 \frac{\delta_2}{p+\delta_2} \lambda_1 + \eta_1 \lambda_1)}}{1 - \sqrt{(\eta_2 \frac{\delta_2}{p+\delta_2} \lambda_1 + \eta_1 \lambda_1)}}} \quad (2.62)$$

Subroutine in VBA is executed to compute $z_0(y, \theta)$ from $\overline{z_0}(y, p)$ is given below as:

```
Function pdt_granular(n, lamda1, lamda2, eta1, eta2, delta2, Qb, t, y) As Double
```

```
'y indicates dimensionless distance
```

```
't indicates dimensionless time
```

```
Dim i, k, kbg, knd, nh, sn As Integer
```

```
Dim v(1 To 50), g(1 To 50), h(1 To 25) As Double
```

```
Dim d, f, r As Double
```

```
Dim u, s As Double
```

```
Dim L, pds_granular, a, p As Double
```

```
Const ln2 = 0.693414718105599
```

```
r = n Mod 2
```

```
If r = 1 Then
```

```
MsgBox "Error: n must be even"
```

```
ElseIf n > 50 Then
```

```
MsgBox "Error:n must be less than 50"
```

```
Else
```

```
g(1) = 1
```

```
nh = Int(n / 2)
```

```
d = nh Mod 2
```

```
sn = 2 * d - g(1)
```

```
For i = 1 To n
```

```
g(i + 1) = i * g(i)
```

```
Next i
```

```
h(1) = 2 / g(nh)
```

```
For i = 2 To nh
```

```
h(i) = (i ^ nh) * g(2 * i + 1) / (g(nh - i + 1) * g(i + 1) * g(i))
```

```

Next i
a = ln2 / t
pdt_granular = 0
For i = 1 To n
    kbg = Int((i + 1) / 2)
    kno = WorksheetFunction.Min(i, nh)
    v(i) = 0
    For k = kbg To kno
        v(i) = v(i) + h(k) / (g(i - k + 1) * g(2 * k - i + 1))
    Next k
    v(i) = sn * v(i)
    sn = -sn
    p = a * i
    f = (eta1 * lamda1) + (eta2 * lamda1 * delta2 / (p + delta2))
    s = Sqr(f)
    u = (s * (Exp(2 * Sqr(p)) + 1)) + (Exp(2 * Sqr(p))) - 1
    pds_granular = (Qb / (p ^ 1.5)) * (s + 1) * Exp(2 * Sqr(p)) * (1 / u) * Exp(-Sqr(p)) *
y) + (Qb / (p ^ 1.5)) * (-s + 1) * (1 / u) * Exp(Sqr(p)) * y
    pdt_granular = pdt_granular + v(i) * pds_granular
Next i
pdt_granular = a * pdt_granular
End If
End Function
Sub granular_aquifer()
Dim number_of_elements, l1, l2, et1, et2, del2, dim_discharge, dim_time, dim_distance
As Double
Dim m, j As Integer
number_of_elements = Cdbl(InputBox("even number value", "number of elements",
"Enter an even number for elements in calculation smaller than 50.))

```

```

l1 = CDbI(InputBox("l1", "ratio of transmissivity coefficient fracture to granular aquifer",
"enter l1 ."))

l2 = CDbI(InputBox("l2", "ratio of transmissivity coefficient blocks to granular aquifer",
"enter l2. "))

et1 = CDbI(InputBox("et1", "ratio of storage coefficient fracture to granular aquifer",
"enter et1 ."))

et2 = CDbI(InputBox("et2", "ratio of storage coefficient blocks to granular aquifer",
"enter et2 ."))

del2 = CDbI(InputBox("delta", "delta coefficient:combined effect of
transmissivity,storage and shape of aquifer ", "enter del2. "))

dim_discharge = CDbI(InputBox("dim_discharge", "dimensionless discharge ", "enter
dim_discharge"))

Cells(1, 1) = "n= " + CStr(number_of_elements) + " " + "l1= " + CStr(l1) + " " + "l2=
" + CStr(l2) + " " + "et1= " + CStr(et1) + " " + "et2= " + CStr(et2) + " " + "del2= " +
CStr(del2) + " " + "Qb=" + CStr(dim_discharge)

dim_time = 0.01

dim_distance = 0

If dim_distance > 1 Then

    MsgBox "Error: distance should be less than 1."

End If

m = 2

For j = 2 To 12

    Cells(1, j) = "y= " + "" + CStr(dim_distance)

    Do While dim_time < 0.1

        Cells(m, 1) = "theta= " + "" + CStr(dim_time)

        Cells(m, j) = pdt_granular(number_of_elements, l1, l2, et1, et2, del2, dim_discharge,
dim_time, dim_distance)

        m = m + 1

        dim_time = dim_time + 0.01

    Loop

    dim_time = dim_time - 0.01

    Do While dim_time < 1

```

```

Cells(m, 1) = "theta= " + "" + CStr(dim_time)

Cells(m, j) = pdt_granular(number_of_elements, l1, l2, et1, et2, del2, dim_discharge,
dim_time, dim_distance)

m = m + 1

dim_time = dim_time + 0.1

Loop

dim_time = dim_time - 0.1

Do While 1 < dim_time < 10

If dim_time > 10 Then Exit Do

Cells(m, 1) = "theta= " + "" + CStr(dim_time)

Cells(m, j) = pdt_granular(number_of_elements, l1, l2, et1, et2, del2, dim_discharge,
dim_time, dim_distance)

m = m + 1

dim_time = dim_time + 1

Loop

dim_time = dim_time - 1

Do While 10 < dim_time < 100

If dim_time > 100 Then Exit Do

Cells(m, 1) = "theta= " + "" + CStr(dim_time)

Cells(m, j) = pdt_granular(number_of_elements, l1, l2, et1, et2, del2, dim_discharge,
dim_time, dim_distance)

m = m + 1

dim_time = dim_time + 10

Loop

dim_time = 0.01

m = 2

dim_distance = dim_distance + 0.1

Next j

End Sub

```

Table B.1: Numerical solution in granular region for $\lambda_1=15, \lambda_2=0.01, \eta_1=0.2, \eta_2=2, \delta_2=0.5, Q_b=0.06$

	y=0	y=0.1	y=0.2	y=0.3	y=0.4	y=0.5	y=0.6	y=0.7	y=0.8	y=0.9	y=1
theta= 0.01	0.006769	0.002395	0.000604	0.000102	9.76E-06	1.23E-06	1.25E-06	7.6E-07	2.3E-07	-1.5E-08	-6.6E-08
theta= 0.02	0.009573	0.004746	0.002	0.000705	0.000202	4.46E-05	7.2E-06	1.82E-06	1.78E-06	1.49E-06	7.56E-07
theta= 0.03	0.011724	0.006689	0.003432	0.001569	0.000633	0.000221	6.45E-05	1.5E-05	3.09E-06	1.53E-06	1.56E-06
theta= 0.04	0.013538	0.008376	0.00479	0.002517	0.001208	0.000525	0.000203	6.8E-05	1.88E-05	4.39E-06	1.56E-06
theta= 0.05	0.015136	0.009887	0.006068	0.003483	0.001863	0.000923	0.00042	0.000173	6.28E-05	1.93E-05	4.01E-06
theta= 0.06	0.016581	0.011267	0.007271	0.004441	0.002559	0.001386	0.000702	0.00033	0.000141	5.29E-05	1.31E-05
theta= 0.07	0.017909	0.012545	0.008409	0.005379	0.003275	0.001894	0.001036	0.000532	0.000254	0.000108	3.21E-05
theta= 0.08	0.019145	0.01374	0.00949	0.006294	0.003999	0.00243	0.001408	0.000774	0.000399	0.000186	6.29E-05
theta= 0.09	0.020306	0.014867	0.010522	0.007184	0.004723	0.002986	0.00181	0.001048	0.000573	0.000285	0.000106
theta= 0.1	0.021403	0.015937	0.01151	0.00805	0.005443	0.003553	0.002234	0.001348	0.000771	0.000403	0.000162
theta= 0.2	0.030259	0.024635	0.019754	0.015588	0.012091	0.009204	0.006856	0.004969	0.003461	0.00225	0.001255
theta= 0.3	0.03699	0.031291	0.026189	0.021665	0.017693	0.014234	0.011242	0.008663	0.006436	0.0045	0.002788
theta= 0.4	0.042508	0.036759	0.031508	0.026741	0.022439	0.018573	0.015108	0.012003	0.009212	0.006683	0.004364
theta= 0.5	0.047154	0.041367	0.036002	0.031049	0.026492	0.022309	0.018471	0.014945	0.011694	0.008676	0.005846
theta= 0.6	0.051111	0.045293	0.039837	0.034734	0.029971	0.02553	0.021387	0.017515	0.013883	0.010456	0.007197
theta= 0.7	0.054504	0.048661	0.043129	0.037902	0.032969	0.028314	0.023917	0.019757	0.015806	0.012036	0.008414
theta= 0.8	0.057426	0.051562	0.045967	0.040637	0.035561	0.030727	0.026118	0.021715	0.017495	0.013435	0.009508
theta= 0.9	0.059953	0.054071	0.048424	0.043006	0.037811	0.032825	0.028037	0.023429	0.018983	0.014678	0.01049
theta= 1	0.062147	0.05625	0.050559	0.045067	0.03977	0.034657	0.029717	0.024936	0.020298	0.015784	0.011376
theta= 2	0.073963	0.067997	0.0621	0.056269	0.050505	0.044804	0.039164	0.033582	0.028055	0.022578	0.017148
theta= 3	0.078873	0.072891	0.066947	0.061038	0.055166	0.04933	0.043529	0.037762	0.032029	0.026328	0.020658
theta= 4	0.082121	0.076135	0.070177	0.064246	0.058343	0.052468	0.04662	0.040799	0.035005	0.029238	0.023498
theta= 5	0.084811	0.078823	0.07286	0.06692	0.061006	0.055115	0.049249	0.043407	0.037589	0.031796	0.026026
theta= 6	0.087227	0.081238	0.075272	0.069329	0.063408	0.057509	0.051633	0.045779	0.039948	0.034139	0.028353
theta= 7	0.089465	0.083475	0.077507	0.07156	0.065635	0.05973	0.053847	0.047985	0.042144	0.036324	0.030525
theta= 8	0.091564	0.085574	0.079605	0.073655	0.067726	0.061817	0.055928	0.050059	0.04421	0.038381	0.032572
theta= 9	0.09355	0.087559	0.081588	0.075636	0.069704	0.06379	0.057896	0.052021	0.046165	0.040328	0.03451
theta= 10	0.095437	0.089446	0.083474	0.07752	0.071585	0.065668	0.059769	0.053888	0.048026	0.042182	0.036356
theta= 20	0.110822	0.104829	0.098849	0.092882	0.086928	0.080988	0.075061	0.069147	0.063246	0.057358	0.051484
theta= 30	0.12267	0.116675	0.110691	0.104718	0.098756	0.092805	0.086864	0.080934	0.075015	0.069107	0.063209
theta= 40	0.132659	0.126664	0.120678	0.114701	0.108734	0.102776	0.096827	0.090888	0.084958	0.079037	0.073126
theta= 50	0.141459	0.135464	0.129476	0.123497	0.117526	0.111564	0.10561	0.099664	0.093726	0.087797	0.081876
theta= 60	0.149415	0.143419	0.13743	0.131449	0.125476	0.11951	0.113552	0.107602	0.101659	0.095723	0.089796
theta= 70	0.156731	0.150734	0.144745	0.138762	0.132787	0.126819	0.120858	0.114903	0.108956	0.103016	0.097083
theta= 80	0.16354	0.157543	0.151553	0.145569	0.139593	0.133622	0.127658	0.121701	0.115751	0.109807	0.103869
theta= 90	0.169935	0.163938	0.157947	0.151963	0.145984	0.140012	0.134047	0.128087	0.122134	0.116186	0.110245
theta= 100	0.175983	0.169986	0.163995	0.15801	0.15203	0.146057	0.140089	0.134128	0.128172	0.122222	0.116278

APPENDIX C

SUBROUTINE OF COMPOSITE AQUIFER IN VBA EXCEL TO SOLVE STEHFEST ALGORITHM FOR DIMENSIONLESS PIEZOMETRIC HEAD OF FRACTURES UNDER CONSTANT DISCHARGE

The numerical inversion method proposed by Stehfest to find real time solution for dimensionless piezometric head in fractures is:

$$z_1(y, \theta) \approx \frac{\ln 2}{\theta} \sum_{i=1}^N V_i \bar{z}_1(y, i \frac{\ln 2}{\theta}) \quad (2.68)$$

$$V_i = (-1)^{i+\frac{N}{2}} \sum_{k=\text{int}(\frac{i+1}{2})}^{\min(i, \frac{N}{2})} \frac{k^{N/2} (2k)!}{(\frac{N}{2} - k)! (k-1)! (i-k)! (2k-1)!} \quad (2.66)$$

where

z_1 is the real time solution for dimensionless head in fractures

\bar{z}_1 is the analytical solution obtained by Laplace transform for dimensionless piezometric head in fractures and it is given below as:

$$\bar{z}_1 = 2 \frac{Q_p}{p\sqrt{p}} e^{\sqrt{p}} \frac{e^{\sqrt{(\frac{\eta_2}{\lambda_1} \frac{\delta_2}{p+\delta_2} + \frac{\eta_1}{\lambda_1})p}}}{-1 + e^{2\sqrt{p}} + (\eta_2 \frac{\delta_2}{p+\delta_2} \lambda_1 + \eta_1 \lambda_1)(1 + e^{2\sqrt{p}})} e^{-\sqrt{(\frac{\eta_2}{\lambda_1} \frac{\delta_2}{p+\delta_2} + \frac{\eta_1}{\lambda_1})p} y} \quad (2.63)$$

Subroutine in VBA is executed to compute $z_1(y, \theta)$ from $\bar{z}_1(y, p)$ is given below as:

```
Function pdt_fracture(n, lamda1, lamda2, eta1, eta2, delta2, Qb, t, y) As Double
```

```
'y indicates dimensionless distance
```

```
't indicates dimensionless time
```

```
Dim i, k, kbg, knd, nh, sn As Integer
```

```
Dim v(1 To 50), g(1 To 50), h(1 To 25) As Double
```

```
Dim d, f, r As Double
```

```
Dim u, s As Double
```

```
Dim L, pds_fracture, a, p As Double
```

```
Const ln2 = 0.693414718105599
```

```
r = n Mod 2
```

```
If r = 1 Then
```

```
MsgBox "Error: n must be even"
```

```
ElseIf n > 50 Then
```

```
MsgBox "Error:n must be less than 50"
```

```
Else
```

```
g(1) = 1
```

```
nh = Int(n / 2)
```

```
d = nh Mod 2
```

```
sn = 2 * d - g(1)
```

```
For i = 1 To n
```

```
g(i + 1) = i * g(i)
```

```
Next i
```

```
h(1) = 2 / g(nh)
```

```
For i = 2 To nh
```

```
h(i) = (i ^ nh) * g(2 * i + 1) / (g(nh - i + 1) * g(i + 1) * g(i))
```

```

Next i
a = ln2 / t
pdt_fracture = 0
For i = 1 To n
    kbg = Int((i + 1) / 2)
    kno = WorksheetFunction.Min(i, nh)
    v(i) = 0
    For k = kbg To kno
        v(i) = v(i) + h(k) / (g(i - k + 1) * g(2 * k - i + 1))
    Next k
    v(i) = sn * v(i)
    sn = -sn
    p = a * i
    f = (eta1 / lamda1) + ((eta2 / lamda1) * (delta2 / (p + delta2)))
    s = (eta1 * lamda1) + (eta2 * lamda1) * (delta2 / (p + delta2))
    u = (Sqr(s) * ((Exp(2 * Sqr(p))) + 1)) + (Exp(2 * Sqr(p))) - 1
    pds_fracture = (2 * Qb / (p ^ 1.5)) * (1 / u) * Exp(2 * Sqr(p)) * Exp(Sqr(p * f)) *
    Exp(-Sqr(p * f) * y) * Exp(-Sqr(p))
    pdt_fracture = pdt_fracture + v(i) * pds_fracture
Next i
pdt_fracture = a * pdt_fracture
End If
End Function
Sub fracture_aquifer()
    Dim number_of_elements, l1, l2, et1, et2, del2, dim_discharge, dim_time, dim_distance
    As Double
    Dim m, j As Integer
    number_of_elements = Cdbl(InputBox("even number value", "number of elements",
    "Enter an even number for elements in calculation smaller than 50.))

```

```

l1 = CDbI(InputBox("l1", "ratio of transmissivity coefficient fracture to fracture aquifer",
"enter l1 ."))

l2 = CDbI(InputBox("l2", "ratio of transmissivity coefficient blocks to fracture aquifer",
"enter l2. "))

et1 = CDbI(InputBox("et1", "ratio of storage coefficient fracture to fracture aquifer",
"enter et1 ."))

et2 = CDbI (InputBox("et2", "ratio of storage coefficient blocks to fracture aquifer",
"enter et2 ."))

del2 = CDbI(InputBox("delta", "delta coefficient:combined effect of
transmissivity,storage and shape of aquifer ", "enter del2. "))

dim_discharge = CDbI(InputBox("dim_discharge", "dimensionless discharge ", "enter
dim_discharge"))

Cells(1, 1) = "n= " + CStr(number_of_elements) + " " + "l1= " + CStr(l1) + " " + "l2=
" + CStr(l2) + " " + "et1= " + CStr(et1) + " " + "et2= " + CStr(et2) + " " + "del2= " +
CStr(del2) + " " + "Qb=" + CStr(dim_discharge)

dim_time = 0.01

dim_distance = 1

m = 2

j = 2

Do While dim_distance < 10
If dim_distance > 10 Then Exit Do
Cells(1, j) = "y= " + "" + CStr(dim_distance)

Do While dim_time < 0.1
Cells(m, 1) = "theta= " + "" + CStr(dim_time)

Cells(m, j) = pdt_fracture(number_of_elements, l1, l2, et1, et2, del2, dim_discharge,
dim_time, dim_distance)

m = m + 1

dim_time = dim_time + 0.01

Loop

dim_time = dim_time - 0.01

Do While dim_time < 1

Cells(m, 1) = "theta= " + "" + CStr(dim_time)

```

```

Cells(m, j) = pdt_fracture(number_of_elements, l1, l2, et1, et2, del2, dim_discharge,
dim_time, dim_distance)

m = m + 1
dim_time = dim_time + 0.1
Loop
dim_time = dim_time - 0.1
Do While 1 < dim_time < 10
If dim_time > 10 Then Exit Do
Cells(m, 1) = "theta= " + "" + CStr(dim_time)
Cells(m, j) = pdt_fracture(number_of_elements, l1, l2, et1, et2, del2, dim_discharge,
dim_time, dim_distance)
m = m + 1
dim_time = dim_time + 1
Loop
dim_time = dim_time - 1
Do While 10 < dim_time < 100
If dim_time > 100 Then Exit Do
Cells(m, 1) = "theta= " + "" + CStr(dim_time)
Cells(m, j) = pdt_fracture(number_of_elements, l1, l2, et1, et2, del2, dim_discharge,
dim_time, dim_distance)
m = m + 1
dim_time = dim_time + 10
Loop
dim_time = 0.01
m = 2
j = j + 1
dim_distance = dim_distance + 1
Loop
Do While 10 < dim_distance < 100

```

```

If dim_distance > 100 Then Exit Do
Cells(1, j) = "y= " + "" + CStr(dim_distance)
Do While dim_time < 0.1
    Cells(m, 1) = "theta= " + "" + CStr(dim_time)
    Cells(m, j) = pdt_fracture(number_of_elements, l1, l2, et1, et2, del2, dim_discharge,
dim_time, dim_distance)
    m = m + 1
    dim_time = dim_time + 0.01
Loop
dim_time = dim_time - 0.01
Do While dim_time < 1
    Cells(m, 1) = "theta= " + "" + CStr(dim_time)
    Cells(m, j) = pdt_fracture(number_of_elements, l1, l2, et1, et2, del2, dim_discharge,
dim_time, dim_distance)
    m = m + 1
    dim_time = dim_time + 0.1
Loop
dim_time = dim_time - 0.1
Do While 1 < dim_time < 10
If dim_time > 10 Then Exit Do
Cells(m, 1) = "theta= " + "" + CStr(dim_time)
Cells(m, j) = pdt_fracture(number_of_elements, l1, l2, et1, et2, del2, dim_discharge,
dim_time, dim_distance)
    m = m + 1
    dim_time = dim_time + 1
Loop
dim_time = dim_time - 1
Do While 10 < dim_time < 100
If dim_time > 100 Then Exit Do

```

```
Cells(m, 1) = "theta= " + "" + CStr(dim_time)

Cells(m, j) = pdt_fracture(number_of_elements, l1, l2, et1, et2, del2, dim_discharge,
dim_time, dim_distance)

m = m + 1

dim_time = dim_time + 10

Loop

dim_time = 0.01

m = 2

j = j + 1

dim_distance = dim_distance + 10

Loop

End Sub
```

Table C.1: Numerical solution of fractures for $\lambda_1=15, \lambda_2=0.01, \eta_1=0.2, \eta_2=2, \delta_2=0.5, Q_b=0.06$

	y=1	y=2	y=3	y=4	y=5	y=6	y=7	y=8	y=9	y=10	y=20	y=30	y=40	y=50	y=60	y=70	y=80	y=90	y=100
theta=0.01	-7E-08	-5E-08	-3E-08	-1E-08	-6E-09	-2E-09	-9E-10	-4E-10	-1E-10	-5E-11	-3E-15	-1E-19	-6E-24	-3E-28	-1E-32	-6E-37	-3E-41	-1E-45	-7E-50
theta=0.02	8E-07	3E-07	5E-08	-5E-08	-6E-08	-5E-08	-3E-08	-2E-08	-1E-08	-6E-09	-6E-12	-5E-15	-3E-18	-2E-21	-2E-24	-1E-27	-8E-31	-5E-34	-4E-37
theta=0.03	2E-06	1E-06	9E-07	4E-07	2E-07	2E-08	-4E-08	-5E-08	-4E-08	-3E-08	-2E-10	-5E-13	-1E-15	-2E-18	-5E-21	-1E-23	-3E-26	-6E-29	-1E-31
theta=0.04	2E-06	2E-06	2E-06	1E-06	8E-07	4E-07	2E-07	6E-08	-8E-09	-3E-08	-1E-09	-7E-12	-3E-14	-1E-16	-6E-19	-3E-21	-1E-23	-5E-26	-2E-28
theta=0.05	4E-06	1E-06	1E-06	2E-06	1E-06	1E-06	6E-07	4E-07	2E-07	7E-08	-4E-09	-4E-11	-3E-13	-2E-15	-1E-17	-9E-20	-6E-22	-4E-24	-3E-26
theta=0.06	1E-05	3E-06	1E-06	1E-06	1E-06	1E-06	1E-06	7E-07	5E-07	3E-07	-7E-09	-1E-10	-2E-12	-1E-14	-1E-16	-1E-18	-1E-20	-1E-22	-1E-24
theta=0.07	3E-05	9E-06	2E-06	9E-07	1E-06	1E-06	1E-06	1E-06	8E-07	5E-07	-1E-08	-3E-10	-5E-12	-7E-14	-8E-16	-1E-17	-1E-19	-1E-21	-2E-23
theta=0.08	6E-05	2E-05	6E-06	1E-06	6E-07	9E-07	1E-06	1E-06	1E-06	8E-07	-9E-09	-7E-10	-1E-11	-2E-13	-3E-15	-5E-17	-7E-19	-1E-20	-2E-22
theta=0.09	0.0001	4E-05	1E-05	3E-06	7E-07	4E-07	7E-07	9E-07	1E-06	9E-07	-1E-09	-1E-09	-3E-11	-6E-13	-1E-14	-2E-16	-3E-18	-5E-20	-9E-22
theta=0.1	0.0002	7E-05	3E-05	8E-06	2E-06	3E-07	3E-07	6E-07	8E-07	8E-07	1E-08	-2E-09	-5E-11	-1E-12	-3E-14	-5E-16	-1E-17	-2E-19	-4E-21
theta=0.2	0.0013	0.0008	0.0005	0.0003	0.0001	8E-05	4E-05	2E-05	8E-06	2E-06	2E-07	1E-08	-2E-10	-5E-11	-3E-12	-2E-13	-7E-15	-3E-16	-1E-17
theta=0.3	0.0028	0.0019	0.0013	0.0008	0.0005	0.0003	0.0002	0.0001	8E-05	5E-05	-3E-07	2E-08	2E-09	-4E-11	-1E-11	-1E-12	-9E-14	-6E-15	-3E-16
theta=0.4	0.0044	0.0031	0.0022	0.0015	0.001	0.0007	0.0005	0.0003	0.0002	0.0001	4E-07	-3E-08	3E-09	1E-10	-2E-11	-4E-12	-4E-13	-3E-14	-3E-15
theta=0.5	0.0058	0.0043	0.0031	0.0022	0.0016	0.0011	0.0008	0.0006	0.0004	0.0003	4E-06	-6E-08	-1E-09	5E-11	-4E-11	-9E-12	-1E-13	-1E-14	-1E-14
theta=0.6	0.0072	0.0053	0.004	0.0029	0.0021	0.0016	0.0011	0.0008	0.0006	0.0004	1E-05	3E-08	-7E-09	-4E-10	-9E-11	-2E-11	-3E-12	-3E-13	-3E-14
theta=0.7	0.0084	0.0063	0.0048	0.0036	0.0026	0.002	0.0015	0.0011	0.0008	0.0006	2E-05	3E-07	-9E-09	-1E-09	-2E-10	-4E-11	-6E-12	-8E-13	-9E-14
theta=0.8	0.0095	0.0072	0.0055	0.0042	0.0031	0.0024	0.0018	0.0013	0.001	0.0007	3E-05	7E-07	-2E-09	-2E-09	-4E-10	-7E-11	-1E-11	-2E-12	-2E-13
theta=0.9	0.0105	0.0081	0.0062	0.0047	0.0036	0.0027	0.0021	0.0016	0.0012	0.0009	4E-05	1E-06	2E-08	-3E-09	-7E-10	-1E-10	-2E-11	-3E-12	-4E-13
theta=1	0.0114	0.0088	0.0068	0.0052	0.004	0.0031	0.0023	0.0018	0.0014	0.001	5E-05	2E-06	4E-08	-4E-09	-1E-09	-2E-10	-4E-11	-6E-12	-8E-13
theta=2	0.0171	0.0139	0.0112	0.009	0.0072	0.0058	0.0046	0.0037	0.0029	0.0023	0.0002	2E-05	1E-06	4E-08	-1E-08	-5E-09	-1E-09	-3E-10	-7E-11
theta=3	0.0207	0.0172	0.0143	0.0118	0.0097	0.008	0.0066	0.0054	0.0044	0.0036	0.0004	4E-05	4E-06	3E-07	-3E-08	-2E-08	-9E-09	-3E-09	-8E-10
theta=4	0.0235	0.0199	0.0169	0.0142	0.0119	0.01	0.0084	0.007	0.0058	0.0048	0.0007	8E-05	9E-06	9E-07	-9E-09	-6E-08	-3E-08	-1E-08	-4E-09
theta=5	0.026	0.0224	0.0192	0.0165	0.014	0.0119	0.0101	0.0086	0.0072	0.0061	0.001	0.0001	2E-05	2E-06	1E-07	-1E-07	-7E-08	-3E-08	-1E-08
theta=6	0.0284	0.0247	0.0215	0.0186	0.016	0.0138	0.0118	0.0101	0.0086	0.0073	0.0013	0.0002	3E-05	4E-06	5E-07	-1E-07	-1E-07	-7E-08	-3E-08
theta=7	0.0305	0.0269	0.0235	0.0206	0.0179	0.0156	0.0135	0.0116	0.01	0.0086	0.0017	0.0003	4E-05	7E-06	1E-06	-2E-08	-2E-07	-1E-07	-6E-08
theta=8	0.0326	0.0289	0.0255	0.0225	0.0197	0.0173	0.0151	0.0131	0.0114	0.0099	0.0021	0.0004	6E-05	1E-05	2E-06	2E-07	-2E-07	-2E-07	-1E-07
theta=9	0.0345	0.0308	0.0274	0.0243	0.0215	0.019	0.0167	0.0146	0.0128	0.0112	0.0025	0.0005	9E-05	2E-05	3E-06	5E-07	-2E-07	-2E-07	-2E-07
theta=10	0.0364	0.0326	0.0292	0.026	0.0232	0.0206	0.0182	0.0161	0.0141	0.0124	0.003	0.0006	0.0001	2E-05	5E-06	1E-06	-4E-08	-3E-07	-2E-07
theta=20	0.0515	0.0477	0.0441	0.0406	0.0374	0.0344	0.0316	0.0289	0.0264	0.0241	0.0088	0.0028	0.0008	0.0002	5E-05	2E-05	7E-06	3E-06	7E-07
theta=30	0.0632	0.0594	0.0557	0.0521	0.0488	0.0456	0.0425	0.0396	0.0369	0.0343	0.0153	0.0061	0.0021	0.0007	0.0002	6E-05	2E-05	1E-05	7E-06
theta=40	0.0731	0.0693	0.0655	0.0619	0.0585	0.0552	0.052	0.0489	0.046	0.0432	0.0219	0.01	0.0041	0.0016	0.0005	0.0002	6E-05	2E-05	2E-05
theta=50	0.0819	0.078	0.0742	0.0706	0.0671	0.0637	0.0604	0.0573	0.0542	0.0513	0.0282	0.0143	0.0066	0.0028	0.0011	0.0004	0.0001	5E-05	2E-05
theta=60	0.0898	0.0859	0.0821	0.0785	0.0749	0.0715	0.0681	0.0649	0.0618	0.0588	0.0343	0.0186	0.0094	0.0044	0.0019	0.0008	0.0003	0.0001	4E-05
theta=70	0.0971	0.0932	0.0894	0.0857	0.0821	0.0786	0.0752	0.072	0.0688	0.0657	0.0402	0.0231	0.0124	0.0063	0.003	0.0013	0.0005	0.0002	8E-05
theta=80	0.1039	0.1	0.0962	0.0924	0.0888	0.0853	0.0819	0.0786	0.0753	0.0722	0.0458	0.0274	0.0156	0.0083	0.0042	0.002	0.0009	0.0004	0.0001
theta=90	0.1102	0.1063	0.1025	0.0988	0.0951	0.0916	0.0881	0.0848	0.0815	0.0783	0.0512	0.0318	0.0188	0.0105	0.0056	0.0028	0.0013	0.0006	0.0002
theta=100	0.1163	0.1124	0.1085	0.1048	0.1011	0.0976	0.0941	0.0907	0.0874	0.0841	0.0564	0.0361	0.0221	0.0129	0.0072	0.0038	0.0019	0.0009	0.0004

APPENDIX D

SUBROUTINE OF COMPOSITE AQUIFER IN VBA EXCEL TO SOLVE STEHFEST ALGORITHM FOR DIMENSIONLESS PIEZOMETRIC HEAD OF BLOCKS UNDER CONSTANT DISCHARGE

The numerical inversion method proposed by Stehfest to find real time solution for dimensionless piezometric head in blocks is:

$$z_2(y, \theta) \approx \frac{\ln 2}{\theta} \sum_{i=1}^N V_i \bar{z}_2(y, i \frac{\ln 2}{\theta}) \quad (2.69)$$

$$V_i = (-1)^{i+\frac{N}{2}} \frac{\sum_{k=\text{int}(\frac{i+1}{2})}^{\min(i, \frac{N}{2})} k^{N/2} (2k)!}{(\frac{N}{2} - k)! k! (k-1)! (i-k)! (2k-1)!} \quad (2.66)$$

where

z_2 is the real time solution for dimensionless head in blocks

\bar{z}_2 is the analytical solution obtained by Laplace transform for dimensionless piezometric head in blocks and it is given below as

$$\bar{z}_2 = 2 \frac{\delta_2}{p + \delta_2} \frac{Q_b}{p \sqrt{p}} e^{\sqrt{p} y} \frac{e^{\sqrt{\left(\frac{\eta_2}{\lambda_1} \frac{\delta_2}{p + \delta_2} + \frac{\eta_1}{\lambda_1}\right) p}}}{-1 + e^{2\sqrt{p} y} + \left(\eta_2 \frac{\delta_2}{p + \delta_2} \lambda_1 + \eta_1 \lambda_1\right) (1 + e^{2\sqrt{p} y})} e^{-\sqrt{\left(\frac{\eta_2}{\lambda_1} \frac{\delta_2}{p + \delta_2} + \frac{\eta_1}{\lambda_1}\right) p} y} \quad (2.64)$$

Subroutine in VBA is executed to compute $z_2(y, \theta)$ from $\overline{z_2}(y, p)$ is given below as:

```
Function pdt_blocks(n, lamda1, lamda2, eta1, eta2, delta2, Qb, t, y) As Double
```

```
'y indicates dimensionless distance
```

```
't indicates dimensionless time
```

```
Dim i, k, kbg, knd, nh, sn As Integer
```

```
Dim v(1 To 50), g(1 To 50), h(1 To 25) As Double
```

```
Dim d, f, r As Double
```

```
Dim u, s As Double
```

```
Dim L, pds_blocks, a, p As Double
```

```
Const ln2 = 0.693414718105599
```

```
r = n Mod 2
```

```
If r = 1 Then
```

```
MsgBox "Error: n must be even"
```

```
ElseIf n > 50 Then
```

```
MsgBox "Error:n must be less than 50"
```

```
Else
```

```
g(1) = 1
```

```
nh = Int(n / 2)
```

```
d = nh Mod 2
```

```
sn = 2 * d - g(1)
```

```
For i = 1 To n
```

```
g(i + 1) = i * g(i)
```

```
Next i
```

```
h(1) = 2 / g(nh)
```

```
For i = 2 To nh
```

```
h(i) = (i ^ nh) * g(2 * i + 1) / (g(nh - i + 1) * g(i + 1) * g(i))
```

```

Next i
a = ln2 / t
pdt_blocks = 0
For i = 1 To n
    kbg = Int((i + 1) / 2)
    kno = WorksheetFunction.Min(i, nh)
    v(i) = 0
    For k = kbg To kno
        v(i) = v(i) + h(k) / (g(i - k + 1) * g(2 * k - i + 1))
    Next k
    v(i) = sn * v(i)
    sn = -sn
    p = a * i
    f = (eta1 / lamda1) + ((eta2 / lamda1) * (delta2 / (p + delta2)))
    s = (eta1 * lamda1) + (eta2 * lamda1) * (delta2 / (p + delta2))
    u = (Sqr(s) * ((Exp(2 * Sqr(p))) + 1)) + (Exp(2 * Sqr(p))) - 1
    pds_blocks = (delta2 / (p + delta2)) * (2 * Qb / (p ^ 1.5)) * (1 / u) * Exp(2 * Sqr(p))
    * Exp(Sqr(p * f)) * Exp(-Sqr(p * f) * y) * Exp(-Sqr(p))
    pdt_blocks = pdt_blocks + v(i) * pds_blocks
Next i
pdt_blocks = a * pdt_blocks
End If
End Function
Sub blocks_aquifer()
Dim number_of_elements, l1, l2, et1, et2, del2, dim_discharge, dim_time, dim_distance
As Double
Dim m, j As Integer
number_of_elements = Cdbl(InputBox("even number value", "number of elements",
"Enter an even number for elements in calculation smaller than 50.))

```

```

l1 = CDbI(InputBox("l1", "ratio of transmissivity coefficient blocks to blocks aquifer",
"enter l1 ."))

l2 = CDbI(InputBox("l2", "ratio of transmissivity coefficient blocks to blocks aquifer",
"enter l2. "))

et1 = CDbI(InputBox("et1", "ratio of storage coefficient blocks to blocks aquifer", "enter
et1 ."))

et2 = CDbI(InputBox("et2", "ratio of storage coefficient blocks to blocks aquifer", "enter
et2 ."))

del2 = CDbI(InputBox("delta", "delta coefficient:combined effect of
transmissivity,storage and shape of aquifer ", "enter del2. "))

dim_discharge = CDbI(InputBox("dim_discharge", "dimensionless discharge ", "enter
dim_discharge"))

Cells(1, 1) = "n= " + CStr(number_of_elements) + " " + "l1= " + CStr(l1) + " " + "l2=
" + CStr(l2) + " " + "et1= " + CStr(et1) + " " + "et2= " + CStr(et2) + " " + "del2= " +
CStr(del2) + " " + "Qb=" + CStr(dim_discharge)

dim_time = 0.01

dim_distance = 1

m = 2

j = 2

Do While dim_distance < 10
If dim_distance > 10 Then Exit Do
Cells(1, j) = "y= " + "" + CStr(dim_distance)

Do While dim_time < 0.1
Cells(m, 1) = "theta= " + "" + CStr(dim_time)

Cells(m, j) = pdt_blocks(number_of_elements, l1, l2, et1, et2, del2, dim_discharge,
dim_time, dim_distance)

m = m + 1

dim_time = dim_time + 0.01

Loop

dim_time = dim_time - 0.01

Do While dim_time < 1

Cells(m, 1) = "theta= " + "" + CStr(dim_time)

```

```

Cells(m, j) = pdt_blocks(number_of_elements, l1, l2, et1, et2, del2, dim_discharge,
dim_time, dim_distance)

m = m + 1
dim_time = dim_time + 0.1
Loop
dim_time = dim_time - 0.1
Do While 1 < dim_time < 10
If dim_time > 10 Then Exit Do
Cells(m, 1) = "theta= " + "" + CStr(dim_time)
Cells(m, j) = pdt_blocks(number_of_elements, l1, l2, et1, et2, del2, dim_discharge,
dim_time, dim_distance)
m = m + 1
dim_time = dim_time + 1
Loop
dim_time = dim_time - 1
Do While 10 < dim_time < 100
If dim_time > 100 Then Exit Do
Cells(m, 1) = "theta= " + "" + CStr(dim_time)
Cells(m, j) = pdt_blocks(number_of_elements, l1, l2, et1, et2, del2, dim_discharge,
dim_time, dim_distance)
m = m + 1
dim_time = dim_time + 10
Loop
dim_time = 0.01
m = 2
j = j + 1
dim_distance = dim_distance + 1
Loop
Do While 10 < dim_distance < 100

```

```

If dim_distance > 100 Then Exit Do
Cells(1, j) = "y= " + "" + CStr(dim_distance)
  Do While dim_time < 0.1
    Cells(m, 1) = "theta= " + "" + CStr(dim_time)
    Cells(m, j) = pdt_blocks(number_of_elements, l1, l2, et1, et2, del2, dim_discharge,
dim_time, dim_distance)
    m = m + 1
    dim_time = dim_time + 0.01
  Loop
  dim_time = dim_time - 0.01
Do While dim_time < 1
  Cells(m, 1) = "theta= " + "" + CStr(dim_time)
  Cells(m, j) = pdt_blocks(number_of_elements, l1, l2, et1, et2, del2, dim_discharge,
dim_time, dim_distance)
  m = m + 1
  dim_time = dim_time + 0.1
Loop
dim_time = dim_time - 0.1
Do While 1 < dim_time < 10
If dim_time > 10 Then Exit Do
Cells(m, 1) = "theta= " + "" + CStr(dim_time)
Cells(m, j) = pdt_blocks(number_of_elements, l1, l2, et1, et2, del2, dim_discharge,
dim_time, dim_distance)
m = m + 1
dim_time = dim_time + 1
Loop
dim_time = dim_time - 1
Do While 10 < dim_time < 100
If dim_time > 100 Then Exit Do

```

```
Cells(m, 1) = "theta= " + "" + CStr(dim_time)

Cells(m, j) = pdt_blocks(number_of_elements, l1, l2, et1, et2, del2, dim_discharge,
dim_time, dim_distance)

m = m + 1

dim_time = dim_time + 10

Loop

dim_time = 0.01

m = 2

j = j + 1

dim_distance = dim_distance + 10

Loop

End Sub
```

Table D.1: Numerical solution of blocks for $\lambda_1=15, \lambda_2=0.01, \eta_1=0.2, \eta_2=2, \delta_2=0.5, Q_b=0.06$

	y=1	y=2	y=3	y=4	y=5	y=6	y=7	y=8	y=9	y=10	y=20	y=30	y=40	y=50	y=60	y=70	y=80	y=90	y=100
theta=0.01	-1E-09	-7E-10	-3E-10	-1E-10	-5E-11	-2E-11	-7E-12	-3E-12	-1E-12	-4E-13	-2E-17	-9E-22	-4E-26	-2E-30	-9E-35	-4E-39	-2E-43	-1E-47	-5E-52
theta=0.02	-9E-09	-8E-09	-6E-09	-4E-09	-2E-09	-1E-09	-8E-10	-4E-10	-2E-10	-1E-10	-9E-14	-7E-17	-5E-20	-3E-23	-2E-26	-2E-29	-1E-32	-8E-36	-5E-39
theta=0.03	9E-09	-5E-09	-1E-08	-1E-08	-1E-08	-7E-09	-5E-09	-3E-09	-2E-09	-1E-09	-4E-12	-1E-14	-2E-17	-5E-20	-1E-22	-2E-25	-5E-28	-1E-30	-3E-33
theta=0.04	7E-08	3E-08	7E-09	-7E-09	-1E-08	-1E-08	-1E-08	-9E-09	-6E-09	-4E-09	-4E-11	-2E-13	-9E-16	-4E-18	-2E-20	-7E-23	-3E-25	-1E-27	-6E-30
theta=0.05	2E-07	1E-07	5E-08	2E-08	3E-09	-8E-09	-1E-08	-1E-08	-1E-08	-9E-09	-2E-10	-1E-12	-1E-14	-7E-17	-5E-19	-3E-21	-2E-23	-2E-25	-1E-27
theta=0.06	3E-07	2E-07	1E-07	7E-08	4E-08	1E-08	-1E-09	-8E-09	-1E-08	-1E-08	-5E-10	-6E-12	-6E-14	-6E-16	-6E-18	-5E-20	-5E-22	-5E-24	-4E-26
theta=0.07	5E-07	3E-07	2E-07	1E-07	9E-08	5E-08	2E-08	6E-09	-4E-09	-8E-09	-1E-09	-2E-11	-3E-13	-3E-15	-4E-17	-5E-19	-6E-21	-7E-23	-8E-25
theta=0.08	8E-07	5E-07	3E-07	2E-07	2E-07	1E-07	6E-08	3E-08	1E-08	1E-09	-2E-09	-5E-11	-8E-13	-1E-14	-2E-16	-3E-18	-4E-20	-6E-22	-8E-24
theta=0.09	1E-06	7E-07	4E-07	3E-07	2E-07	2E-07	1E-07	7E-08	4E-08	2E-08	-3E-09	-9E-11	-2E-12	-4E-14	-6E-16	-1E-17	-2E-19	-3E-21	-6E-23
theta=0.1	2E-06	1E-06	6E-07	4E-07	3E-07	2E-07	2E-07	1E-07	7E-08	4E-08	-3E-09	-2E-10	-4E-12	-9E-14	-2E-15	-4E-17	-7E-19	-1E-20	-3E-22
theta=0.2	3E-05	2E-05	1E-05	5E-06	3E-06	2E-06	1E-06	6E-07	4E-07	3E-07	2E-08	-1E-09	-2E-10	-1E-11	-5E-13	-2E-14	-9E-16	-4E-17	-1E-18
theta=0.3	0.0001	8E-05	5E-05	3E-05	2E-05	1E-05	6E-06	3E-06	2E-06	1E-06	6E-08	3E-09	-3E-10	-5E-11	-5E-12	-3E-13	-2E-14	-1E-15	-6E-17
theta=0.4	0.0003	0.0002	0.0001	8E-05	5E-05	3E-05	2E-05	1E-05	8E-06	5E-06	5E-08	7E-09	-2E-10	-1E-10	-2E-11	-1E-12	-1E-13	-9E-15	-6E-16
theta=0.5	0.0005	0.0004	0.0002	0.0002	0.0001	8E-05	5E-05	3E-05	2E-05	1E-05	1E-07	5E-09	-3E-10	-2E-10	-4E-11	-5E-12	-4E-13	-4E-14	-3E-15
theta=0.6	0.0008	0.0006	0.0004	0.0003	0.0002	0.0001	1E-04	7E-05	4E-05	3E-05	4E-07	7E-10	-1E-09	-4E-10	-8E-11	-1E-11	-1E-12	-1E-13	-1E-14
theta=0.7	0.0012	0.0008	0.0006	0.0004	0.0003	0.0002	0.0002	0.0001	8E-05	5E-05	1E-06	3E-09	-3E-09	-8E-10	-2E-10	-2E-11	-3E-12	-3E-13	-4E-14
theta=0.8	0.0015	0.0011	0.0008	0.0006	0.0004	0.0003	0.0002	0.0002	0.0001	8E-05	2E-06	2E-08	-5E-09	-1E-09	-3E-10	-5E-11	-6E-12	-8E-13	-9E-14
theta=0.9	0.002	0.0014	0.0011	0.0008	0.0006	0.0004	0.0003	0.0002	0.0002	0.0001	4E-06	7E-08	-7E-09	-2E-09	-5E-10	-8E-11	-1E-11	-2E-12	-2E-13
theta=1	0.0024	0.0018	0.0013	0.001	0.0007	0.0005	0.0004	0.0003	0.0002	0.0002	6E-06	2E-07	-8E-09	-3E-09	-8E-10	-1E-10	-2E-11	-3E-12	-4E-13
theta=2	0.0073	0.0058	0.0045	0.0035	0.0028	0.0022	0.0017	0.0013	0.001	0.0008	6E-05	4E-06	2E-07	-2E-08	-1E-08	-4E-09	-1E-09	-2E-10	-4E-11
theta=3	0.012	0.0097	0.0078	0.0063	0.0051	0.0041	0.0033	0.0026	0.0021	0.0017	0.0002	1E-05	1E-06	2E-08	-5E-08	-2E-08	-8E-09	-2E-09	-6E-10
theta=4	0.016	0.0132	0.0109	0.009	0.0074	0.006	0.0049	0.004	0.0033	0.0027	0.0003	3E-05	4E-06	3E-07	-8E-08	-7E-08	-3E-08	-1E-08	-3E-09
theta=5	0.0195	0.0164	0.0138	0.0115	0.0096	0.008	0.0067	0.0055	0.0046	0.0038	0.0005	6E-05	8E-06	1E-06	-4E-08	-1E-07	-7E-08	-3E-08	-1E-08
theta=6	0.0225	0.0192	0.0164	0.0139	0.0118	0.01	0.0084	0.0071	0.0059	0.005	0.0008	0.0001	1E-05	2E-06	2E-07	-2E-07	-1E-07	-7E-08	-3E-08
theta=7	0.0253	0.0218	0.0188	0.0162	0.0139	0.0118	0.0101	0.0086	0.0073	0.0062	0.001	0.0002	2E-05	4E-06	6E-07	-1E-07	-2E-07	-1E-07	-6E-08
theta=8	0.0278	0.0242	0.0211	0.0183	0.0158	0.0137	0.0118	0.0101	0.0087	0.0074	0.0014	0.0002	4E-05	7E-06	1E-06	7E-09	-2E-07	-2E-07	-1E-07
theta=9	0.0301	0.0265	0.0232	0.0203	0.0178	0.0155	0.0134	0.0116	0.01	0.0087	0.0018	0.0003	5E-05	1E-05	2E-06	3E-07	-2E-07	-2E-07	-2E-07
theta=10	0.0322	0.0286	0.0253	0.0223	0.0196	0.0172	0.015	0.0131	0.0114	0.0099	0.0022	0.0004	7E-05	1E-05	4E-06	7E-07	-2E-07	-3E-07	-2E-07
theta=20	0.0487	0.0449	0.0413	0.038	0.0348	0.0318	0.0291	0.0265	0.0241	0.0219	0.0076	0.0023	0.0006	0.0001	4E-05	1E-05	6E-06	3E-06	6E-07
theta=30	0.061	0.0572	0.0535	0.05	0.0466	0.0434	0.0404	0.0376	0.0349	0.0323	0.014	0.0054	0.0018	0.0005	0.0002	5E-05	2E-05	1E-05	7E-06
theta=40	0.0712	0.0674	0.0636	0.0601	0.0566	0.0533	0.0502	0.0471	0.0442	0.0415	0.0206	0.0092	0.0037	0.0013	0.0004	0.0001	5E-05	2E-05	1E-05
theta=50	0.0802	0.0763	0.0725	0.0689	0.0654	0.062	0.0588	0.0557	0.0526	0.0498	0.027	0.0134	0.0061	0.0025	0.001	0.0003	0.0001	4E-05	2E-05
theta=60	0.0883	0.0844	0.0806	0.0769	0.0734	0.0699	0.0666	0.0634	0.0603	0.0573	0.0331	0.0178	0.0088	0.0041	0.0017	0.0007	0.0002	9E-05	4E-05
theta=70	0.0957	0.0918	0.088	0.0843	0.0807	0.0772	0.0738	0.0706	0.0674	0.0643	0.039	0.0222	0.0118	0.0059	0.0027	0.0012	0.0005	0.0002	7E-05
theta=80	0.1025	0.0986	0.0948	0.0911	0.0875	0.084	0.0806	0.0773	0.074	0.0709	0.0447	0.0266	0.0149	0.0079	0.0039	0.0018	0.0008	0.0003	0.0001
theta=90	0.109	0.1051	0.1013	0.0975	0.0939	0.0904	0.0869	0.0836	0.0803	0.0771	0.0501	0.0309	0.0181	0.0101	0.0053	0.0026	0.0012	0.0005	0.0002
theta=100	0.1151	0.1112	0.1073	0.1036	0.1	0.0964	0.0929	0.0895	0.0862	0.083	0.0553	0.0352	0.0214	0.0124	0.0068	0.0036	0.0018	0.0008	0.0004

APPENDIX E

SUBROUTINE OF FINITE AQUIFER WITH IMPERVIOUS BOUNDARY IN VBA EXCEL TO SOLVE STEHFEST ALGORITHM FOR DIMENSIONLESS PIEZOMETRIC HEAD UNDER CONSTANT DISCHARGE

The numerical inversion method proposed by Stehfest to find real time solution for dimensionless piezometric head in finite homogeneous aquifer with impervious boundary is:

$$z_0(y, \theta) \approx \frac{\ln 2}{\theta} \sum_{i=1}^N V_i \bar{z}_0(y, i \frac{\ln 2}{\theta}) \quad (2.67)$$

$$V_i = (-1)^{i+\frac{N}{2}} \sum_{k=\text{int}(\frac{i+1}{2})}^{\min(i, \frac{N}{2})} \frac{k^{N/2} (2k)!}{(\frac{N}{2} - k)! k! (k-1)! (i-k)! (2k-1)!} \quad (2.66)$$

where

z_0 is the real time solution for dimensionless head in finite homogeneous aquifer with impervious boundary.

\bar{z}_0 is the analytical solution obtained by Laplace transform for dimensionless head in finite homogeneous aquifer with impervious boundary and it is below given as:

$$\bar{z}_0 = \frac{Q_b}{(e^{2\sqrt{p}} - 1)\sqrt{p}} e^{2\sqrt{p}} e^{-\sqrt{p}y} + \frac{Q_b}{(e^{2\sqrt{p}} - 1)\sqrt{p}} e^{\sqrt{p}y} \quad (5.7)$$

Subroutine in VBA is executed to compute $z_0(y, \theta)$ from $\overline{z_0}(y, p)$ is given below

as:

```
Function pdt_granular_impervious_boundary (n, Qb, t, y) As Double
```

```
'y indicates dimensionless distance
```

```
't indicates dimensionless time
```

```
Dim i, k, kbg, knd, nh, sn As Integer
```

```
Dim v(1 To 50), g(1 To 50), h(1 To 25) As Double
```

```
Dim d, f, r As Double
```

```
Dim u, s As Double
```

```
Dim L, pds_granular_impervious_boundary, a, p As Double
```

```
Const ln2 = 0.693414718105599
```

```
r = n Mod 2
```

```
If r = 1 Then
```

```
MsgBox "Error: n must be even"
```

```
ElseIf n > 50 Then
```

```
MsgBox "Error:n must be less than 50"
```

```
Else
```

```
g(1) = 1
```

```
nh = Int(n / 2)
```

```
d = nh Mod 2
```

```
sn = 2 * d - g(1)
```

```
For i = 1 To n
```

```
g(i + 1) = i * g(i)
```

```
Next i
```

```
h(1) = 2 / g(nh)
```

```
For i = 2 To nh
```

```
h(i) = (i ^ nh) * g(2 * i + 1) / (g(nh - i + 1) * g(i + 1) * g(i))
```

```

Next i
a = ln2 / t
pdt_granular_impervious_boundary = 0
For i = 1 To n
    kbg = Int((i + 1) / 2)
    kno = WorksheetFunction.Min(i, nh)
    v(i) = 0
    For k = kbg To kno
        v(i) = v(i) + h(k) / (g(i - k + 1) * g(2 * k - i + 1))
    Next k
    v(i) = sn * v(i)
    sn = -sn
    p = a * i
    f = (Exp(2 * Sqr(p))) - 1
    s = f * (p ^ 1.5)
    u = (Exp(2 * Sqr(p))) / s
    pds_granular_impervious_boundary = (Qb * u * Exp(-Sqr(p) * y)) + (Qb / s) *
    Exp(Sqr(p) * y)
    pdt_granular_impervious_boundary = pdt_granular_impervious_boundary + v(i) *
    pds_granular_impervious_boundary
Next i
pdt_granular_impervious_boundary = a * pdt_granular_impervious_boundary
End If
End Function
Sub granular_impervious_boundary()

Dim number_of_elements, dim_discharge, dim_time, dim_distance As Double
Dim m, j As Integer

```

```

number_of_elements = CDbI(InputBox("even number value", "number of elements",
"Enter an even number for elements in calculation smaller than 50.))

dim_discharge = CDbI(InputBox("dim_discharge", "dimensionless discharge ", "enter
dim_discharge"))

Cells(1, 1) = "n= " + CStr(number_of_elements) + " " + "Qb= " + CStr(dim_discharge)

dim_time = 0.01

dim_distance = 0

If dim_distance > 1 Then
    MsgBox "Error: distance should be less than 1."
End If

m = 2

For j = 2 To 12
    Cells(1, j) = "y= " + "" + CStr(dim_distance)

    Do While dim_time < 0.1

        Cells(m, 1) = "theta= " + "" + CStr(dim_time)

        Cells(m, j) = pdt_granular_impervious_boundary(number_of_elements,
dim_discharge, dim_time, dim_distance)

        m = m + 1

        dim_time = dim_time + 0.01

    Loop

    dim_time = dim_time - 0.01

    Do While dim_time < 1

        Cells(m, 1) = "theta= " + "" + CStr(dim_time)

        Cells(m, j) = pdt_granular_impervious_boundary(number_of_elements,
dim_discharge, dim_time, dim_distance)

        m = m + 1

        dim_time = dim_time + 0.1

    Loop

    dim_time = dim_time - 0.1

    Do While 1 < dim_time < 10

```

```

If dim_time > 10 Then Exit Do

Cells(m, 1) = "theta= " + "" + CStr(dim_time)

Cells(m, j) = pdt_granular_impervious_boundary(number_of_elements,
dim_discharge, dim_time, dim_distance)

m = m + 1

dim_time = dim_time + 1

Loop

dim_time = dim_time - 1

Do While 10 < dim_time < 100

If dim_time > 100 Then Exit Do

Cells(m, 1) = "theta= " + "" + CStr(dim_time)

Cells(m, j) = pdt_granular_impervious_boundary(number_of_elements,
dim_discharge, dim_time, dim_distance)

m = m + 1

dim_time = dim_time + 10

Loop

dim_time = 0.01

m = 2

dim_distance = dim_distance + 0.1

Next j

End Sub

```

Table E.1: Numerical solution by Stehfest Algorithm in finite aquifer with impervious boundary, $Q_b=0.06$

n= 8 $Q_b= 0.06$	y= 0	y= 0.1	y= 0.2	y= 0.3	y= 0.4	y= 0.5	y= 0.6	y= 0.7	y= 0.8	y= 0.9	y= 1
theta= 0.01	0.006769	0.002395	0.000604	0.000102	9.75E-06	1.22E-06	1.23E-06	7.25E-07	1.66E-07	-1.2E-07	-1.9E-07
theta= 0.02	0.009573	0.004746	0.002	0.000705	0.000202	4.45E-05	7.01E-06	1.7E-06	1.86E-06	2.03E-06	2E-06
theta= 0.03	0.011724	0.006688	0.003431	0.001569	0.000633	0.000221	6.48E-05	1.59E-05	4.8E-06	3.99E-06	4.37E-06
theta= 0.04	0.013538	0.008376	0.00479	0.002517	0.001209	0.000526	0.000205	7.06E-05	2.2E-05	7.6E-06	4.88E-06
theta= 0.05	0.015136	0.009887	0.006068	0.003484	0.001865	0.000926	0.000423	0.000177	6.63E-05	2.32E-05	1.23E-05
theta= 0.06	0.016582	0.011268	0.007273	0.004443	0.002562	0.00139	0.000706	0.000333	0.000145	6.15E-05	3.81E-05
theta= 0.07	0.017912	0.012548	0.008412	0.005383	0.003279	0.001898	0.00104	0.000537	0.000263	0.00013	9.14E-05
theta= 0.08	0.01915	0.013745	0.009496	0.006299	0.004004	0.002435	0.001413	0.000782	0.000418	0.000234	0.000178
theta= 0.09	0.020313	0.014875	0.010529	0.00719	0.004729	0.002991	0.001818	0.001064	0.000611	0.000374	0.0003
theta= 0.1	0.021413	0.015946	0.011518	0.008057	0.00545	0.003561	0.002249	0.001379	0.00084	0.00055	0.000459
theta= 0.2	0.030297	0.02468	0.01982	0.015696	0.012269	0.009495	0.007321	0.005698	0.004576	0.003919	0.003703
theta= 0.3	0.037342	0.031674	0.026667	0.02231	0.018592	0.015494	0.012997	0.01108	0.009726	0.00892	0.008653
theta= 0.4	0.043744	0.038056	0.032992	0.028547	0.024717	0.021494	0.018872	0.016842	0.015397	0.014533	0.014245
theta= 0.5	0.049903	0.044208	0.039121	0.034641	0.030766	0.027493	0.024821	0.022746	0.021265	0.020378	0.020082
theta= 0.6	0.055967	0.050268	0.045172	0.040678	0.036784	0.033492	0.030799	0.028706	0.027211	0.026314	0.026016
theta= 0.7	0.061991	0.056291	0.051191	0.046691	0.042791	0.039491	0.03679	0.03469	0.033189	0.032289	0.031989
theta= 0.8	0.067998	0.062298	0.057197	0.052695	0.048792	0.045489	0.042786	0.040683	0.039181	0.038279	0.037979
theta= 0.9	0.073999	0.068298	0.063197	0.058694	0.054791	0.051488	0.048784	0.046681	0.045178	0.044276	0.043976
theta= 1	0.079996	0.074296	0.069195	0.064692	0.06079	0.057486	0.054783	0.05268	0.051177	0.050276	0.049975
theta= 2	0.139971	0.134271	0.129171	0.124672	0.120772	0.117472	0.114772	0.112673	0.111173	0.110273	0.109973
theta= 3	0.199957	0.194257	0.189157	0.184657	0.180758	0.177458	0.174759	0.172659	0.171159	0.17026	0.16996
theta= 4	0.259943	0.254243	0.249144	0.244644	0.240744	0.237444	0.234745	0.232645	0.231145	0.230245	0.229945
theta= 5	0.31993	0.31423	0.30913	0.30463	0.30073	0.29743	0.294731	0.292631	0.291131	0.290231	0.289931
theta= 6	0.379916	0.374216	0.369116	0.364616	0.360716	0.357417	0.354717	0.352617	0.351117	0.350217	0.349917
theta= 7	0.439902	0.434202	0.429102	0.424602	0.420703	0.417403	0.414703	0.412603	0.411103	0.410203	0.409903
theta= 8	0.499889	0.494189	0.489089	0.484589	0.480689	0.477389	0.474689	0.472589	0.471089	0.470189	0.469889
theta= 9	0.559875	0.554175	0.549075	0.544575	0.540675	0.537375	0.534675	0.532575	0.531075	0.530175	0.529875
theta= 10	0.619861	0.614161	0.609061	0.604561	0.600661	0.597361	0.594661	0.592561	0.591061	0.590161	0.589861
theta= 20	1.219722	1.214022	1.208922	1.204422	1.200522	1.197222	1.194522	1.192422	1.190922	1.190022	1.189722
theta= 30	1.819583	1.813883	1.808783	1.804283	1.800383	1.797083	1.794383	1.792283	1.790783	1.789883	1.789583
theta= 40	2.419444	2.413744	2.408644	2.404144	2.400244	2.396944	2.394244	2.392144	2.390644	2.389744	2.389444
theta= 50	3.019305	3.013605	3.008505	3.004005	3.000105	2.996805	2.994105	2.992005	2.990505	2.989605	2.989305
theta= 60	3.619165	3.613465	3.608365	3.603865	3.599965	3.596665	3.593965	3.591865	3.590365	3.589465	3.589165
theta= 70	4.219026	4.213326	4.208226	4.203726	4.199826	4.196526	4.193826	4.191726	4.190226	4.189326	4.189026
theta= 80	4.818887	4.813187	4.808087	4.803587	4.799687	4.796387	4.793687	4.791587	4.790087	4.789187	4.788887
theta= 90	5.418748	5.413048	5.407948	5.403448	5.399548	5.396248	5.393548	5.391448	5.389948	5.389048	5.388748
theta= 100	6.018609	6.012909	6.007809	6.003309	5.999409	5.996109	5.993409	5.991309	5.989809	5.988909	5.988609

APPENDIX F

SUBROUTINE OF FINITE AQUIFER WITH RECHARGE BOUNDARY IN VBA EXCEL TO SOLVE STEHFEST ALGORITHM FOR DIMENSIONLESS PIEZOMETRIC HEAD UNDER CONSTANT DISCHARGE

The numerical inversion method proposed by Stehfest to find real time solution for dimensionless piezometric head in finite homogeneous aquifer with impervious boundary is:

$$z_0(y, \theta) \approx \frac{\ln 2}{\theta} \sum_{i=1}^N V_i \bar{z}_0(y, i \frac{\ln 2}{\theta}) \quad (2.67)$$

$$V_i = (-1)^{i+\frac{N}{2}} \sum_{k=\text{int}(\frac{i+1}{2})}^{\min(i, \frac{N}{2})} \frac{k^{N/2} (2k)!}{(\frac{N}{2} - k)! (k-1)! (i-k)! (2k-1)!} \quad (2.66)$$

where

z_0 is the real time solution for dimensionless head in finite homogeneous aquifer with impervious boundary

\bar{z}_0 is the analytical solution obtained by Laplace transform for dimensionless head in finite homogeneous aquifer with recharge boundary and it is below given as:

$$\bar{z}_0 = \frac{Q_b}{(e^{2\sqrt{p}} + 1)\sqrt{p}} e^{2\sqrt{p}} e^{-\sqrt{p}y} - \frac{Q_b}{(e^{2\sqrt{p}} + 1)\sqrt{p}} e^{\sqrt{p}y} \quad (5.14)$$

Subroutine in VBA is executed to compute $z_0(y, \theta)$ from $\overline{z_0}(y, p)$ is given below

as:

```
Function pdt_granular_recharge_boundary(n, Qb, t, y) As Double
```

```
'y indicates dimensionless distance
```

```
't indicates dimensionless time
```

```
Dim i, k, kbg, knd, nh, sn As Integer
```

```
Dim v(1 To 50), g(1 To 50), h(1 To 25) As Double
```

```
Dim d, f, r As Double
```

```
Dim u, s As Double
```

```
Dim L, pds_granular_recharge_boundary, a, p As Double
```

```
Const ln2 = 0.693414718105599
```

```
r = n Mod 2
```

```
If r = 1 Then
```

```
MsgBox "Error: n must be even"
```

```
ElseIf n > 50 Then
```

```
MsgBox "Error: n must be less than 50"
```

```
Else
```

```
g(1) = 1
```

```
nh = Int(n / 2)
```

```
d = nh Mod 2
```

```
sn = 2 * d - g(1)
```

```
For i = 1 To n
```

```
g(i + 1) = i * g(i)
```

```
Next i
```

```
h(1) = 2 / g(nh)
```

```
For i = 2 To nh
```

```
h(i) = (i ^ nh) * g(2 * i + 1) / (g(nh - i + 1) * g(i + 1) * g(i))
```

```

Next i
a = ln2 / t
pdt_granular_recharge_boundary = 0
For i = 1 To n
    kbg = Int((i + 1) / 2)
    kno = WorksheetFunction.Min(i, nh)
    v(i) = 0
    For k = kbg To kno
        v(i) = v(i) + h(k) / (g(i - k + 1) * g(2 * k - i + 1))
    Next k
    v(i) = sn * v(i)
    sn = -sn
    p = a * i
    f = (Exp(2 * Sqr(p))) + 1
    s = f * (p ^ 1.5)
    u = (Exp(2 * Sqr(p))) / s
    pds_granular_recharge_boundary = (Qb * u * Exp(-Sqr(p) * y)) - (Qb / s) * Exp(Sqr(p) * y)
    pdt_granular_recharge_boundary = pdt_granular_recharge_boundary + v(i) * pds_granular_recharge_boundary
Next i
pdt_granular_recharge_boundary = a * pdt_granular_recharge_boundary
End If
End Function
Sub granular_recharge_boundary()
Dim number_of_elements, dim_discharge, dim_time, dim_distance As Double
Dim m, j As Integer
number_of_elements = CDBl(InputBox("even number value", "number of elements",
"Enter an even number for elements in calculation smaller than 50.))

```

```

dim_discharge = CDBl(InputBox("dim_discharge", "dimensionless discharge ", "enter
dim_discharge"))

Cells(1, 1) = "n= " + CStr(number_of_elements) + " " + "Qb= " + CStr(dim_discharge)

dim_time = 0.01

dim_distance = 0

If dim_distance > 1 Then

    MsgBox "Error: distance should be less than 1."

End If

m = 2

For j = 2 To 12

    Cells(1, j) = "y= " + "" + CStr(dim_distance)

        Do While dim_time < 0.1

            Cells(m, 1) = "theta= " + "" + CStr(dim_time)

            Cells(m, j) = pdt_granular_recharge_boundary(number_of_elements, dim_discharge,
dim_time, dim_distance)

            m = m + 1

            dim_time = dim_time + 0.01

        Loop

        dim_time = dim_time - 0.01

        Do While dim_time < 1

            Cells(m, 1) = "theta= " + "" + CStr(dim_time)

            Cells(m, j) = pdt_granular_recharge_boundary(number_of_elements, dim_discharge,
dim_time, dim_distance)

            m = m + 1

            dim_time = dim_time + 0.1

        Loop

        dim_time = dim_time - 0.1

        Do While 1 < dim_time < 10

            If dim_time > 10 Then Exit Do

```

```

Cells(m, 1) = "theta= " + "" + CStr(dim_time)

Cells(m, j) = pdt_granular_recharge_boundary(number_of_elements, dim_discharge,
dim_time, dim_distance)

m = m + 1

dim_time = dim_time + 1

Loop

dim_time = dim_time - 1

Do While 10 < dim_time < 100

If dim_time > 100 Then Exit Do

Cells(m, 1) = "theta= " + "" + CStr(dim_time)

Cells(m, j) = pdt_granular_recharge_boundary(number_of_elements, dim_discharge,
dim_time, dim_distance)

m = m + 1

dim_time = dim_time + 10

Loop

dim_time = 0.01

m = 2

dim_distance = dim_distance + 0.1

Next j

End Sub

```

Table F.1: Numerical solution by Stehfest Algorithm in finite aquifer with recharge boundary under constant discharge, $Q_b=0.06$

n=8 $Q_b=0.06$	y=0	y=0.1	y=0.2	y=0.3	y=0.4	y=0.5	y=0.6	y=0.7	y=0.8	y=0.9	y=1
theta= 0.01	0.006769	0.002395	0.000604	0.000102	9.76E-06	1.23E-06	1.26E-06	7.8E-07	2.65E-07	4.07E-08	7.62E-22
theta= 0.02	0.009573	0.004746	0.002	0.000705	0.000202	4.47E-05	7.28E-06	1.87E-06	1.69E-06	1.15E-06	2.13E-21
theta= 0.03	0.011725	0.006689	0.003432	0.001569	0.000633	0.000221	6.42E-05	1.43E-05	2.05E-06	9.5E-08	-2.6E-19
theta= 0.04	0.013539	0.008376	0.004791	0.002517	0.001208	0.000524	0.000202	6.65E-05	1.7E-05	2.72E-06	2.09E-18
theta= 0.05	0.015136	0.009887	0.006068	0.003483	0.001862	0.000922	0.000418	0.000171	6.11E-05	1.76E-05	-5E-18
theta= 0.06	0.01658	0.011266	0.00727	0.004439	0.002557	0.001384	0.0007	0.000328	0.000139	4.88E-05	3.03E-18
theta= 0.07	0.017907	0.012543	0.008407	0.005377	0.003273	0.001891	0.001034	0.000531	0.00025	9.69E-05	-2.7E-18
theta= 0.08	0.019142	0.013737	0.009487	0.006291	0.003997	0.002428	0.001406	0.000771	0.00039	0.00016	1.59E-17
theta= 0.09	0.020301	0.014863	0.010518	0.00718	0.004721	0.002983	0.001807	0.001041	0.000553	0.000236	7.55E-18
theta= 0.1	0.021398	0.015932	0.011506	0.008046	0.00544	0.00355	0.002228	0.001333	0.000735	0.000323	-1.5E-17
theta= 0.2	0.030247	0.02462	0.019728	0.015539	0.012004	0.009056	0.006615	0.00459	0.002882	0.001388	-4.8E-16
theta= 0.3	0.036821	0.031107	0.025957	0.021349	0.01725	0.013612	0.010378	0.007479	0.004839	0.002375	-5.6E-17
theta= 0.4	0.041907	0.036129	0.030791	0.025876	0.021357	0.017199	0.013357	0.009778	0.006403	0.003166	-6.4E-16
theta= 0.5	0.045859	0.040033	0.03455	0.029398	0.024556	0.019996	0.015683	0.011575	0.007626	0.003786	1.08E-15
theta= 0.6	0.048933	0.043069	0.037474	0.032138	0.027045	0.022172	0.017492	0.012973	0.008578	0.004267	7.93E-17
theta= 0.7	0.051324	0.045431	0.039749	0.03427	0.028981	0.023865	0.0189	0.01406	0.009318	0.004642	-3.6E-15
theta= 0.8	0.053188	0.047272	0.041521	0.035931	0.030489	0.025183	0.019996	0.014907	0.009895	0.004934	-4.8E-16
theta= 0.9	0.054643	0.048709	0.042905	0.037227	0.031667	0.026213	0.020852	0.015569	0.010345	0.005162	4.49E-15
theta= 1	0.055782	0.049834	0.043989	0.038242	0.032588	0.027018	0.021522	0.016086	0.010697	0.00534	2.74E-15
theta= 2	0.059643	0.053647	0.04766	0.041682	0.035711	0.029748	0.02379	0.017838	0.01189	0.005944	-4.7E-15
theta= 3	0.060027	0.054026	0.048025	0.042024	0.036022	0.030019	0.024016	0.018012	0.012008	0.006004	-9.5E-15
theta= 4	0.060042	0.054042	0.04804	0.042038	0.036034	0.03003	0.024025	0.018019	0.012013	0.006007	-1.9E-15
theta= 5	0.060024	0.054023	0.048022	0.042021	0.036019	0.030017	0.024014	0.018011	0.012007	0.006004	4.57E-15
theta= 6	0.060009	0.054009	0.048009	0.042008	0.036007	0.030006	0.024005	0.018004	0.012003	0.006001	3.49E-14
theta= 7	0.060001	0.054001	0.048001	0.042001	0.036001	0.030001	0.024001	0.018	0.012	0.006	4.14E-15
theta= 8	0.059997	0.053997	0.047997	0.041997	0.035997	0.029998	0.023998	0.017998	0.011999	0.005999	1.88E-14
theta= 9	0.059995	0.053995	0.047995	0.041995	0.035996	0.029996	0.023997	0.017998	0.011998	0.005999	4.27E-14
theta= 10	0.059994	0.053994	0.047994	0.041995	0.035995	0.029996	0.023996	0.017997	0.011998	0.005999	-2.4E-14
theta= 20	0.059998	0.053998	0.047998	0.041998	0.035998	0.029998	0.023999	0.017999	0.011999	0.006	-1.2E-14
theta= 30	0.059999	0.053999	0.047999	0.041999	0.035999	0.029999	0.024	0.018	0.012	0.006	2.12E-14
theta= 40	0.06	0.054	0.048	0.042	0.036	0.03	0.024	0.018	0.012	0.006	-8E-14
theta= 50	0.06	0.054	0.048	0.042	0.036	0.03	0.024	0.018	0.012	0.006	-2.5E-14
theta= 60	0.06	0.054	0.048	0.042	0.036	0.03	0.024	0.018	0.012	0.006	-4.3E-14
theta= 70	0.06	0.054	0.048	0.042	0.036	0.03	0.024	0.018	0.012	0.006	-1.4E-15
theta= 80	0.06	0.054	0.048	0.042	0.036	0.03	0.024	0.018	0.012	0.006	-3.5E-14
theta= 90	0.06	0.054	0.048	0.042	0.036	0.03	0.024	0.018	0.012	0.006	-1.3E-13
theta= 100	0.06	0.054	0.048	0.042	0.036	0.03	0.024	0.018	0.012	0.006	-1.2E-14